2 (mx)

NASA CR-72816
AiResearch 70-7045

PRELIMINARY DESIGN STUDY
of
NUCLEAR BRAYTON CYCLE HEAT EXCHANGER AND DUCT ASSEMBLY (HXDA)

by

M. G. Coombs, C. J. Morse, and C. E. Richard

AIRESEARCH MANUFACTURING COMPANY

prepared for

NATIONAL AERONAUTICS AND SPACE ADMINISTRATION
NASA Lewis Research Center

Contract No. NAS3-13453
P. T. Kerwin, Project Manager

33

~~Requests for copies of this report should be referred to~~

~~National Aeronautics and Space Administration~~
~~Scientific and Technical Information Facility~~
~~P. O. Box 33~~
~~College Park, Md. 20740~~

NASA CR- 72816
AiResearch 70-7045

TOPICAL REPORT
(PHASE III)

PRELIMINARY DESIGN STUDY OF NUCLEAR BRAYTON CYCLE HEAT EXCHANGER AND DUCT ASSEMBLY (HXDA)

by

M. G. Coombs, C. J. Morse, and C. E. Richard

AIRESEARCH MANUFACTURING COMPANY
Los Angeles, California

prepared for

NATIONAL AERONAUTICS AND SPACE ADMINISTRATION

January 4, 1971

CONTRACT NO. NAS3-13453

NASA Lewis Research Center
Cleveland, Ohio 44135
P. T. Kerwin, Project Manager
Space Power Systems Division

FOREWORD

The studies described herein, which were performed by the AiResearch Manufacturing Company, a division of The Garrett Corporation, were performed under NASA Contract NAS3-13453. The work was done under the direction of the NASA Program Manager, Mr. P.T. Kerwin, Space Power Systems Division, NASA-Lewis Research Center. The AiResearch Program Manager was Mr. M.G. Coombs.

ABSTRACT

The preliminary designs of two Brayton-cycle heat exchanger and duct assemblies (HXDA's) suitable for operation with a liquid-metal-cooled reactor are developed. One system was designed to be compatible with the SNAP-8 reactor capabilities, i.e., 1150°F (894°K) turbine inlet temperature and 300 kw_t, while the other system requires more advanced reactor capabilities, i.e., 1600°F (1144°K) turbine inlet temperature and 650 kw_t.

CONTENTS

ILLUSTRATIONS

ILLUSTRATIONS (Continued)

ILLUSTRATIONS (Continued)

DRAWINGS

TABLES

TABLES (Continued)

SECTION I

INTRODUCTION

As part of their advanced space power systems studies, NASA is investigating the performance characteristics of advanced closed-loop Brayton-cycle electric power generating sytems employing liquid-metal-cooled reactors. The heat exchangers associated with this type of power conversion system are the waste heat exchanger, the heat source heat exchanger, and the recuperator. These three heat exchangers and their associated interconnecting ducting define the heat exchanger and duct assembly (HXDA). The HXDA constitutes a large fraction of the Brayton-cycle power conversion system weight and volume. The weight and volume of the HXDA are highly dependent on the selected cycle operating and design parameters. The definition of the set of design parameters which yields the minimum overall system weight requires extensive studies on the component and systems level.

To aid in the development of advanced Brayton-cycle space power systems, NASA formulated a study to define the associated HXDA heat exchangers and suitable overall packaging configurations. This study was organized in three phases:

Phase I - Parametric Optimization Studies

Phase II - Pressure Containment Tests

Phase III - Preliminary Designs

The Phase I effort was concerned with the selection of basic types of heat transfer surfaces for each of the three sytem heat exchangers and the development of optimum (i.e., minimum weight) HXDA designs and configurations over a wide range of cycle operating conditions and design variables. The results of the Phase I studies are presented in NASA report CR-72783.

The Phase II effort involved the structural testing of plate-fin heat transfer surfaces at the elevated temperatures and pressures associated with advanced Brayton-cycle systems. The results of this experimental program are summarized in NASA report CR-72815.

After reviewing the Phase I and Phase II studies, NASA defined two Brayton-cycle design points for the Phase III preliminary design effort. One of the selected design points is a 300-kw_t system operating at a turbine inlet temperature of 1150^oF (894^oK). This power and temperature level are representative of the capabilities of the SNAP-8 reactor. The second design point involves a Brayton-cycle system operating at approximately 650 kw_t with a turbine inlet temperature of 1600^oF (1144^oK). This system would be representative of the capabilities of a more advanced reactor system. In addition to the base design points defined above, a certain growth potential, in terms of higher operating temperature and pressure capabilities, is designed into both systems. This report describes the Phase III studies and the resulting two HXDA preliminary designs.

PRECEDING PAGE BLANK NOT FILMED

SECTION 2

SUMMARY

This topical report summarizes the Phase III work performed by AiResearch on NASA Contract NAS3-13453 entitled "Conceptual Design Study of Nuclear Brayton-Cycle Heat Exchanger and Duct Assembly (HXDA)." The major elements of the closed-loop Brayton-cycle power conversion package are the turbo-alternator-compressor (TAC), recuperator, waste heat exchanger, heat source heat exchanger, and the interconnecting ducting. This study was concerned with the three system heat exchangers and the interconnecting ducting which, together constitute the HXDA.

The Phase I studies centered around defining optimum heat exchanger designs, system operating parameters, and overall equipment configurations for a closed-loop Brayton-cycle space power conversion system operating in the power range of 80 to 160 kw_e and coupled to a liquid-metal-cooled reactor. The results of this study are presented in NASA CR-72783. The Phase II studies were concerned with the testing of plate-fin heat exchanger matrices suitable for application to advanced Brayton-cycle systems. The Phase II studies are summarized in NASA CR-72815. The Phase III studies are presented in this report and were concerned with the development of two HXDA preliminary designs based on operating conditions defined by NASA. The first system was designed to operate at conditions associated with the SNAP-8 reactor capabilities. The second system was designed for a more advanced reactor system exhibiting higher temperature and power output. Thus, the two designs represent Brayton-cycle systems of increasing power and temperature capabilities. The cycle conditions for the two design cases are shown in Figure 2-1.

CASE I, SNAP-8 DESIGN

The Brayton-cycle nominal operating conditions defined for the SNAP-8 HXDA preliminary design are shown in Figure 2-1a. The system is basically a 300 kw_t design that operates at a turbine inlet temperature of 1150°F (894°K). Heat input to the Brayton-cycle working fluid (He - Xe, molecular weight = 39.94) is accomplished in the NaK-to-gas heat source heat exchanger (HSHX). This NaK is heated in the intermediate heat exchanger (IHX) by the NaK that flows through the reactor. Thus, the Brayton-cycle HXDA is coupled to the reactor by an intermediate NaK heat transfer loop. This technique is used so that no radioactive fluid will be associated with the Brayton-cycle power conversion loop. The IHX was not considered a part of the HXDA study because of its remote location from the HXDA package. Heat is extracted from the Brayton-cycle working fluid by circulating a cooled organic fluid through the waste heat exchanger and subsequently through the space radiator where the heat is ultimately rejected to space. The radiator was not included in the HXDA study. The waste heat exchanger contains dual organic liquid heat transfer circuits to provide redundant heat rejection loops. Total system heat rejection can be accomplished with either one of the two organic loops in operation.

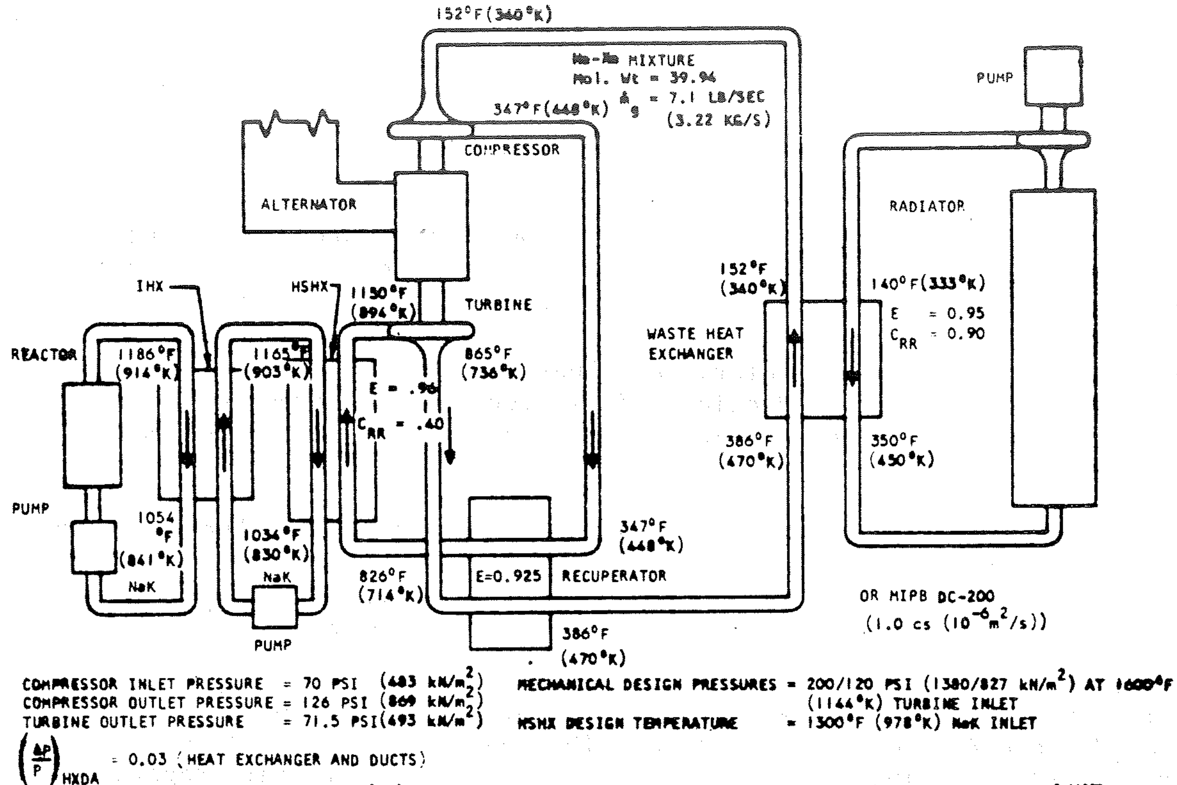

(a) Case I, SNAP-8 System

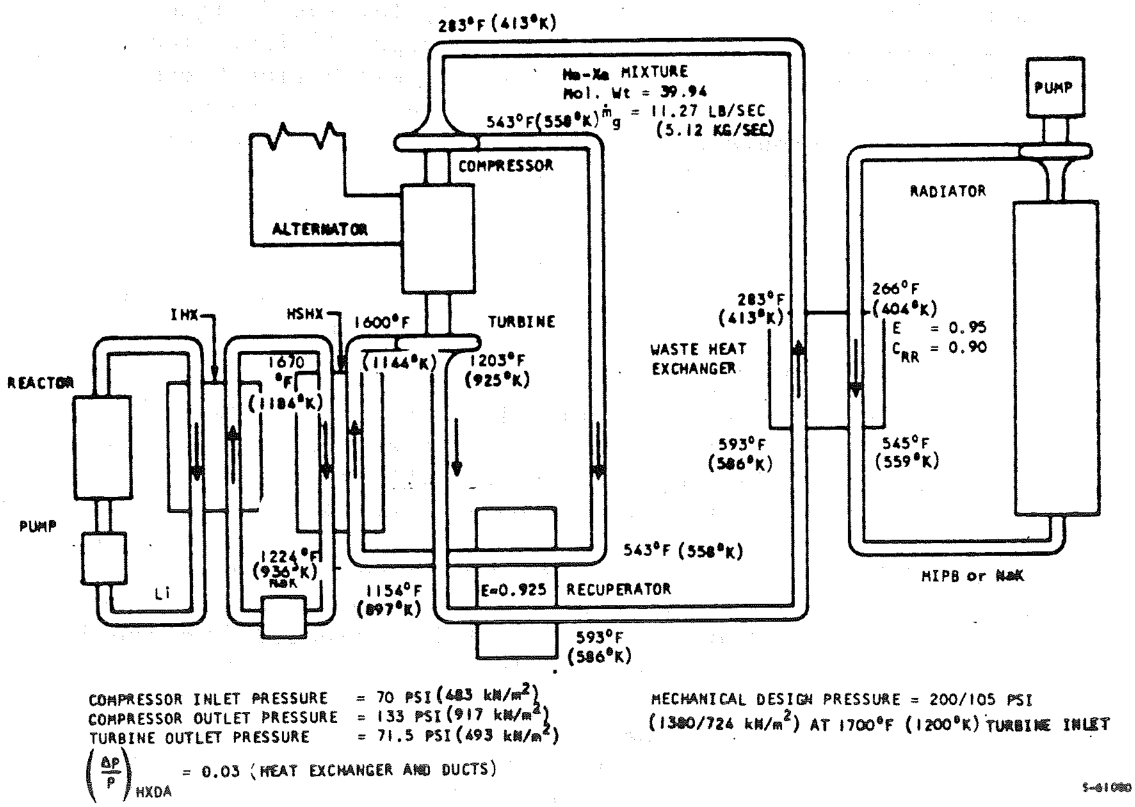

(b) Case II, Advanced Reactor System

Figure 2-1. Brayton-Cycle Design Conditions

To provide some growth potential in the HXDA design, the structural design is based on pressure and temperature levels somewhat higher than the nominal values shown in Figure 2-1a. For the structural design, the system pressure levels are 200 and 120 psi (1380 and 827 kN/m^2), and the temperatures are those associated with the cycle conditions of a 1600^{0}F (1144^{0}K) turbine inlet temperature system. The HSHX structural design, however, is limited to a maximum temperature of 1300^{0}F (978^{0}K) because this is a reasonable limit for SNAP-8 reactor operation.

The resulting set of heat exchanger designs selected for Case I are shown in Figure 2-2; some pertinent design data are also shown. The analysis and system studies leading to the selection of these heat exchanger designs are presented in Section 3 of this report. The weight of the complete HXDA system is 1987 lb (902 kg), which is broken down as follows:

Recuperator	=	732 lb (332 kg)
Waste heat exchanger	=	543 lb (246 kg)
Heat source heat exchanger	=	135 lb (61 kg)
Ducting and manifolds	=	147 lb (67 kg)
Support frame	=	120 lb (55 kg)
Insulation	=	310 lb (141 kg)
HXDA-Total	=	1987 lb (902 kg)

The packaging configuration developed for this design is shown in Figure 2-3. The frame picks up the heat exchanger loads and supports the TAC. The frame-to-spacecraft interface will depend on the particular installation involved; therefore, it was not considered in this study.

CASE II, ADVANCE REACTOR SYSTEM

The operating conditions for the Case II Brayton-cycle system, which employs an advanced reactor, are shown in Figure 2-1b. The reactor is lithium cooled, and the reactor heat is transferred to the Brayton-cycle power conversion system through an intermediate NaK loop similar to that described for the Case I design. The nominal system operating conditions are 650 kw_t at a turbine inlet temperature of 1600^{0}F (1144^{0}K).

To provide some growth potential in the HXDA capabilities, the structural design is based on somewhat higher pressures and temperatures than the nominal values given in Figure 2-1b. The structural design pressures are 200 and 105 psi (1380 and 724 kN/m^2) at compressor and turbine outlets. While it was desired to base the structural design on temperatures associated with a 2100^{0}F (1421^{0}K) turbine inlet temperature, it was found that this would require a

Recuperator

Gas pressure drop	1.18 percent
Weight	732 lb (332 kg)
Core length	13.8 in. (0.351 m)
End section height, hot end	4.9 in. (0.124 m)
cold end	3.2 in. (0.0813 m)
End section ratio, hot end	0.65
cold end	0.59
Width	19.0 in. (0.483 m)
Stack height	37.9 in. (0.963 m)

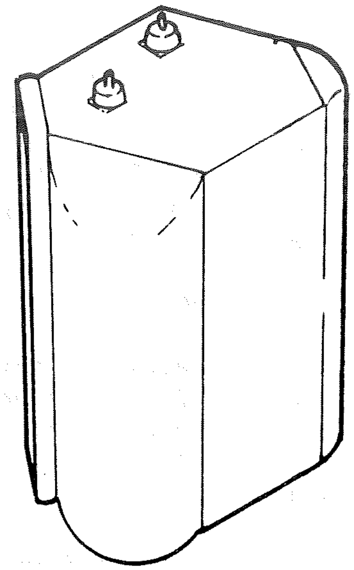

Waste Heat Exchanger

Gas pressure drop	0.94 percent
Weight	543 lb (246 kg)
Liquid pressure drop	13.5 psi (9.3 kN/m^2)
Gas-flow length	19.0 in. (0.483 m)
Liquid-flow length	37.9 in. (0.963 m)
Stack height	11.8 in. (0.300 m)

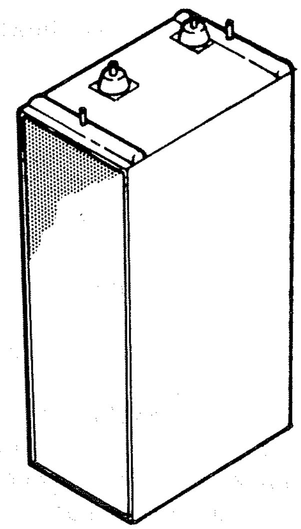

Heat Source Heat Exchanger

Gas pressure drop	0.38 percent
Weight	135 lb (61 kg)
Liquid pressure drop	1 psi (7 kN/m^2)
Gas-flow length	6.0 in. (0.152 m)
Tube length	37.7 in. (0.958 m)
No-flow length	8.9 in. (0.226 m)
Number of tubes	75
Number of tube rows	10
Number of passes	2

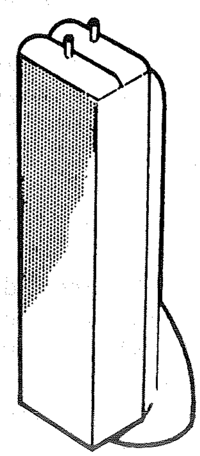

S-61553

Figure 2-2. Case I, SNAP-8 HXDA Heat Exchanger Design Summary

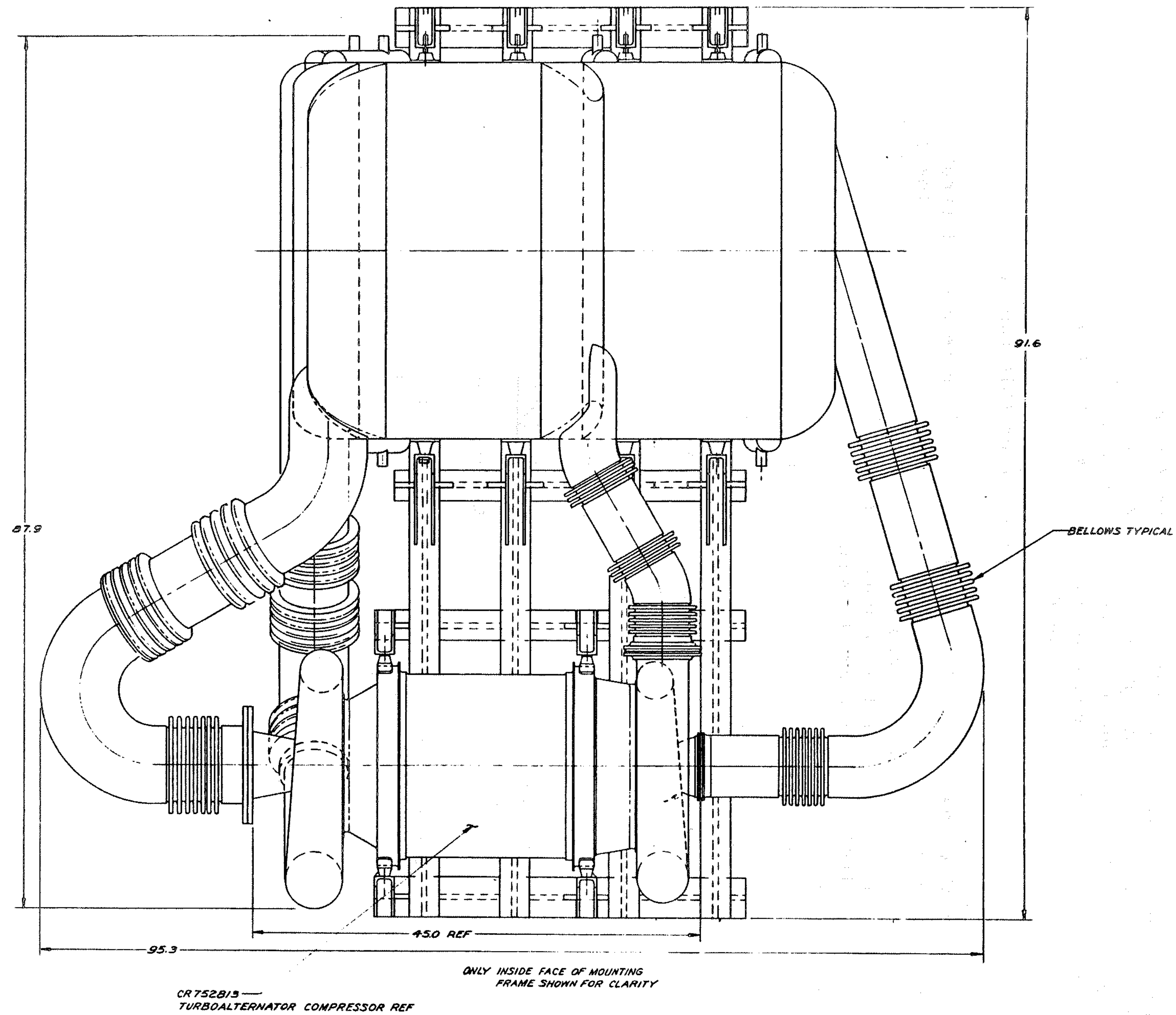

Figure 2-3. Case I, SNAP-8 HXDA Packaging Configuration

major change in heat exchanger materials and/or heat exchanger design approach. Therefore, to provide some growth potential for the HXDA, while maintaining a design approach consistent with requirements at nominal operating conditions, the structural design is based on system cycle temperatures associated with a 1700°F (1200°K) turbine inlet temperature. A discussion of what modifications to the HXDA design would be required to provide the full 2100°F (1421°K) temperature capability is presented in Section 4 of this report.

The heat exchanger designs developed for this case are illustrated in Figure 2-4, which also lists some pertinent design information. The detailed development and optimization procedures employed in selecting these designs are given in Section 4 of this report. The weight of the complete HXDA system is 4383 lb (1990 kg), which can be subdivided as follows:

Recuperator	1778 lb (807 kg)
Waste heat exchanger	866 lb (393 kg)
Heat source heat exchanger	374 lb (170 kg)
Ducting and manifolds	556 lb (253 kg)
Frame	300 lb (136 kg)
Insulation	509 lb (231 kg)
Total	4383 lb (1990 kg)

The package configuration is illustrated in Figure 2-5, which shows the three system heat exchangers, the interconnecting ducts, and the larger TAC required for this higher power system.

Structural design considerations for both the heat exchangers and the overall HXDA assemblies for both Case I and Case II designs are given in Section 6 of this report.

Recuperator

Gas pressure drop	1.18 percent
Weight	1778 lb (807 kg)
Core length	10.0 in. (0.254 m)
End section height, hot end	7.1 in. (0.180 m)
cold end	4.1 in. (0.104 m)
End section ratio, hot end	0.65
cold end	0.58
Width	27.8 in. (0.706 m)
Stack height	55.6 in. (1.41 m)

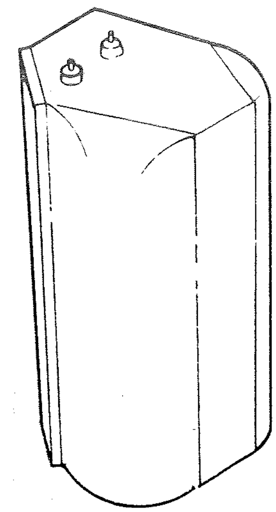

Waste Heat Exchanger

Gas pressure drop	0.75 percent
Weight	866 lb (393 kg)
Liquid pressure drop	10 psi (68.9 kN/m^2)
Gas-flow length	15.0 in. (0.318 m)
Liquid-flow length	55.6 in. (1.41 m)
Stack height	16.4 in. (0.416 m)

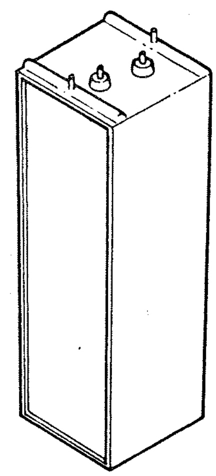

Heat Source Heat Exchanger

Gas pressure drop	0.57 percent
Weight	374 lb (170 kg)
Liquid pressure drop	1.1 psi (7.59 kN/m^2)
Gas-flow length	7.1 in. (0.180 m)
Tube length	56.2 in. (1.43 m)
No-flow length	11.1 in. (0.282 m)
Number of tubes	154
Number of tube rows	14
Number of passes	4

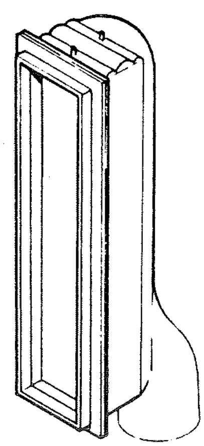

S-61554

Figure 2-4. Case II, Advanced Reactor HXDA Heat Exchanger Design Summary

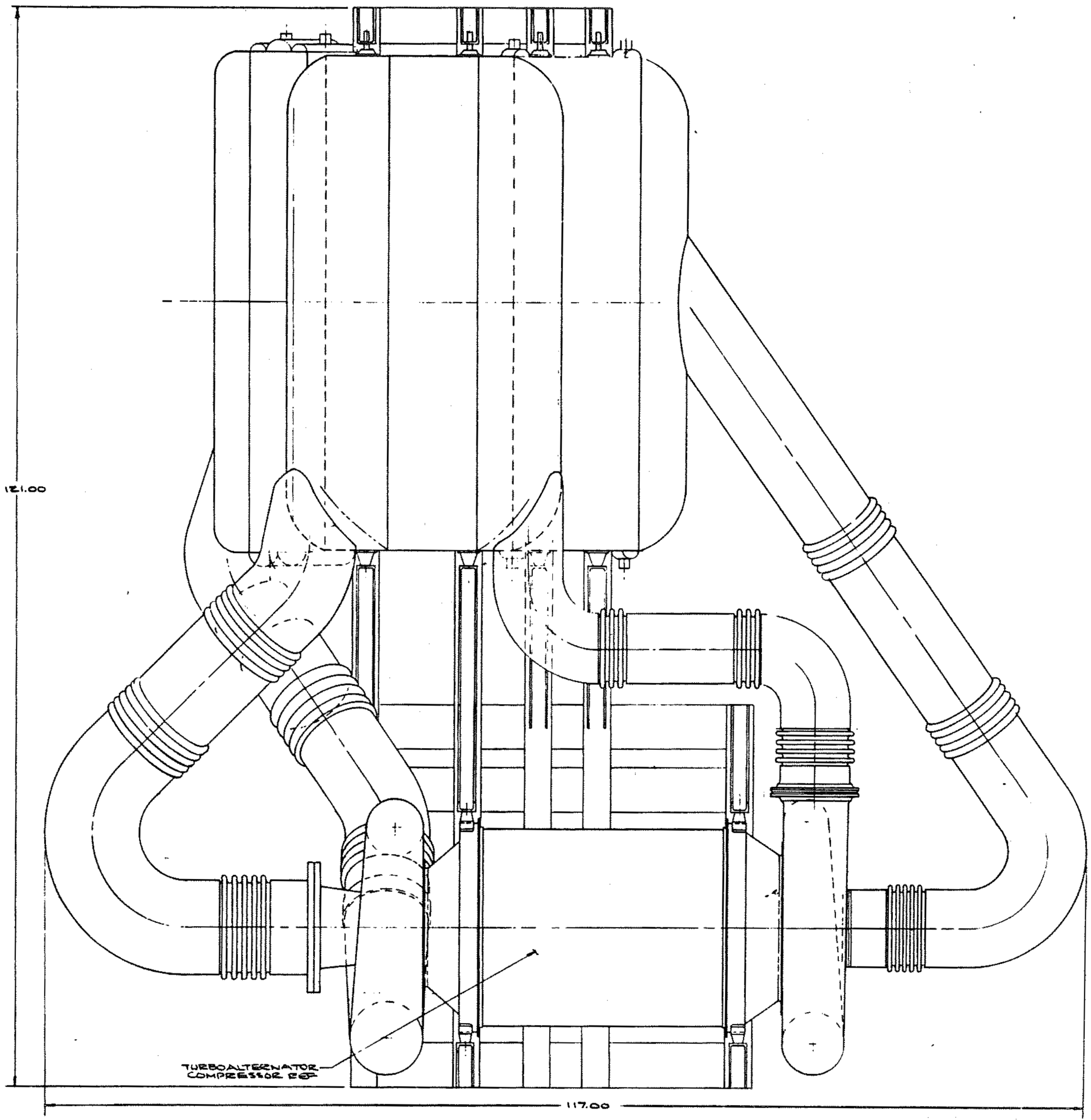

Figure 2-5. Case II, Advanced Reactor, HXDA Packaging Configuration

SECTION 3

CASE I DESIGN STUDIES

INTRODUCTION

The parametric analyses and preliminary design of the HXDA for the Phase 3, Case I design conditions are presented in this section. The Case I cycle conditions, shown in Table 3-1 and on the system schematic of Figure 3-1, define a system operating at a turbine inlet temperature of 1150°F (894°K) (compatible with a SNAP-8 heat source), but with additional structural capability to provide system flexibility and growth potential to higher temperatures and pressures. Thus, the heat exchangers and ducts, with the exception of the heat source heat exchanger and turbine inlet duct, are designed structurally for a set of system temperatures consistent with a 1600°F (1144°K) turbine inlet. The heat source heat exchanger and turbine inlet duct are designed structurally for 1300°F (978°K) at the heat source heat exchanger NaK inlet. Gas pressure levels for the system structural design are 120 and 200 psi (827 and 1380 kN/m^2), respectively, at compressor inlet and outlet.

Fluids used in the Case I system are NaK-78 in the heat source coolant loop, a xenon-helium mixture with a molecular weight of 39.94 as the cycle working fluid, and either Dow-Corning 200 (1.0 centistoke, or 10^{-6} m^2/sec) fluid or monoisopropyl-biphenyl (MIPB) as the heat rejection fluid. The use of MIPB is considered because it has higher temperature capability than the Dow-Corning fluid and is thus preferred for the 1600°F (1144°K) growth system. Design pressure drops are 3.0 percent total for the gas system heat exchangers and ducting, 10.0 psi (68.9 kN/m^2) maximum for the waste heat exhanger liquid side, and 5.0 psi (34.5 kN/m^2) maximum for the heat source heat exchanger liquid side.

COMPONENT DESIGNS

Recuperator

Recuperators were sized as a function of gas fractional pressure drop for the Case I problem statement. Several core fin sets were used to obtain the optimum core geometry. The construction material is Hastelloy X, which is sized for structural capability in a system operating at 1600°F (1144°K) turbine inlet and respective high- and low-pressure levels of 200 and 120 psi (1380 and 827 kN/m^2). The recuperator geometry is pure counterflow with either triangular or rectangular crossflow end sections.

To obtain the optimum pressure drop split between recuperator core and end sections, a series of end section designs for several end section pressure drops was calculated for each of several counterflow core pressure drops and each core fin set. The end section designs were obtained using AiResearch

TABLE 3-1

CASE I DESIGN CONDITIONS

Thermodynamic	
Gas flow rate	7.1 lb/sec (3.22 kg/sec)
Recuperator effectiveness	0.925
Waste heat exchanger effectiveness	0.95
Capacity-rate ratio (gas ÷ liquid)	0.90
Heat source heat exchanger effectiveness	0.9558
Capacity-rate ratio (gas ÷ liquid)	0.404
Temperatures	See Figure 3-1
Compressor inlet pressure	70 psi (483 kN/m^2)
Compressor outlet pressure	126 psi (869 kN/m^2)
Pressure drops	
Gas system, total HXDA	3.0 percent
Waste heat exchanger liquid, maximum	10.0 psi (68.9 kN/m^2)
Heat source heat exchanger liquid, maximum	5.0 psi (34.5 kN/m^2)
Structural	
Temperatures	
Heat source heat exchanger, maximum	1300°F (978°K)
Recuperator, maximum	1216°F (931°K)
Waste heat exchanger, maximum	542°F (557°K)
Compressor inlet duct	240°F (389°K)
Compressor outlet duct	487°F (526°K)
Turbine inlet duct	1285°F (969°K)
Turbine outlet duct	1216°F (931°K)
Pressures	
Compressor inlet	120 psi (827 kN/m^2)
Compressor outlet	200 psi (1380 kN/m^2)
Heat source loop, maximum	30 psi (207 kN/m^2)
Heat rejection loop, maximum	75 psi (517 kN/m^2)

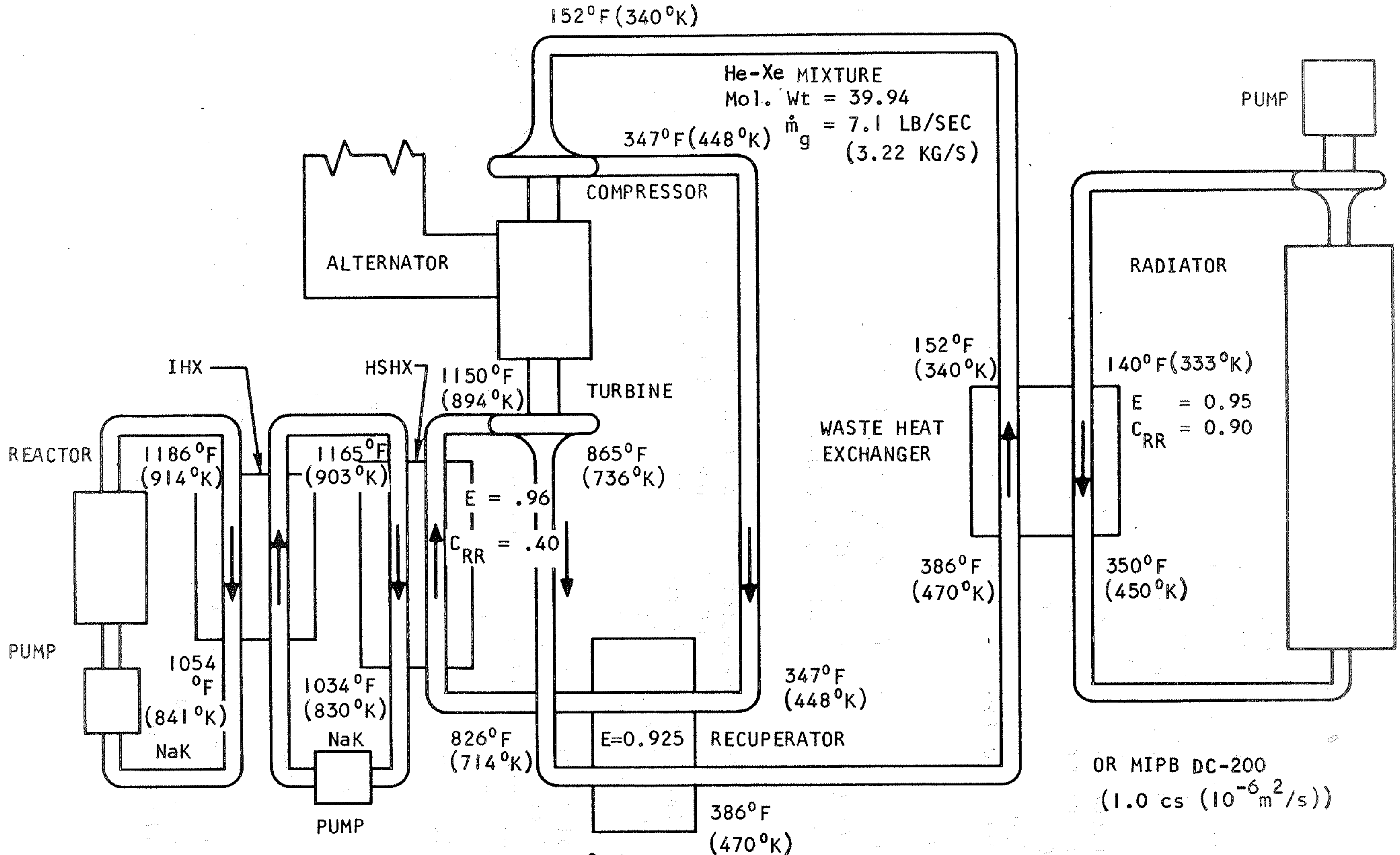

COMPRESSOR INLET PRESSURE = 70 PSI (483 kN/m^2)
COMPRESSOR OUTLET PRESSURE = 126 PSI (869 kN/m^2)
TURBINE OUTLET PRESSURE = 71.5 PSI (493 kN/m^2)

$\left(\frac{\Delta P}{P}\right)_{HXDA}$ = 0.03 (HEAT EXCHANGER AND DUCTS)

MECHANICAL DESIGN PRESSURES = 200/120 PSI (1380/827 kN/m^2) AT 1600°F (1144°K) TURBINE INLET
HSHX DESIGN TEMPERATURE = 1300°F (978°K) NaK INLET

S-61079

Figure 3-1. Case I Cycle Conditions

computer program H1440 (see Section 5), which calculates end section geometry combinations that provide uniform core flow distribution.

The combined weights of counterflow and end sections are shown in Figures 3-2 through 3-9. The core fin sets used are shown in Table 3-2. The dashed lines in the figures represent the recuperator weight variations corresponding to optimum pressure drop splits between counterflow and end sections. The optimized weight variations are summarized in Figures 3-10 and 3-11 for the two types of end sections. As shown, the weight advantage of triangular end sections in comparison with rectangular ends varies from about 70 lb (32 kg) at a total recuperator pressure drop of 3.0 percent to 170 lb (75 kg) at a pressure drop of 0.5 percent. Since this weight advantage is quite small relative to anticipated total HXDA weights, both recuperator types were included in the more detailed studies of HXDA system configurations.

Waste Heat Exchanger

Plate-fin units were sized for the waste heat exchanger design conditions using both DC-200 (1.0 centistoke, or 10^{-6} m^2/sec) fluid and MIPB as the heat rejection fluid. Heat exchanger weights and dimensions are shown in Figure 3-12. Since MIPB is the required fluid for system operation at advanced (1600°F, or 1144°K) turbine inlet conditions, the larger heat exchanger associated with the use of MIPB is selected. This selection results in a slight over-design capability using DC-200 at the nominal SNAP-8 conditions, but provides growth potential without the requirement for a change in heat rejection fluid if MIPB is used. The penalty incurred by this selection is approximately 8 percent in waste heat exchanger weight.

The waste heat exchanger is an eight-pass cross-counterflow unit with two separate liquid circuits in the core. Liquid passages are alternately active and redundant; i.e., the ordering of passages is liquid 1, gas, liquid 2, gas, liquid 1, etc. The gas-side fin geometry is 20 fins/inch (788 fins/m), 0.100 in. (0.00254 m) high, and 0.003 in. (0.762×10^{-4}m) thick. The liquid-side geometry is 20 fins/inch (788 fins/m), 0.075 in. (0.00190 m) high, and 0.002 in. (0.508×10^{-4}m) thick. The fins are nickel, and the plates and header bars are 347 stainless steel.

Heat Source Heat Exchanger

Size and weight for the heat source heat exchanger are shown as a function of gas pressure drop in Figure 3-13. The core matrix for this heat exchanger is the SFT 18* finned tube bundle with 0.500 in. (0.0127 m) OD tubes. The SFT 18* matrix has the following geometry:

Transverse tube spacing = 2.34 x (tube OD)

Tube row spacing = 1.17 x (tube OD)

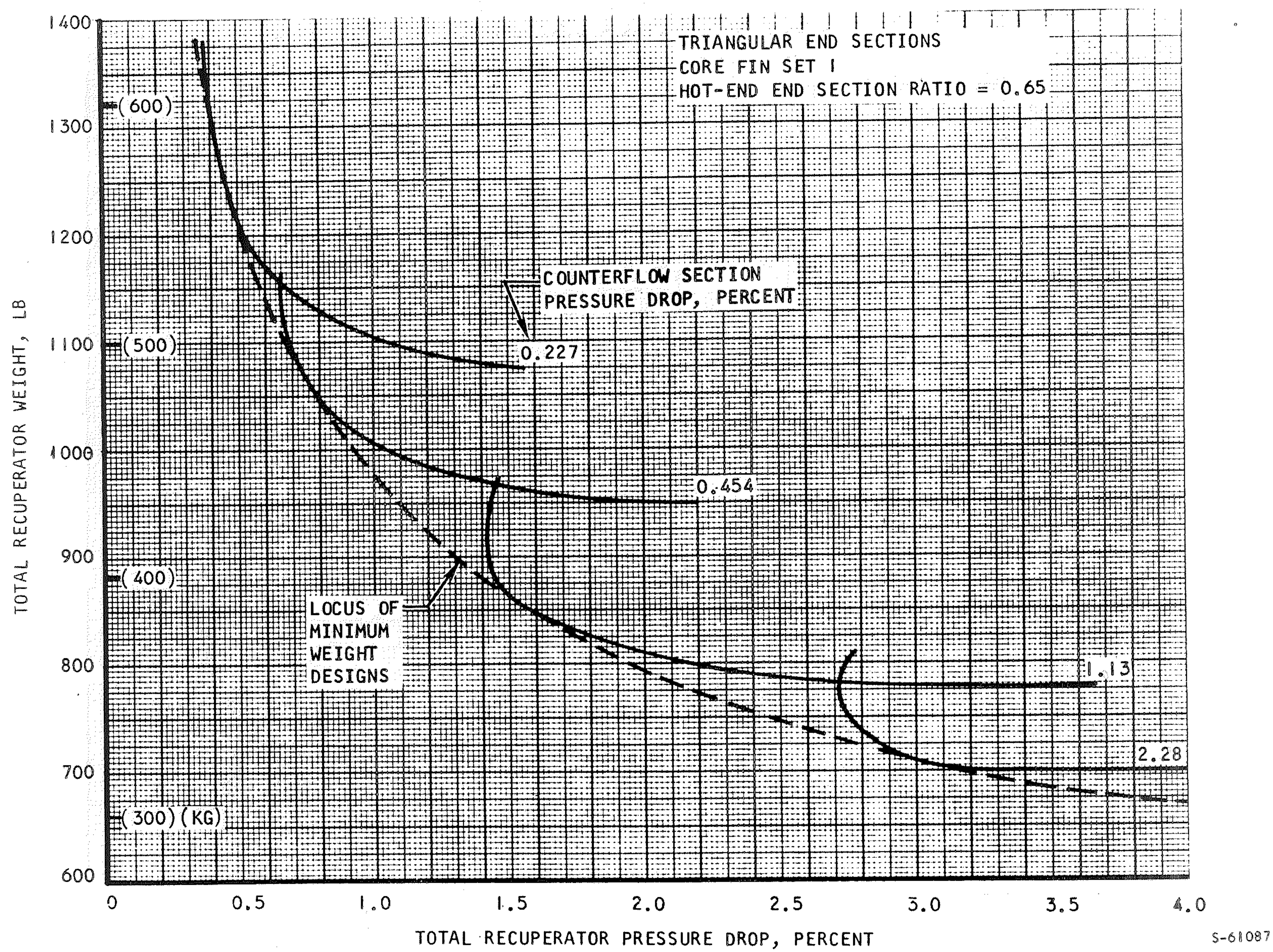

Figure 3-2. Variation of Total Weight with Total Pressure Drop for Case I Recuperator

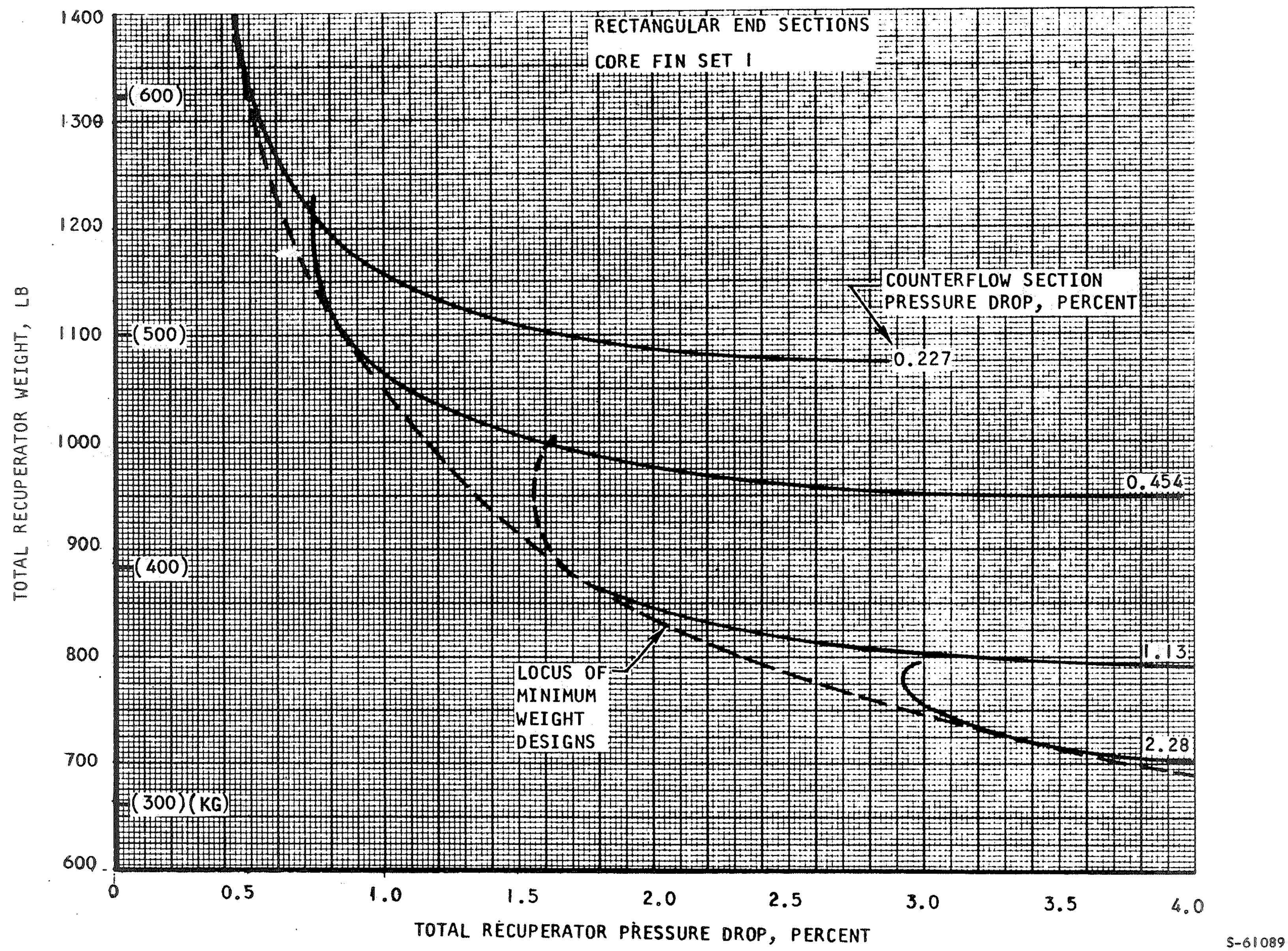

Figure 3-3. Variation of Total Weight with Total Pressure Drop

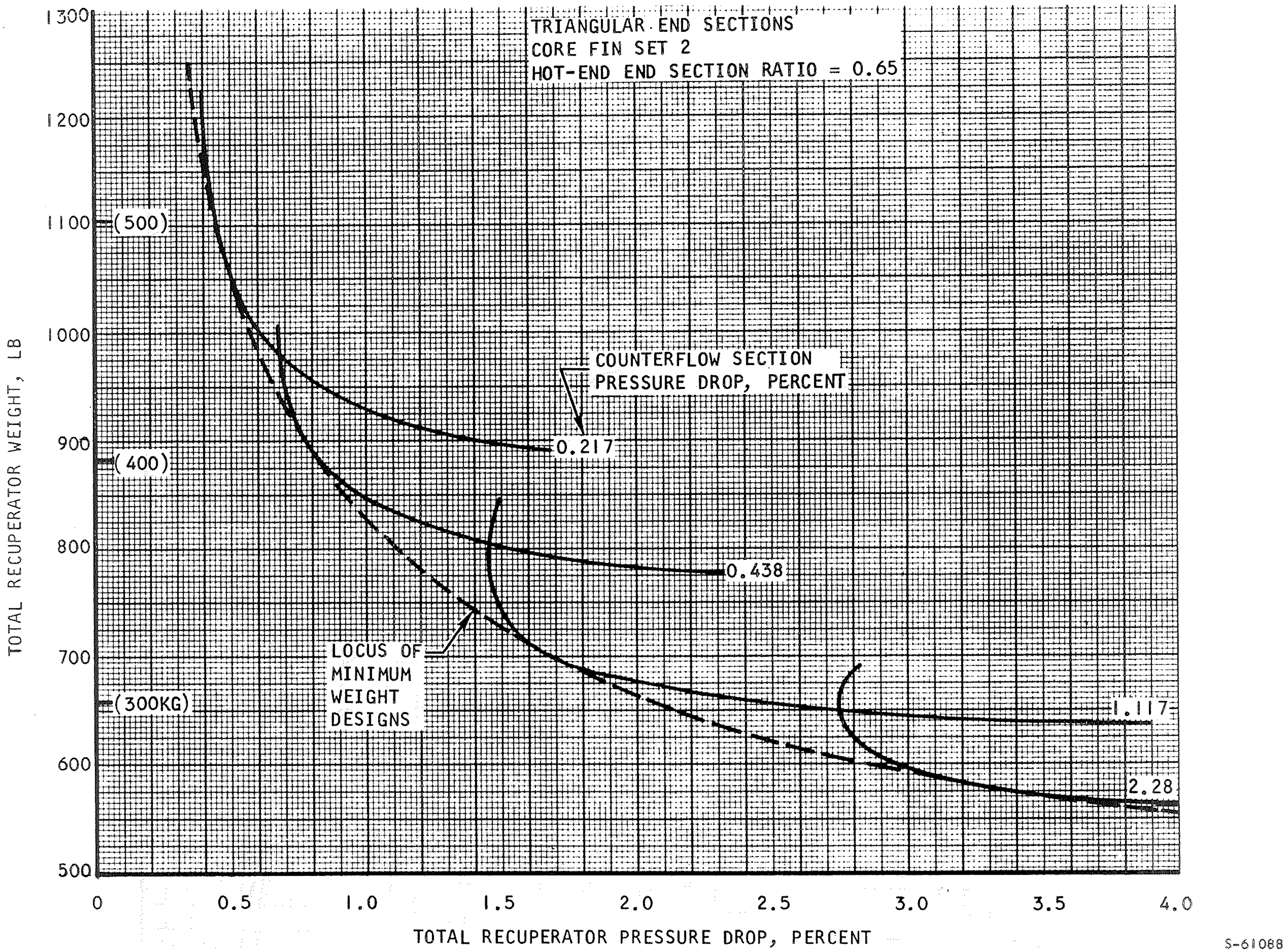

Figure 3-4. Variation of Total Weight with Total Pressure Drop for Case I Recuperator

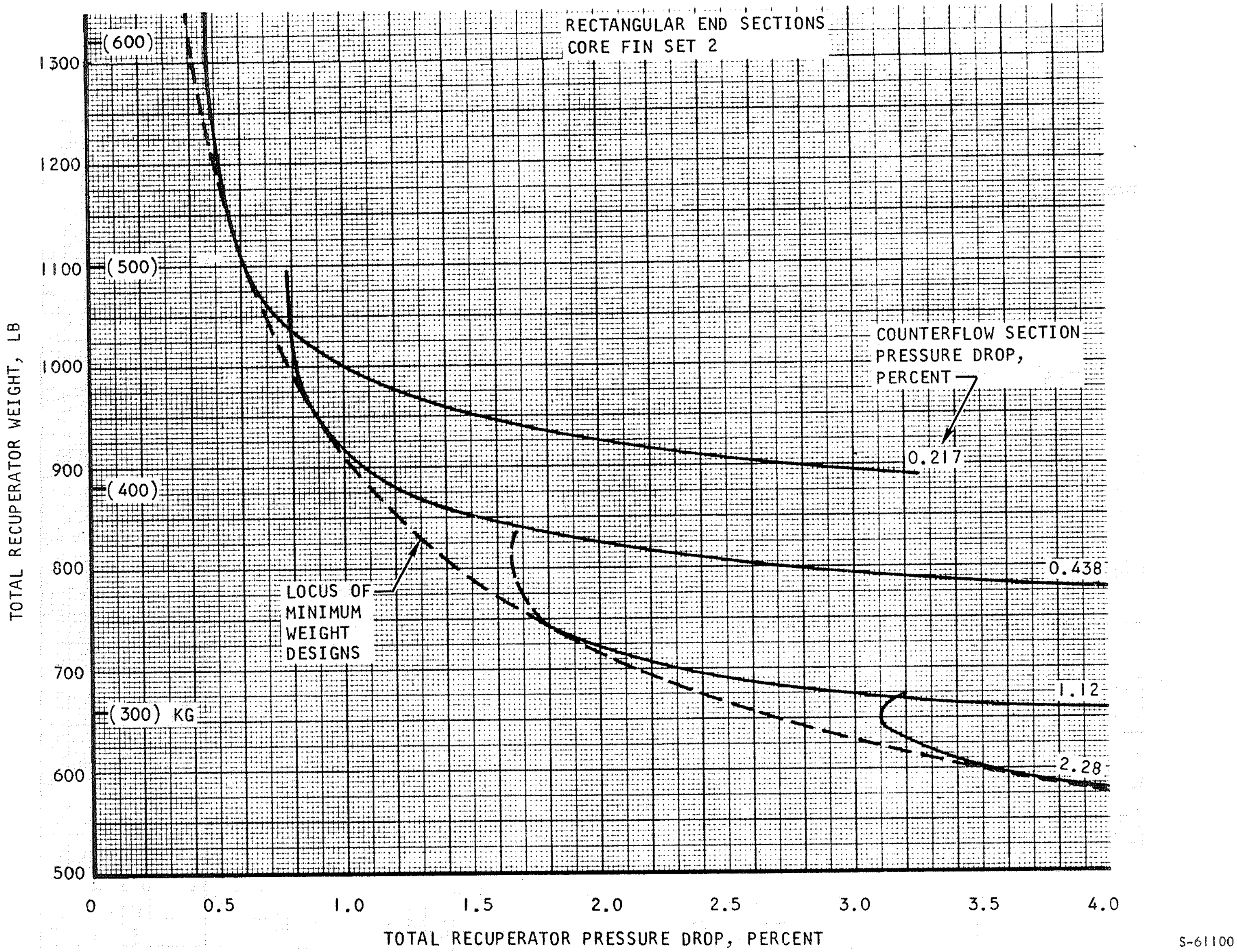

Figure 3-5. Variation of Total Weight with Total Pressure Drop for Case I Recuperator

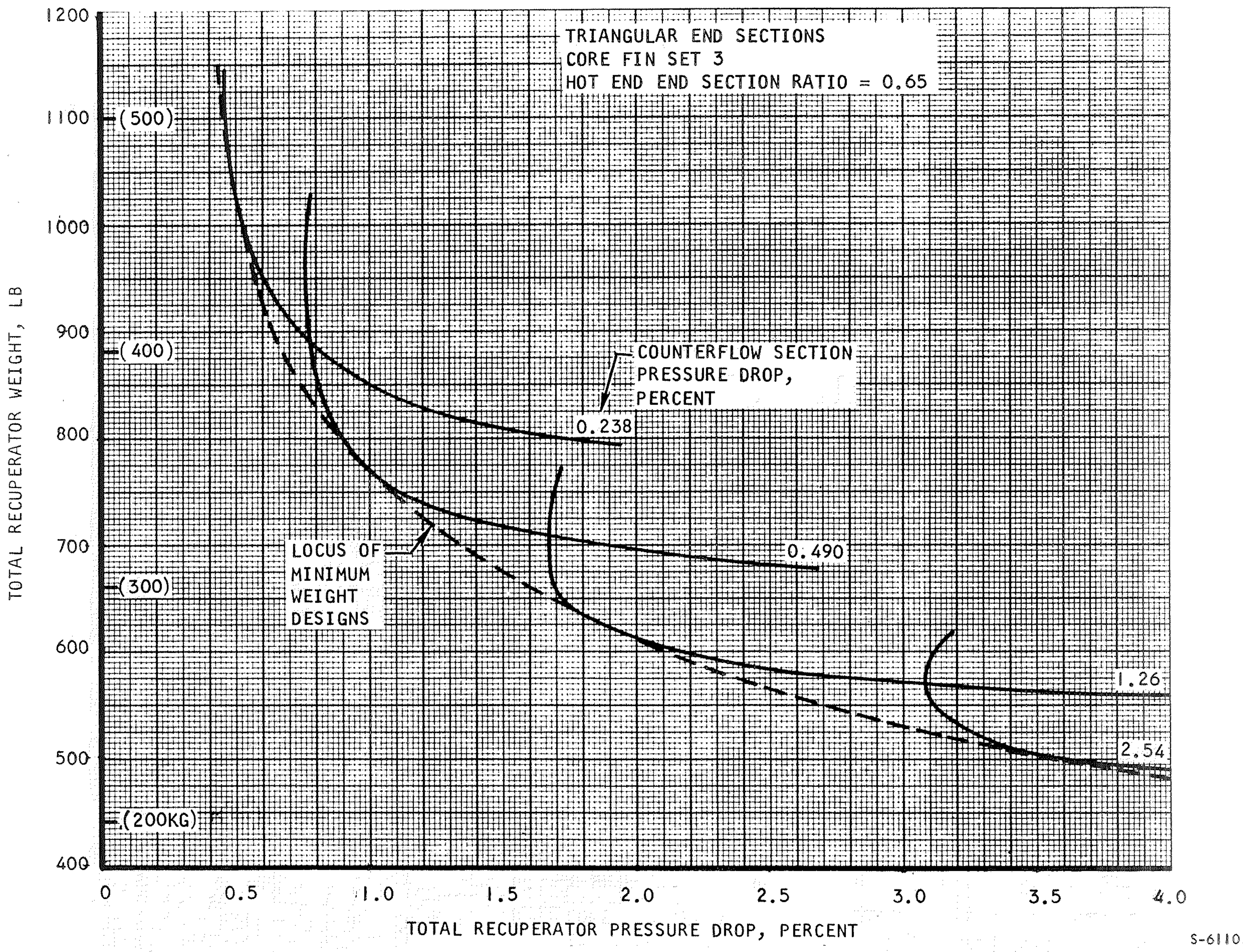

Figure 3-6. Variation of Total Weight with Total Pressure Drop for Case I Recuperator

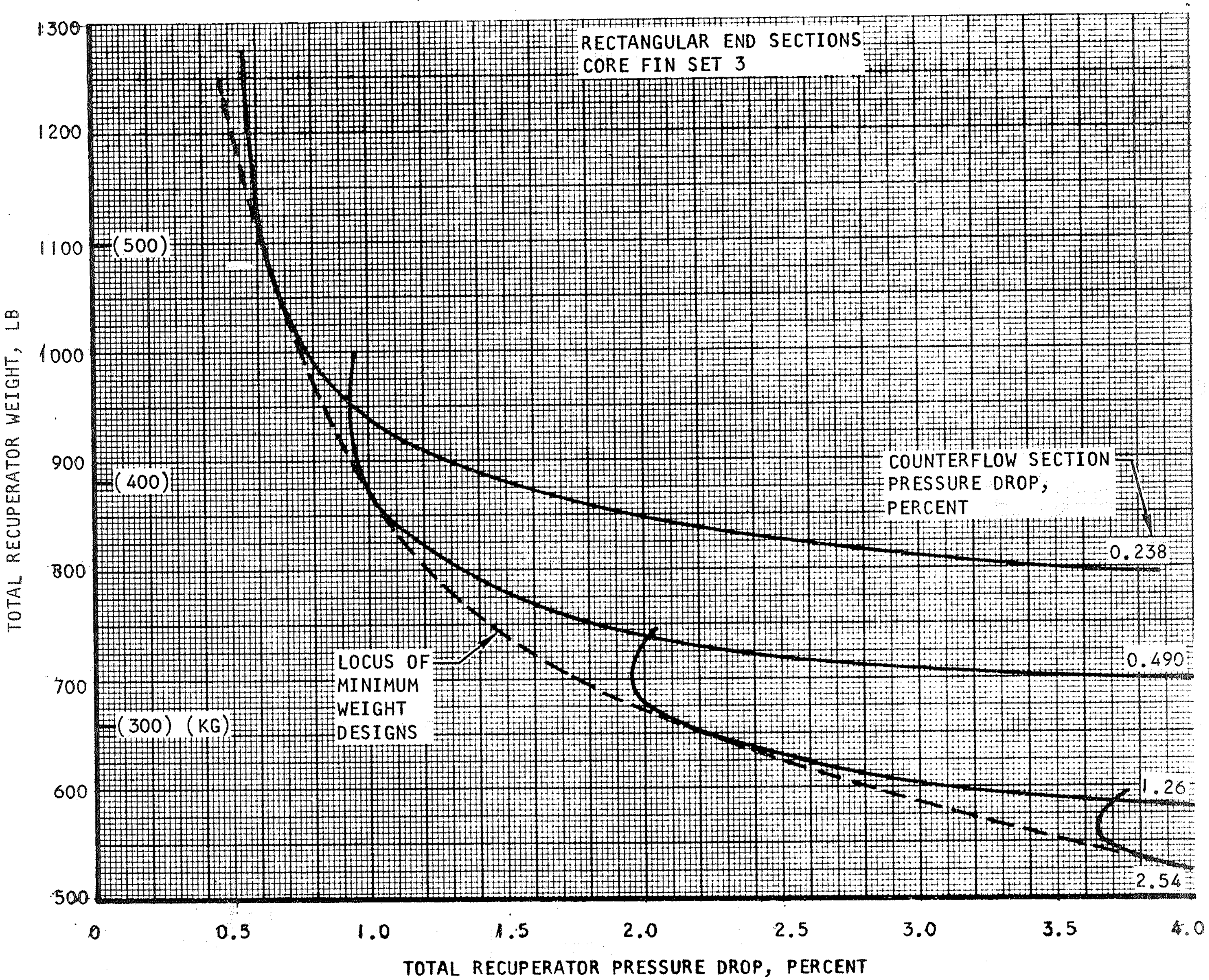

S-61077

Figure 3-7. Variation of Total Weight with Total Pressure Drop for Case I Recuperator

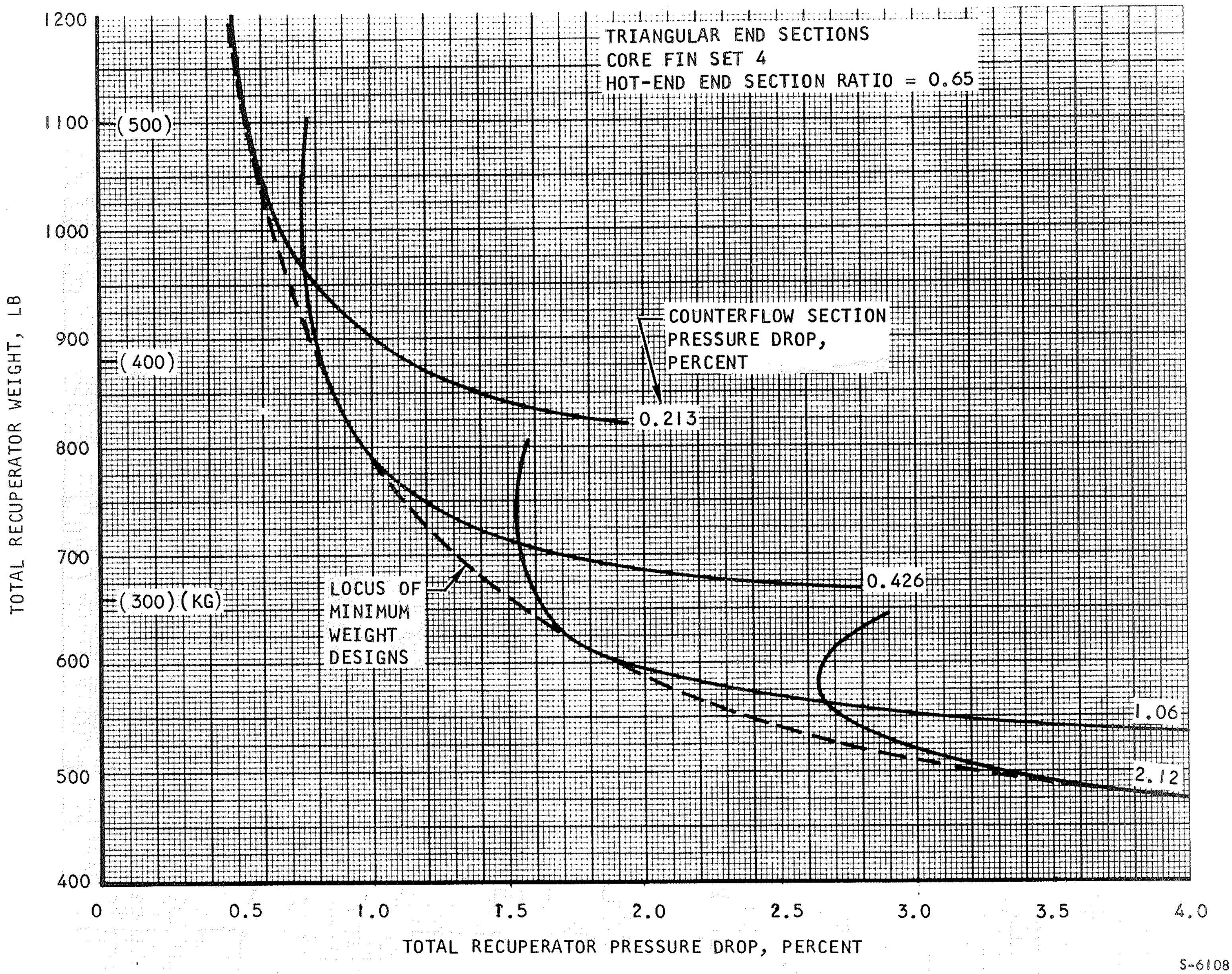

Figure 3-8. Variation of Total Weight with Total Pressure Drop for Case I Recuperator

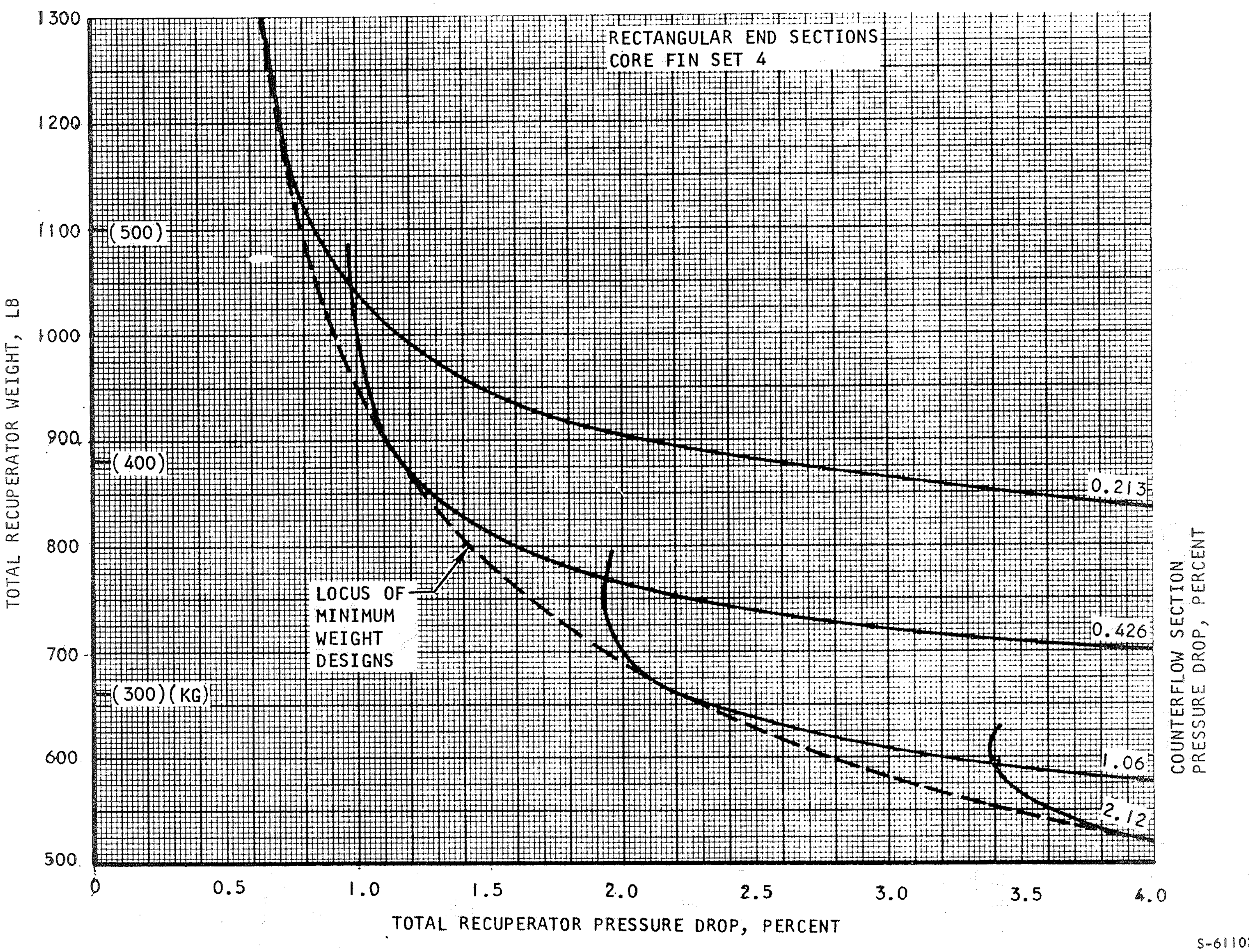

Figure 3-9. Variation of Total Weight with Total Pressure Drop for Case I Recuperator

TABLE 3-2

RECUPERATOR CORE FIN SETS (CASE I)

Fin Set	Fins/In. (Fins/m)	Fin Ht, in. (m)	Fin Thick., in. (m)
Low-Pressure Side			
1	12 (473)	0.178 (0.00452)	0.00515 (1.31×10^{-4})
2	16 (630)	0.153 (0.00388)	0.00386 (0.980×10^{-4})
3	16 (630)	0.125 (0.00317)	0.00386 (0.980×10^{-4})
4	20 (788)	0.100 (0.00254)	0.00309 (0.785×10^{-4})
High-Pressure Side			
Fin Set	Fins/In. (Fins/m)	Fin Ht, in. (m)	Fin Thick., in. (m)
1	16 (630)	0.153 (0.00388)	0.00618 (1.57×10^{-4})
2	16 (630)	0.125 (0.00317)	0.00618 (1.57×10^{-4})
3	20 (788)	0.100 (0.00254)	0.00495 (1.26×10^{-4})
4	20 (788)	0.075 (0.00190)	0.00495 (1.26×10^{-4})

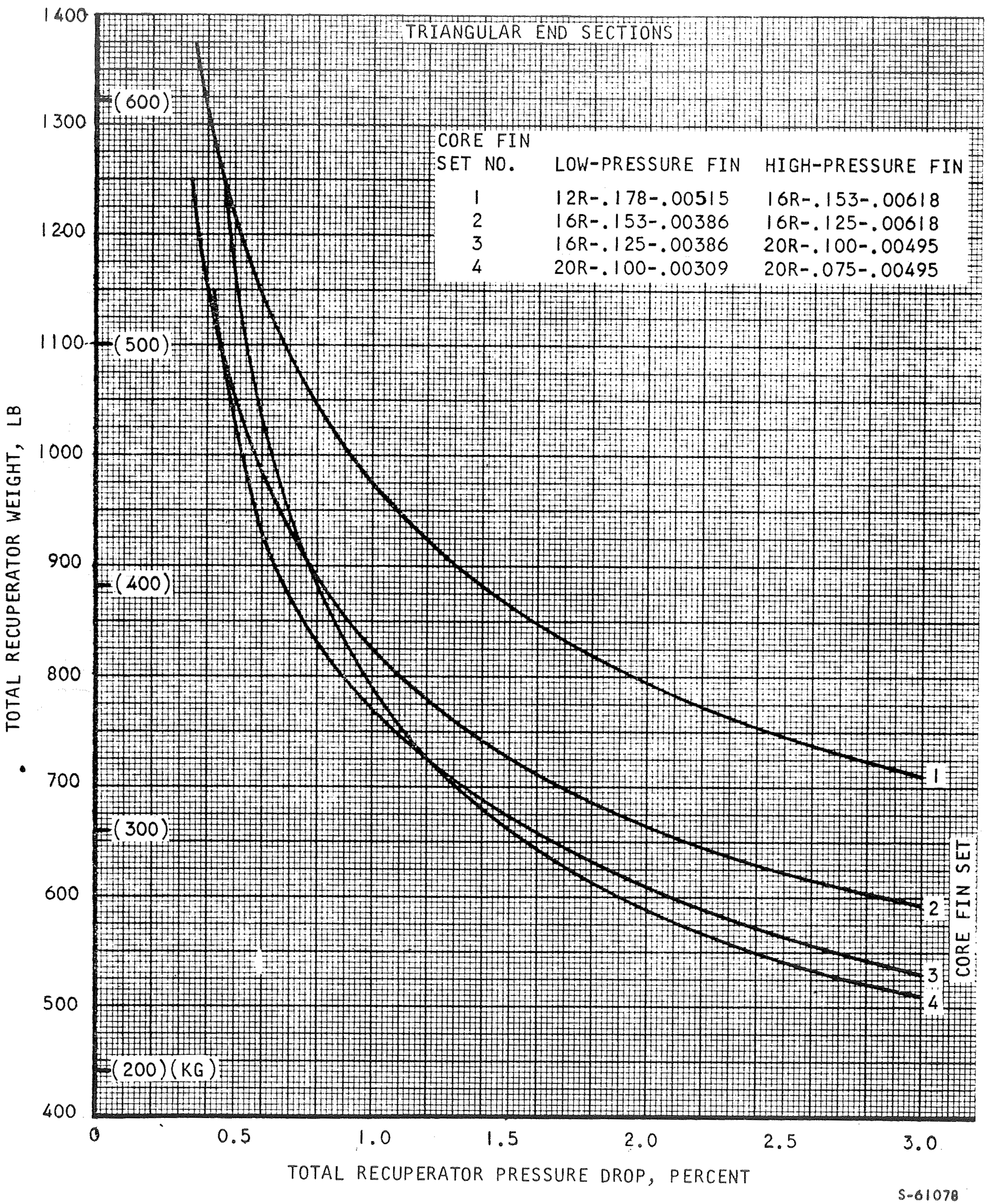

Figure 3-10. Variation of Total Weight with Total Pressure Drop for Case I Recuperator, Minimum-Weight Curves

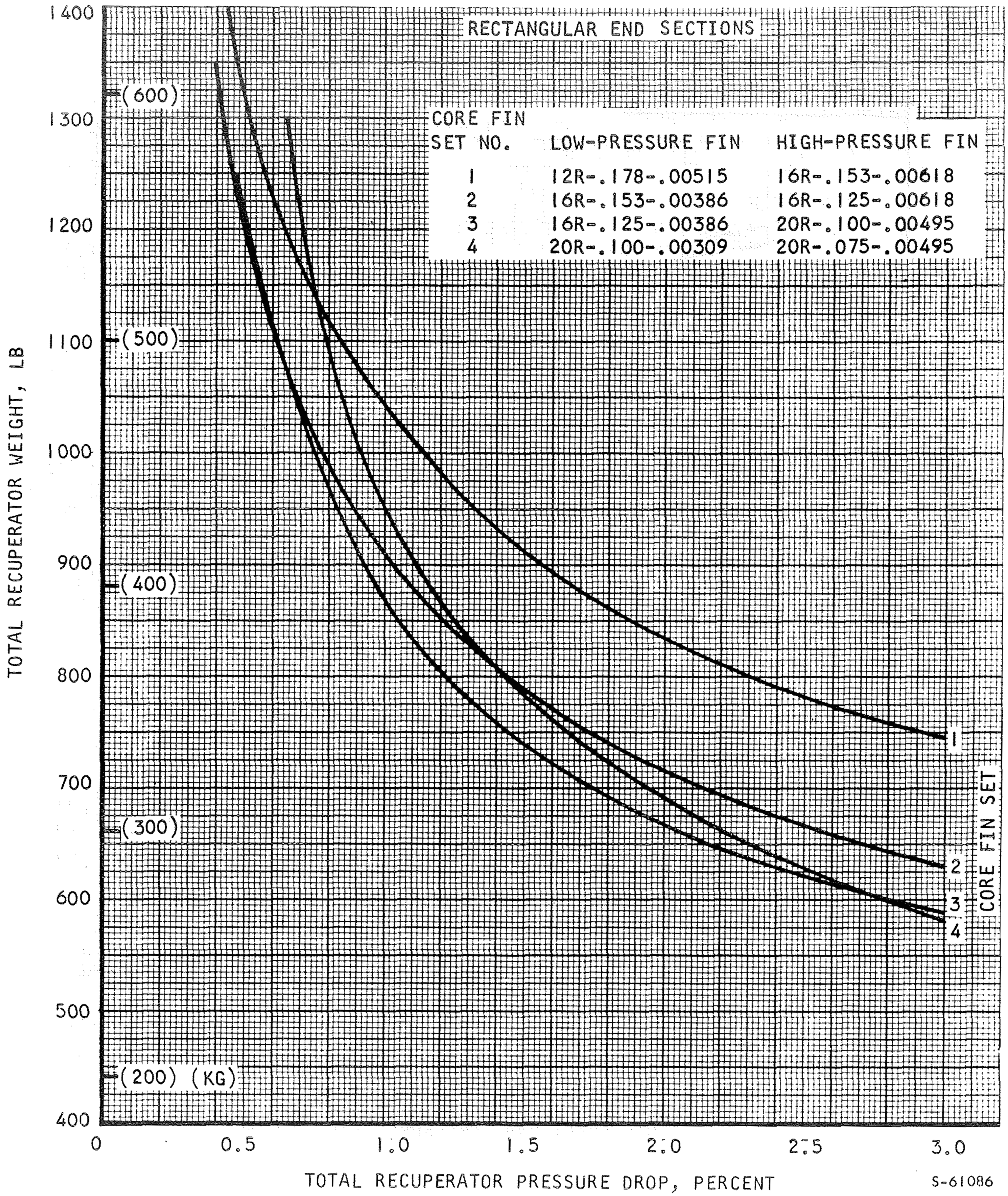

Figure 3-11. Variation of Total Weight with Total Pressure Drop for Case I Recuperator, Minimum-Weight Curves

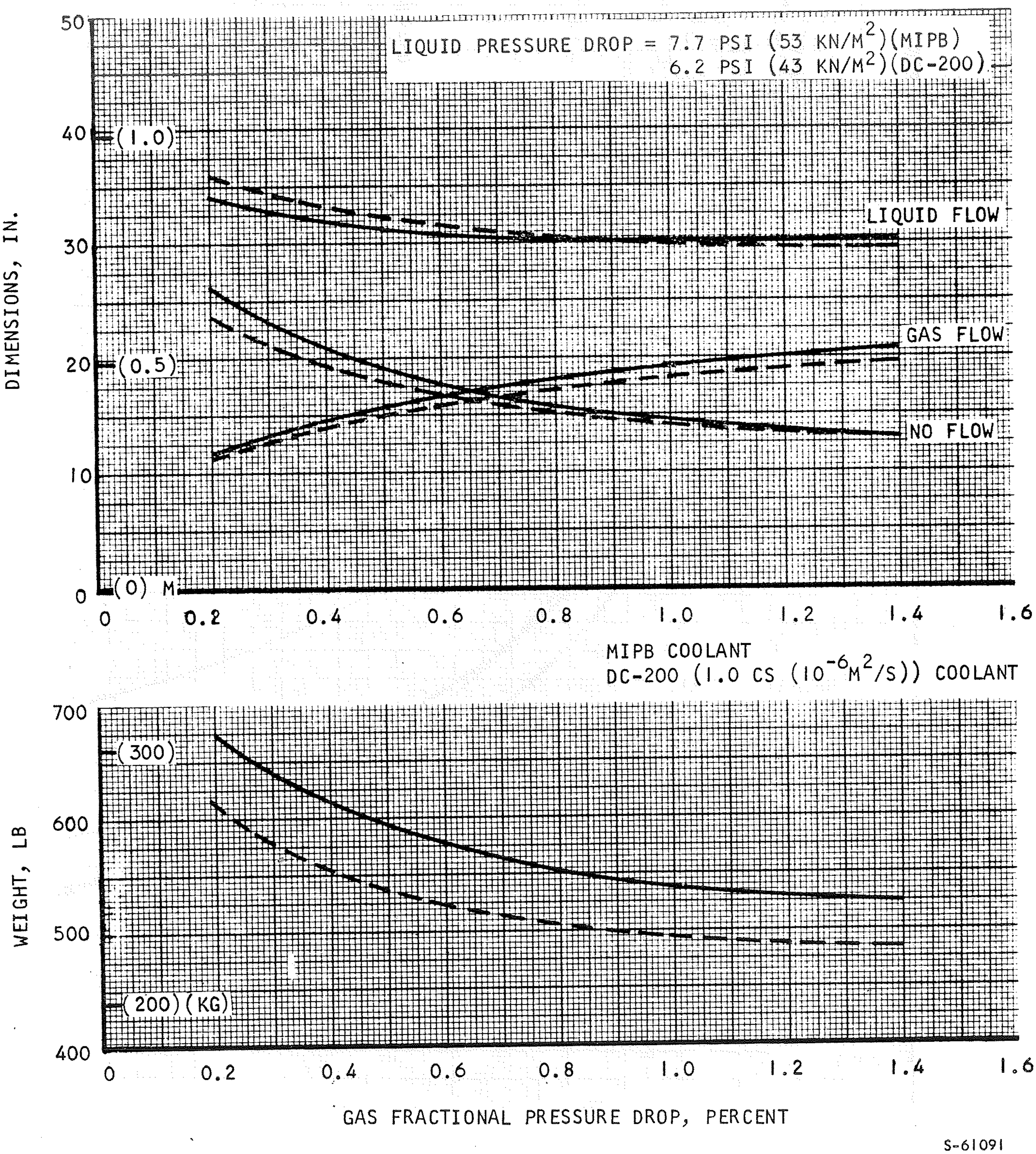

Figure 3-12. Variation of Size and Weight with Gas Pressure Drop for Case I Waste Heat Exchanger

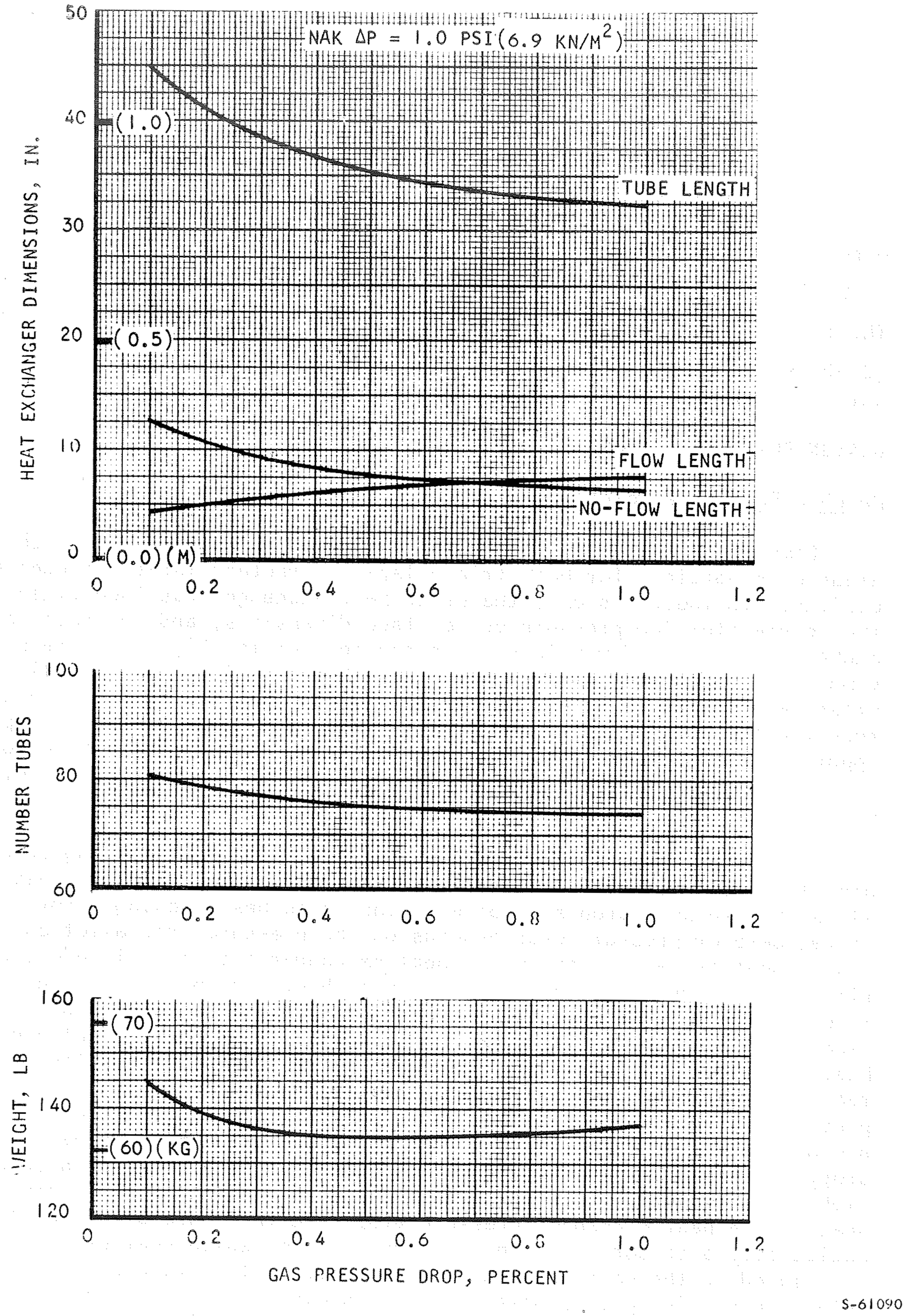

Figure 3-13. Case I Heat Source Heat Exchanger

Fin diameter = 1.5 x (tube OD)

Fins per inch = 30 (fins per meter = 1180)

Staggered tubes

Other characteristics of the core matrix used here are a tube wall thickness of 0.020 in. (5.08×10^{-4}m) and a fin thickness of 0.005 in. (1.27×10^{-4}m). The fin consists of 0.003 in. (0.762×10^{-4}m) of copper clad with 0.002 in. (0.508×10^{-4}m) stainless steel. The tube material is Haynes 25. The overall flow configuration is two-pass cross-counterflow.

DESIGN POINT SELECTION

Matched Face Area Solutions

Complete HXDA system configurations based on matched heat exchanger face areas were obtained for both triangular- and rectangular-end recuperator designs. In these systems, the waste heat exchanger gas face dimensions match the recuperator low-pressure outlet face dimensions, and the heat source heat exchanger gas face dimensions match the recuperator high-pressure outlet face dimensions as closely as possible. For these studies, the overall HXDA gas pressure drop was fixed at 3.0 percent, and a pressure drop of 0.5 percent was reserved for the manifolds and ducts. Thus, the total pressure drop to be apportioned among the three heat exchangers is 2.5 percent. Based on Figures 3-10 and 3-11, the recuperator design utilized in the analysis incorporates core fin set 3.

Figure 3-14 shows the face areas of the waste heat exchanger and recuperator low-pressure outlet plotted as a function of recuperator pressure drop. Since the pressure drop available to the waste heat exchanger for a given value of recuperator pressure drop depends on the pressure drop allotted to the heat source heat exchanger, the waste heat exchanger face area is plotted parametrically for several values of heat source heat exchanger pressure drop. Each intersection between a waste heat exchanger face area curve and a recuperator face area curve represents a design point for the specified value of heat source heat exchanger pressure drop. Since only one such value results in an exact face area match between heat source heat exchanger and the recuperator high-pressure outlet, a unique solution is defined in which both face area matches are obtained. To determine the required heat source heat exchanger pressure drop, recuperator low-pressure outlet face area is plotted as a function of high-pressure outlet face area, as shown in Figure 3-15. For each value of heat source heat exchanger pressure drop used in Figure 3-14, the low-pressure outlet face area corresponding to a recuperator/waste heat exchanger match can be related to the corresponding high-pressure outlet face area through Figure 3-15. Successive points obtained in this manner result in the curve of recuperator high-pressure outlet face area plotted as a function of heat source heat exchanger pressure drop in Figure 3-16. Each point on the recuperator curve in this figure corresponds to a face area match between recuperator low-pressure outlet and waste heat exchanger. The intersection between the

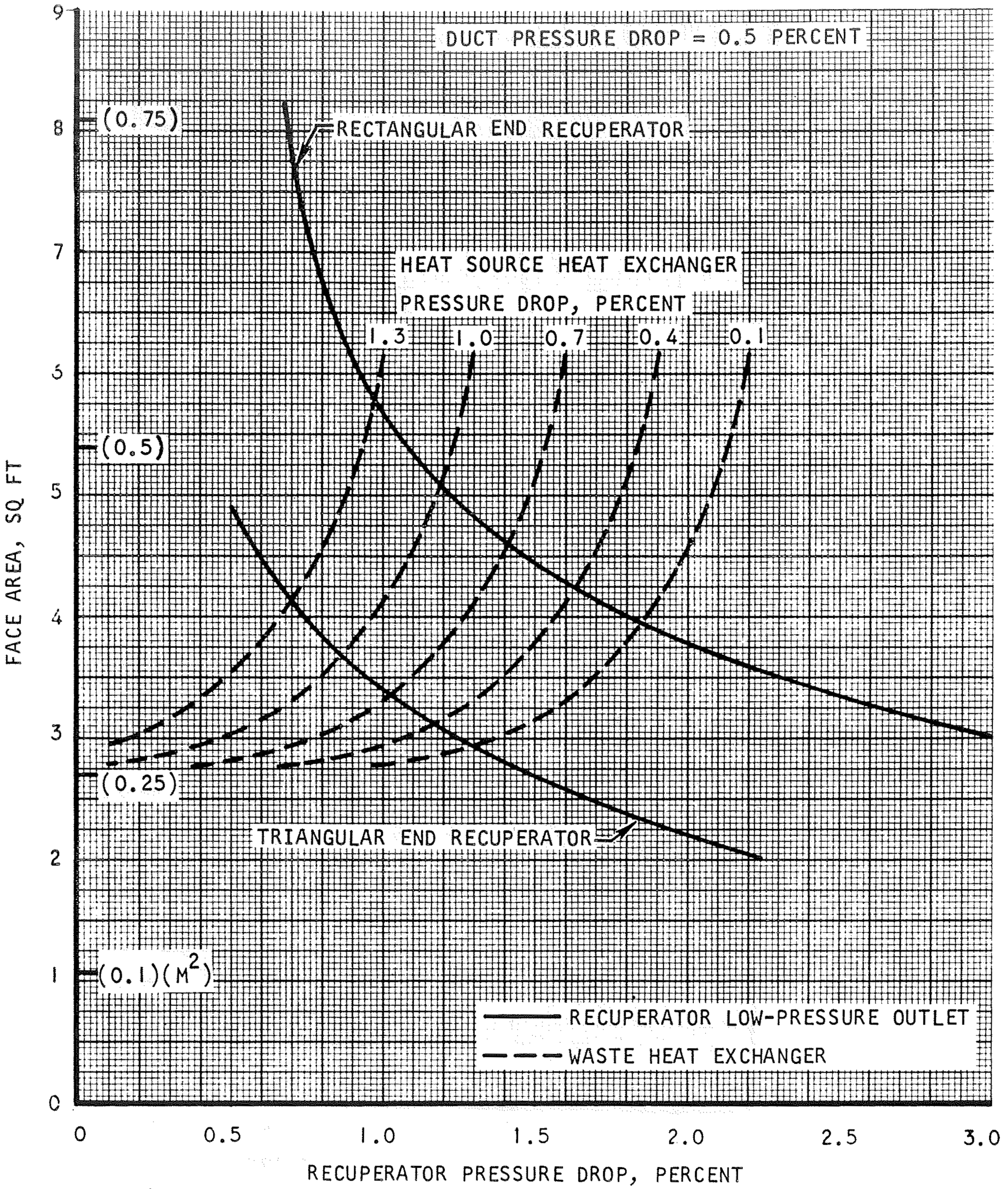

Figure 3-14. Recuperator and Waste Heat Exchanger Face Areas for Case I

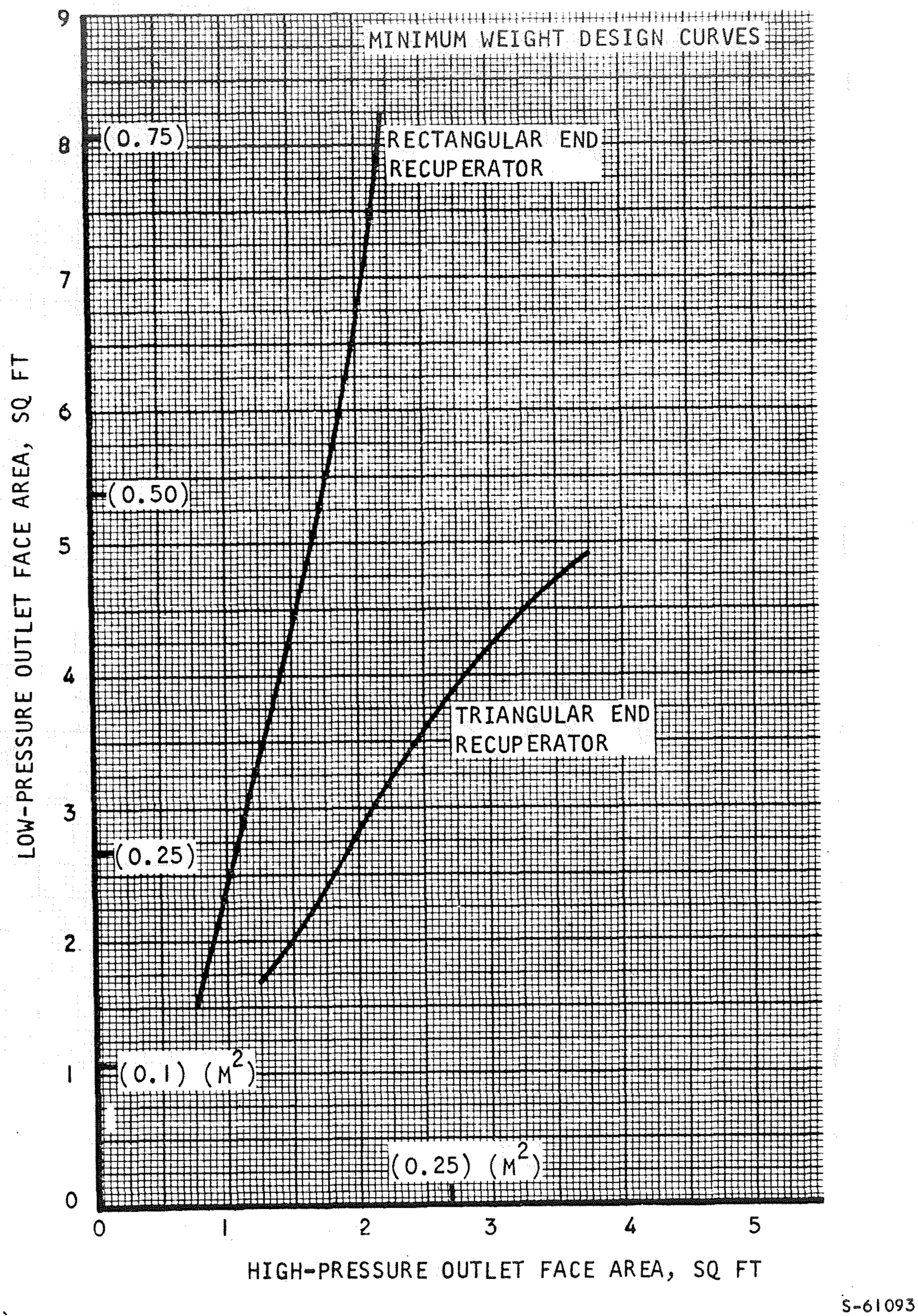

Figure 3-15. Variation of Recuperator Face Areas for Case I

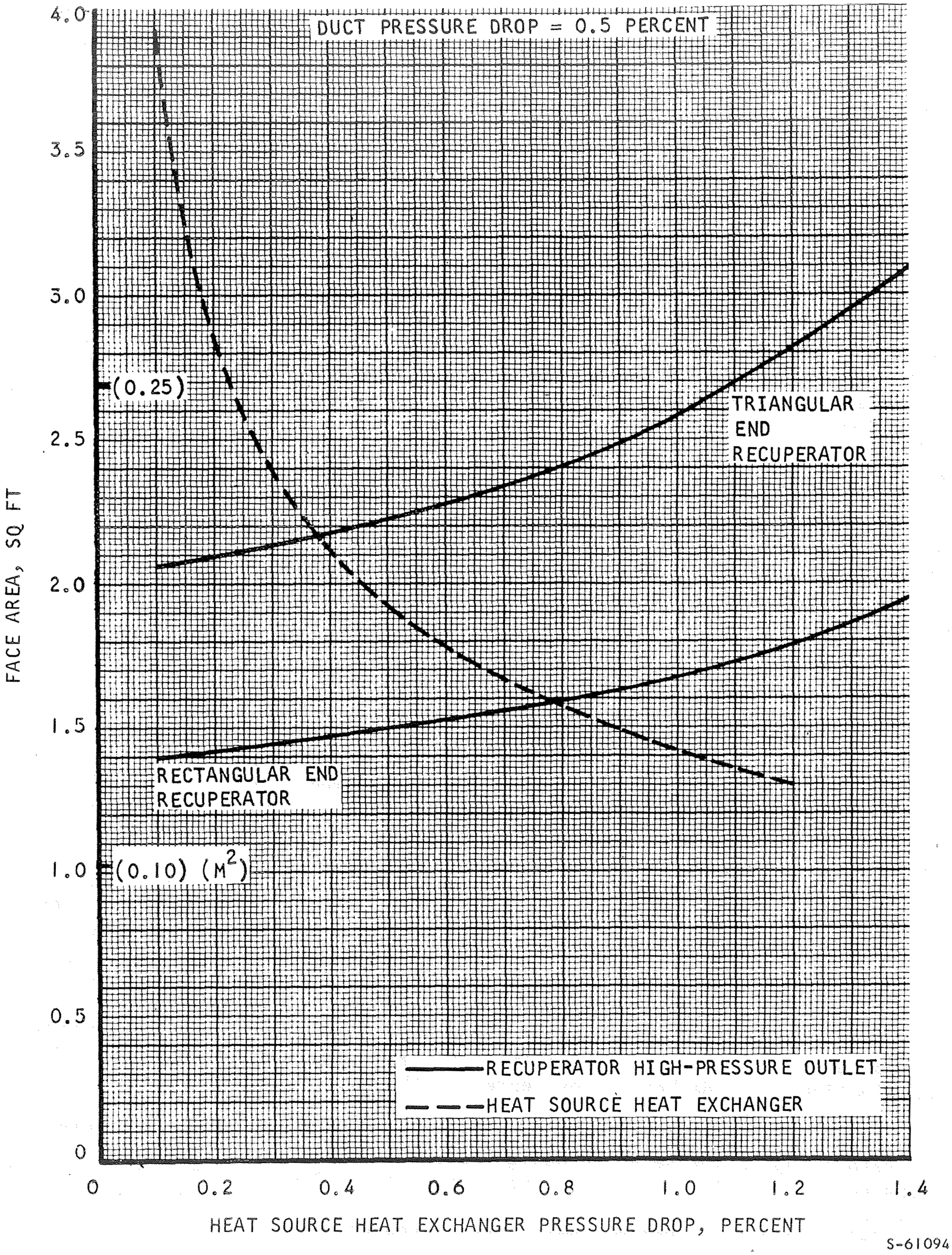

Figure 3-16. Recuperator and Heat Source Heat Exchanger Face Areas for Case I

heat source heat exchanger and recuperator face area curves of Figure 3-16 represents a unique solution in which the two face area matches are obtained coincidentally. Since the above procedure was implemented for both rectangular- and triangular-end recuperator designs, two distinct system design points are obtained.

The HXDA system configuration based on a triangular-end recuperator is summarized in Table 3-3, and the configuration incorporating a rectangular-end recuperator is summarized in Table 3-4. Comparison of the gas pressure drop allocations in Tables 3-3 and 3-4 with those established during the Task 3 design studies indicates that the effect of face area matching is to increase heat source heat exchanger and/or waste heat exchanger pressure drop at the expense of recuperator pressure drop. Dimensional matching of the three exchangers also requires adjustments to the liquid pressure drops in the heat source and waste heat exchangers to obtain the correct liquid-flow and no-flow dimensions.

Minimum Weight Solutions

Solutions were obtained for minimum-weight system configurations utilizing both triangular-end and rectangular-end recuperator designs. In these solutions, the pressure drop allocations to recuperator, recuperator end sections, heat source heat exchanger, and waste heat exchanger were optimized to obtain minimum total heat exchanger weight without regard to the degree of face area mismatch between recuperator and adjoining heat exchangers. The recuperator weight variation used for this optimization is based on the minimum of the applicable weight curves, i.e., fin sets 2, 3, and 4 over the appropriate gas pressure drop ranges in Figures 3-10 and 3-11.

The optimization curves for these two cases are shown in Figures 3-17 through 3-20. In Figures 3-17 and 3-19, the optimum pressure drop split between recuperator and waste heat exchanger is determined as a function of total pressure drop allocated to these two components. The solid curves in these figures represent the variation of total weight with total gas pressure drop for the two heat exchangers at fixed values of the waste heat exchanger pressure drop. The dashed curves represent the loci of minimum-weight designs. Using the dashed curves of Figures 3-17 and 3-19 to represent the weight variation of the recuperator/waste heat exchanger combination, the optimum pressure drop allocation among all three heat exchangers is obtained in Figures 3-18 and 3-20. The solid curves in these figures represent the variations of total heat exchanger weight with total gas pressure drop in the three heat exchangers for fixed values of pressure drop in the optimized recuperator/waste heat exchanger combination. The dashed curves represent the loci of selected system designs.

From Figures 3-18 and 3-20, the heat source heat exchanger pressure drop corresponding to the selected design curve is in all cases the minimum value considered, or 0.10 percent. Using a value of 0.10 percent for the heat source heat exchanger, and reserving 0.50 percent for manifolds and ducts, Figures 3-17 and 3-19 indicate an optimum waste heat exchanger pressure drop of 0.5 percent for both systems.

TABLE 3-3

CASE I HXDA
TRIANGULAR-END RECUPERATOR
MATCHED FACE AREA SOLUTION

Recuperator	
Gas pressure drop	1.18 percent
Weight	732 lb (332 kg)
Core length	13.8 in. (0.351 m)
End section height, hot end	4.9 in. (0.124 m)
cold end	3.2 in. (0.0813 m)
End section ratio, hot end	0.65
cold end	0.59
Width	19.0 in. (0.483 m)
Stack height	37.9 in. (0.963 m)
Waste Heat Exchanger	
Gas pressure drop	0.94 percent
Weight	543 lb (246 kg)
Liquid pressure drop	13.5 psi (9.3 kN/m^2)
Gas-flow length	19.0 in. (0.483 m)
Liquid-flow length	37.9 in. (0.963 m)
Stack height	11.8 in. (0.300 m)
Heat Source Heat Exchanger	
Gas pressure drop	0.38 percent
Weight	135 lb (61 kg)
Liquid pressure drop	1 psi (7 kN/m^2)
Gas-flow length	6.0 in. (0.152 m)
Tube length	37.7 in. (0.958 m)
No-flow length	8.9 in. (0.226 m)
Number of tubes	75
Number of tube rows	10
Number of passes	2

TABLE 3-4

CASE I HXDA
RECTANGULAR-END RECUPERATOR
MATCHED FACE AREA SOLUTION

Recuperator	
Gas pressure drop	1.35 percent
Weight	772 lb (351 kg)
Core average length	14.3 in. (0.363 m)
End section height, hot end	6.3 in. (0.160 m)
cold end	5.1 in. (0.130 m)
Total length	20.0 in. (0.509 m)
Width	18.4 in. (0.467 m)
Stack height	36.8 in. (0.935 m)
Waste Heat Exchanger	
Gas pressure drop	0.37 percent
Weight	623 lb (283 kg)
Liquid pressure drop	10.9 psi (75.1 kN/m^2)
Gas-flow length	14.2 in. (0.361 m)
Liquid-flow length	36.9 in. (0.937 m)
Stack height	18.6 in. (0.472 m)
Heat Source Heat Exchanger	
Gas pressure drop	0.78 percent
Weight	136 lb (61.8 kg)
Liquid pressure drop	1.3 psi (8.96 kN/m^2)
Gas-flow length	7.2 in. (0.183 m)
Tube length	37.3 in. (0.947 m)
No-flow length	6.6 in. (0.168 m)
Number of tubes	66
Number of tube rows	12
Number of passes	2

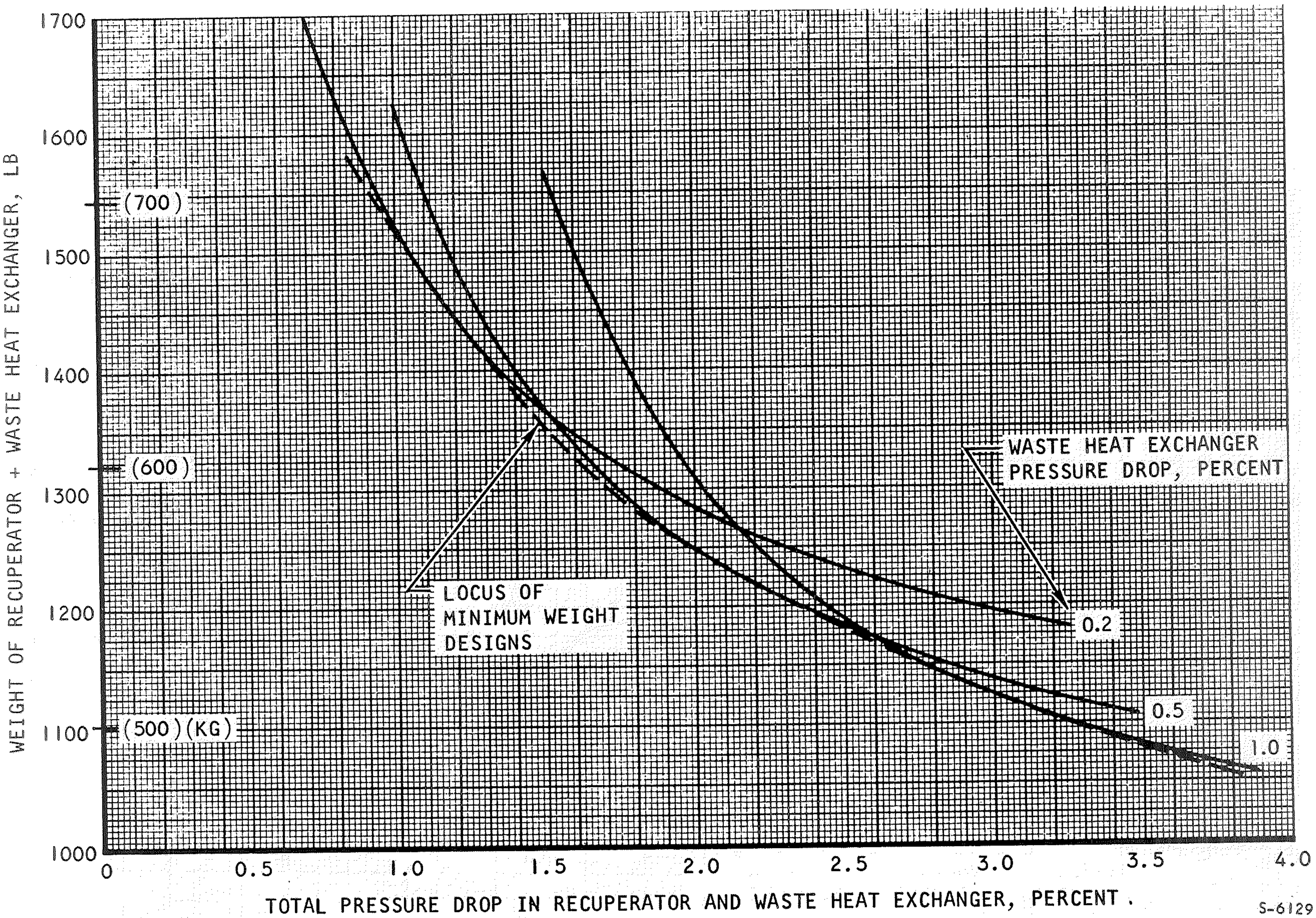

Figure 3-17. Waste Heat Exchanger/Recuperator Optimization for Case I with Triangular-End Recuperator

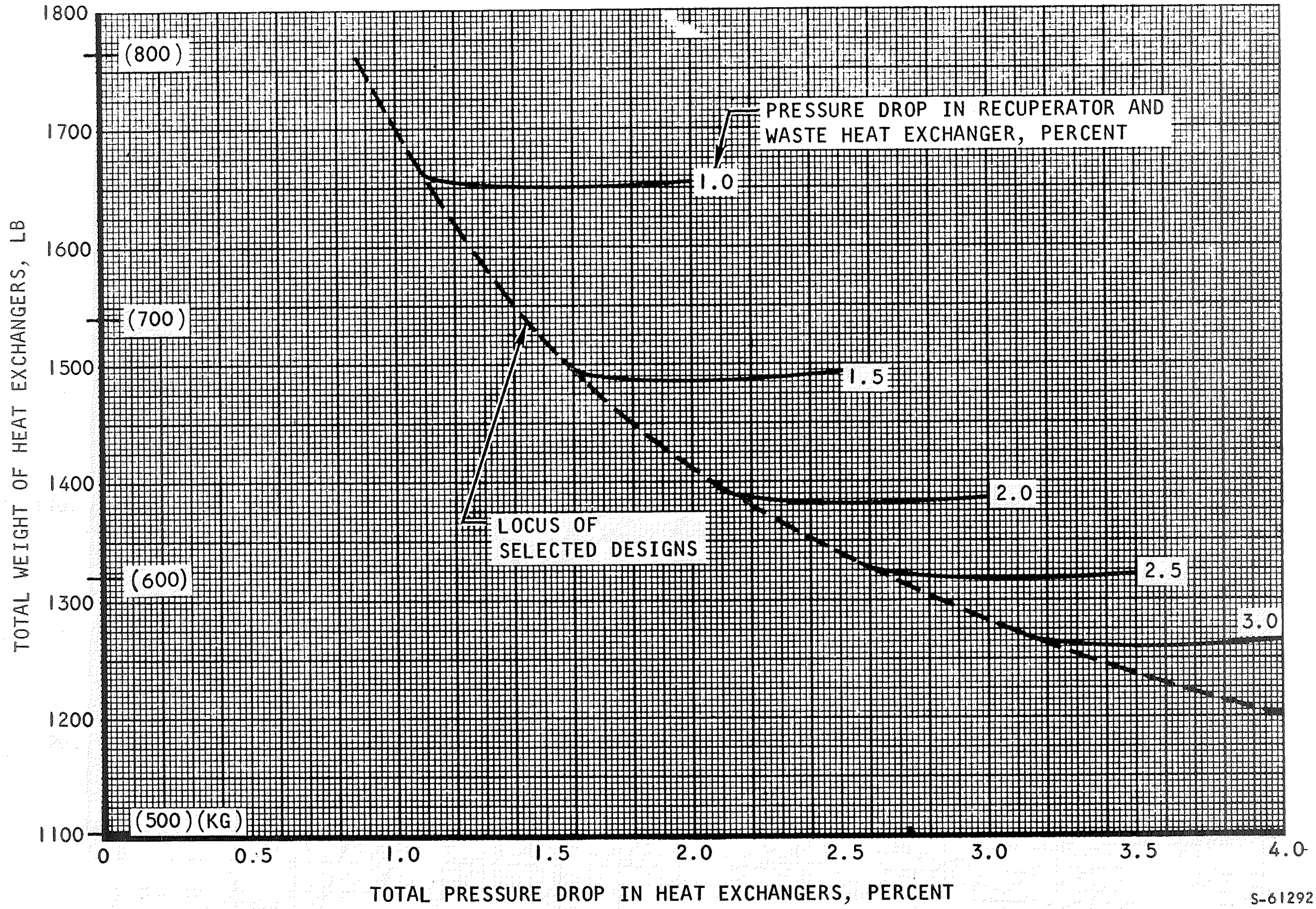

Figure 3-18. System Optimization for Case I with Triangular-End Recuperator

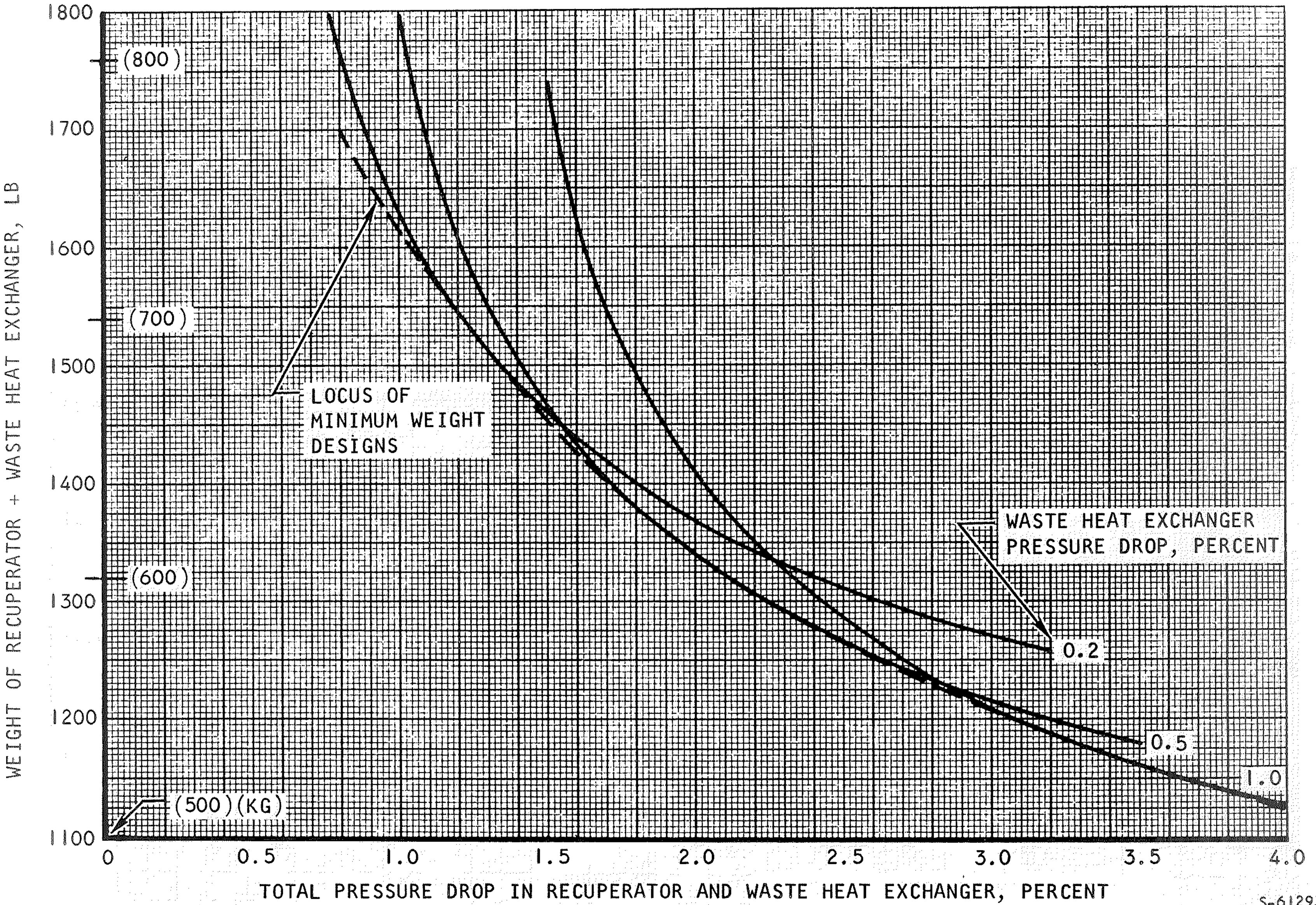

Figure 3-19. Waste Heat Exchanger/Recuperator Optimization for Case I with Rectangular-End Recuperator

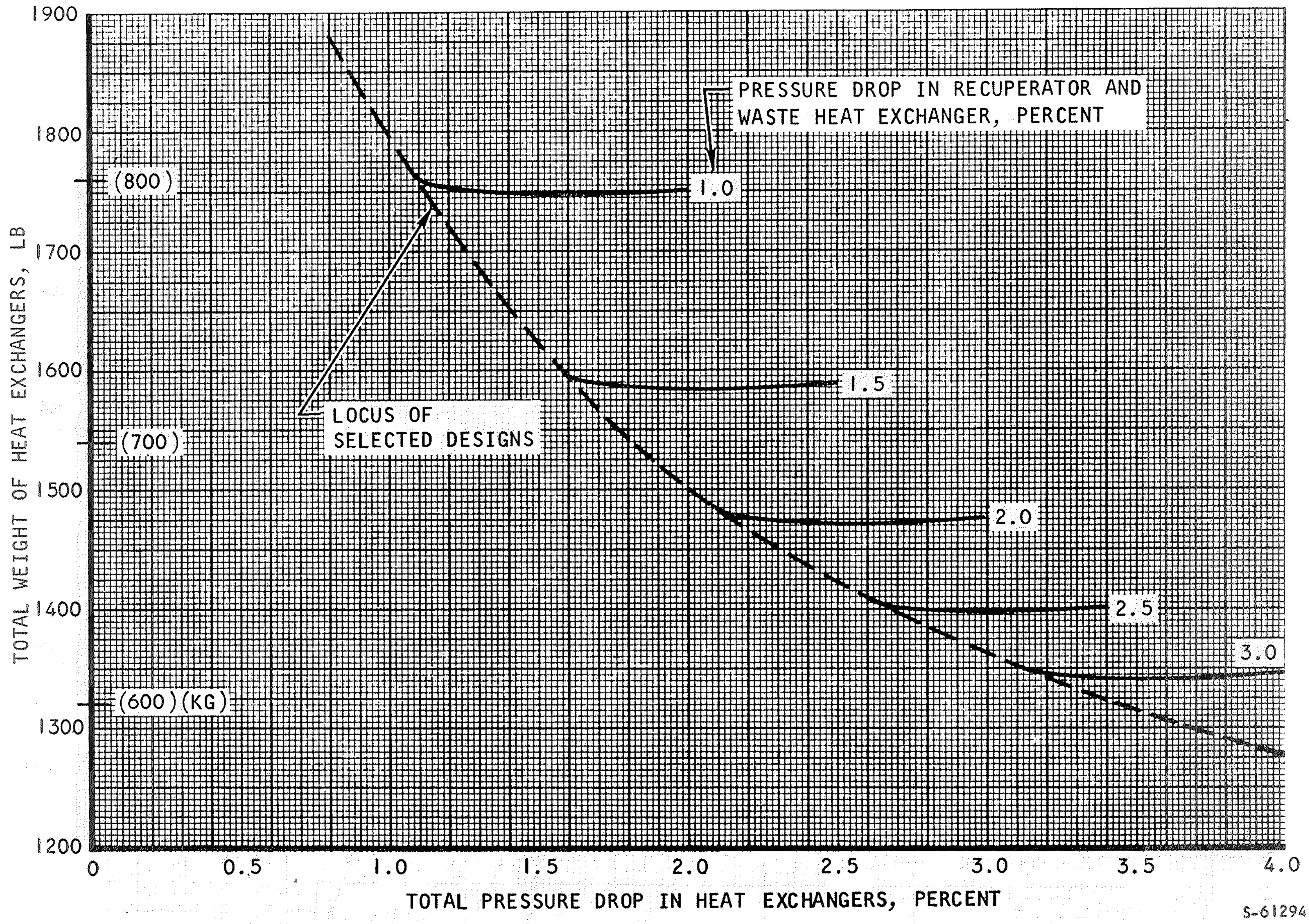

Figure 3-20. System Optimization for Case I with Rectangular-End Recuperator

Based on these pressure drop allocations, the heat exchanger designs for the two minimum-weight systems are summarized in Tables 3-5 and 3-6. Total heat exchanger weight for the triangular-end recuperator system is 1340 lb (609 kg), and total weight for the rectangular-end recuperator system is 1421 lb (646 kg). In both system designs, the heat source heat exchanger tube length and the waste heat exchanger liquid flow length have been set approximately equal to the recuperator stack height, which limits the mismatch in face areas between these components to one dimension only. The liquid pressure drops of Tables 3-5 and 3-6 reflect these adjustments to the heat source heat exchanger and waste heat exchanger dimensions.

PACKAGING

Package Configuration

A number of HXDA packaging arrangements were studied for the Case I matched-area systems. The major features looked for in the overall layout were (1) minimum size of the HXDA/TAC package, (2) minimum number and severity of gas ducting bends, and (3) favorable gas flow paths at the HXDA and TAC inlets. In addition, three bellows arranged in two different alignments are required in each duct to completely accommodate differential thermal expansions between HXDA and TAC. For uniform flow distribution in the recuperator core, gas velocities at the high- and low-pressure recuperator inlets should be parallel to the inlet faces. The parallel flow direction, in conjunction with tapered flow areas in the manifolds, provides constant static pressure profiles along the inlet manifolds.

The selected packaging configurations are shown in Drawing SK51802. Overall dimensions of the HXDA/TAC package are essentially independent of the type of recuperator (triangular-end or rectangular-end) used in the system. The total of gas ducting bends is also virtually equal for the two systems. At a constant pressure loss of 0.5 percent for the ducts and manifolds, slightly larger ducting is required for the rectangular-end recuperator system, due primarly to a high expansion loss associated with the large recuperator low-pressure inlet manifold. The individual heat exchangers that comprise the triangular-end recuperator system are shown in Drawings SK51812, SK51813, and SK51814.

Ducting

Gas duct and manifold sizes were calculated for both the triangular-end and rectangular-end recuperator systems, based on the packaging configurations of Drawing SK51802. With two exceptions, the manifolds are all full-radius manifolds, with sizes thus dependent on heat exchanger core dimensions. Diameters of the recuperator high-pressure inlet manifold and heat source heat exchanger outlet manifold in the rectangular-end recuperator system were set equal to the connecting duct diameters, and are thus sized slightly larger than full-radius. Individual duct sizes were established to maintain a constant gas velocity head in all four ducts while meeting the manifold/ducting pressure drop allocation of 0.5 percent. The major losses comprising the total manifold/ducting pressure drop are (1) the duct bend losses, (2) losses due to area change between ducts and manifolds, and (3) losses associated with flow turning and area change between manifolds and heat exchanger cores.

TABLE 3-5

CASE I HXDA
TRIANGULAR-END RECUPERATOR
MINIMUM-WEIGHT SOLUTION

Recuperator	
Gas pressure drop	1.9 percent
Weight	600 lb (272 kg)
Core length	12.9 in. (0.328 m)
End section height, hot end	5.3 in. (0.135 m)
cold end	3.3 in. (0.0839 m)
End section ratio, hot end	0.65
cold end	0.55
Width	16.9 in. (0.429 m)
Stack height	33.7 in. (0.856 m)
Waste Heat Exchanger	
Gas pressure drop	0.5 percent
Weight	595 lb (270 kg)
Liquid pressure drop	9.4 psi (64.9 kN/m^2)
Gas-flow length	15.6 in. (0.396 m)
Liquid-flow length	33.7 in. (0.856 m)
Stack height	17.6 in. (0.447 m)
Heat Source Heat Exchanger	
Gas pressure drop	0.1 percent
Weight	145 lb (65.9 kg)
Liquid pressure drop	0.5 psi (3.45 kN/m^2)
Gas-flow length	4.4 in. (0.112 m)
Tube length	33.6 in. (0.854 m)
No-flow length	18.3 in. (0.465 m)
Number of tubes	108
Number of tube rows	7
Number of passes	2

TABLE 3-6

CASE I HXDA
RECTANGULAR-END RECUPERATOR
MINIMUM-WEIGHT SOLUTION

Recuperator	
Gas pressure drop	1.9 percent
Weight	681 lb (309 kg)
Core length	15.8 in. (0.401 m)
End section height, hot end	6.0 in. (0.152 m)
cold end	4.8 in. (0.122 m)
Total length	21.2 in. (0.539 m)
Width	17.2 in. (0.437 m)
Stack height	34.3 in. (0.871 m)
Waste Heat Exchanger	
Gas pressure drop	0.5 percent
Weight	595 lb (270 kg)
Liquid pressure drop	9.8 psi (67.6 kN/m^2)
Gas-flow length	15.6 in. (0.396 m)
Liquid-flow length	34.3 in. (0.871 m)
Stack height	17.3 in. (0.440 m)
Heat Source Heat Exchanger	
Gas pressure drop	0.1 percent
Weight	145 lb (65.9 kg)
Liquid pressure drop	0.5 psi (3.45 kN/m^2)
Gas-flow length	4.4 in. (0.112 m)
Tube length	34.4 in. (0.874 m)
No-flow length	17.8 in. (0.452 m)
Number of tubes	105
Number of tube rows	7
Number of passes	2

PRECEDING PAGE BLANK NOT FILMED

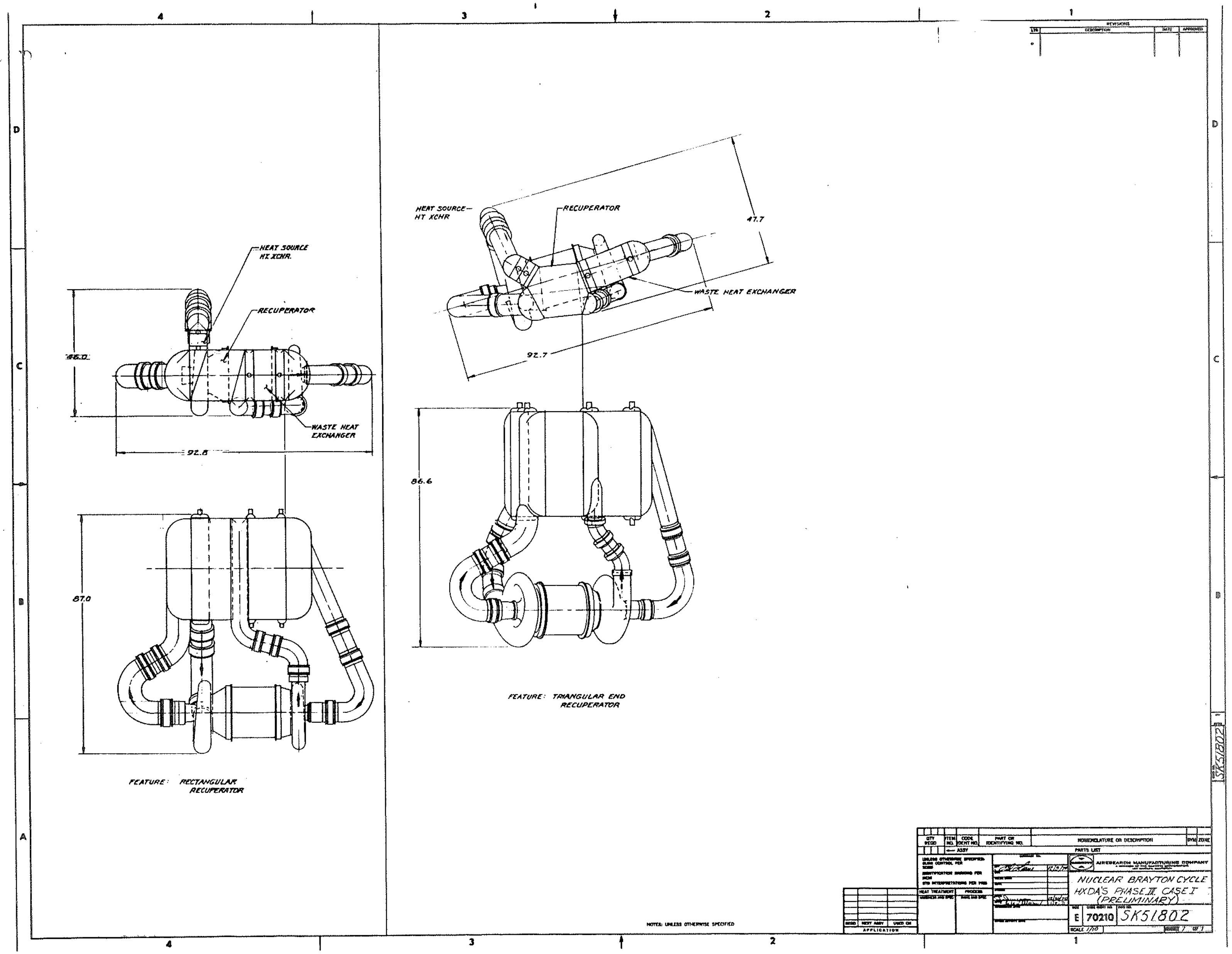

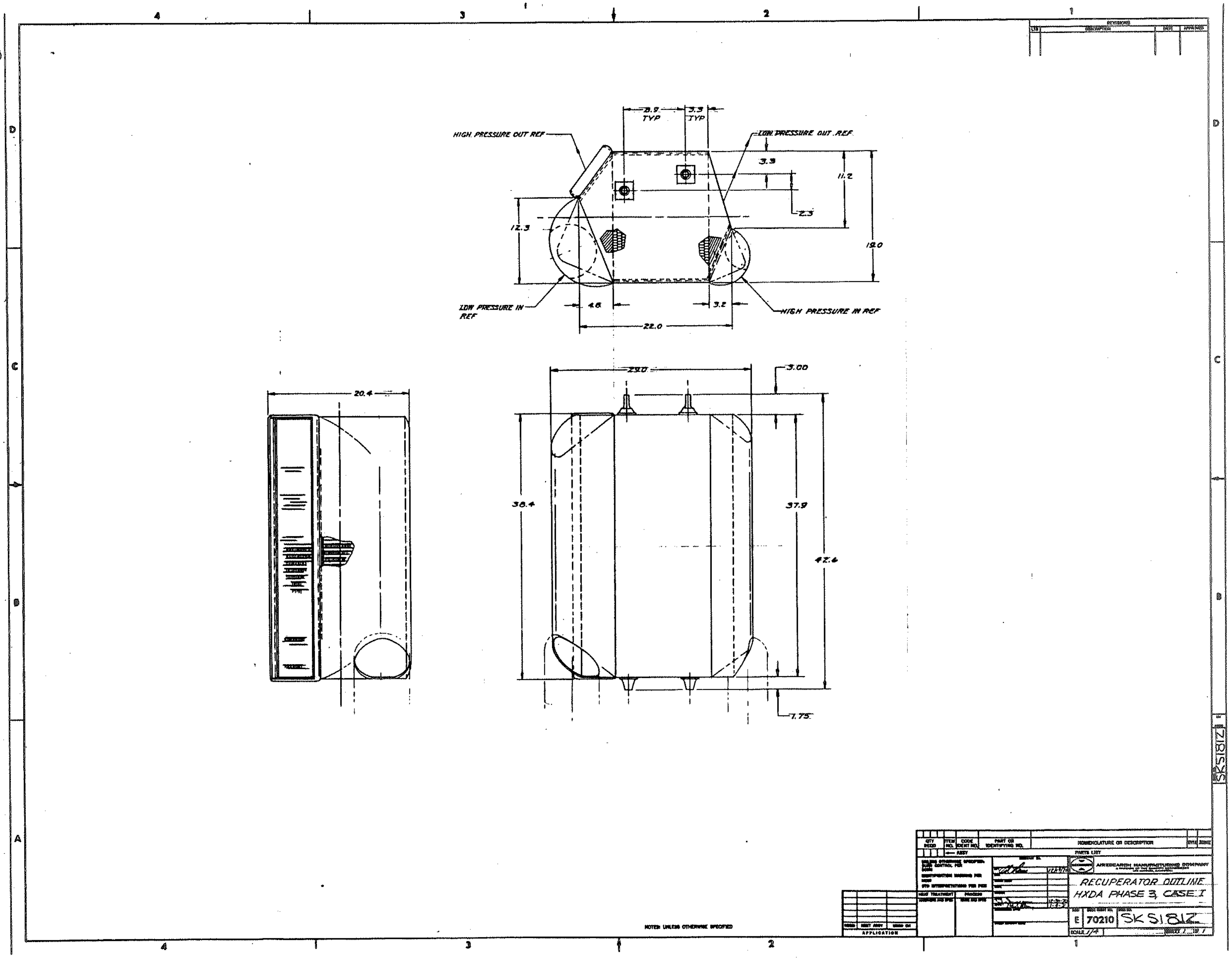
HIGH PRESSURE OUT REF
LOW PRESSURE OUT REF
LOW PRESSURE IN REF
HIGH PRESSURE IN REF
8.9 TYP
3.3 TYP
3.3
2.3
11.2
19.0
12.3
4.6
3.2
22.0
29.0
3.00
20.4
38.4
37.9
42.6
1.75
NOTES: UNLESS OTHERWISE SPECIFIED
RECUPERATOR OUTLINE
HXDA PHASE 3, CASE I
E 70210 SK 51812
SK51812

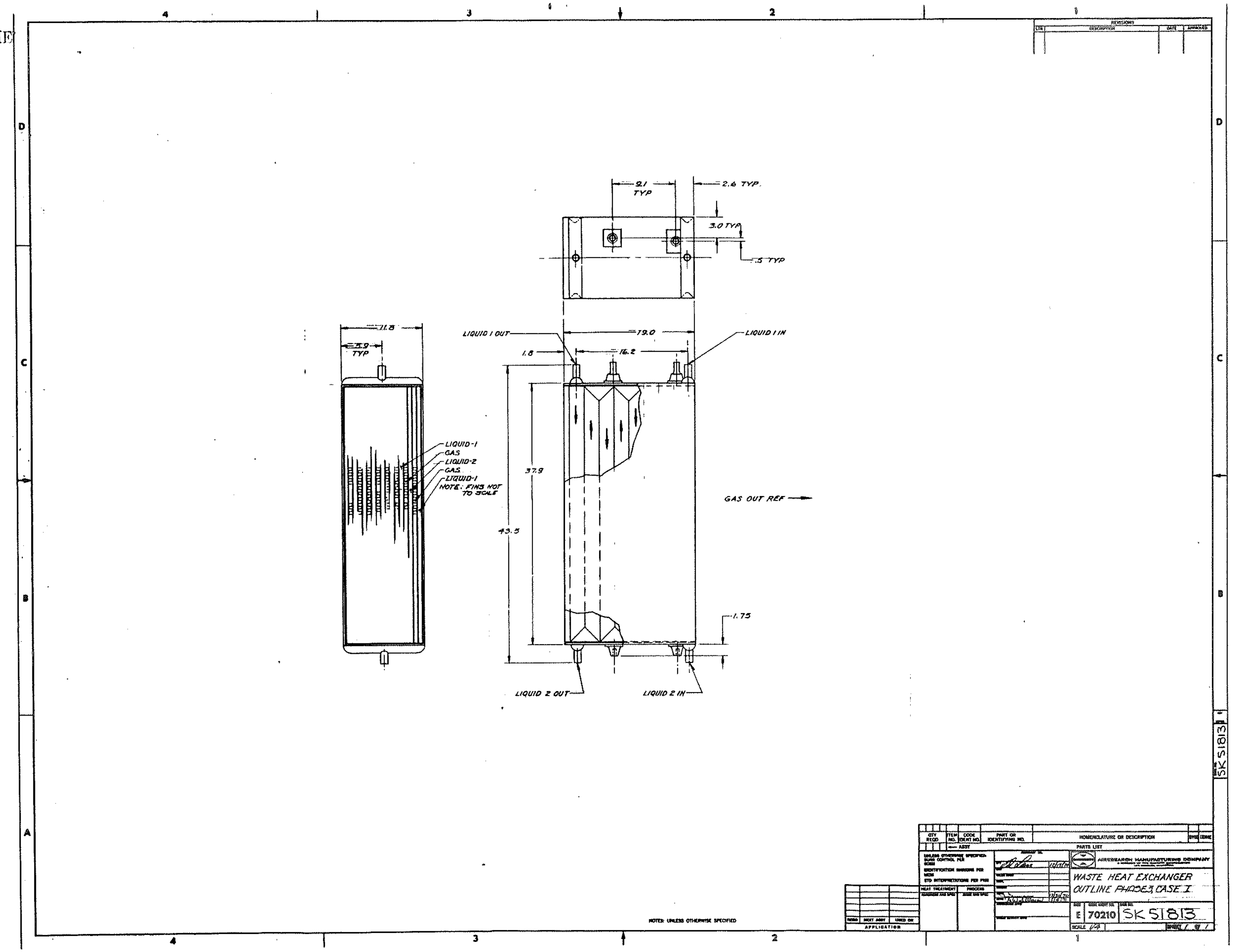

11.8
3.9 TYP
LIQUID-1
GAS
LIQUID-2
GAS
LIQUID-1
NOTE: FINS NOT TO SCALE
9.1 TYP
2.6 TYP.
3.0 TYP
.5 TYP
LIQUID 1 OUT
19.0
LIQUID 1 IN
1.8
16.2
37.9
43.5
GAS OUT REF
1.75
LIQUID 2 OUT
LIQUID 2 IN
NOTES: UNLESS OTHERWISE SPECIFIED
AIRESEARCH MANUFACTURING COMPANY
WASTE HEAT EXCHANGER
OUTLINE PHASE 3 CASE I
E 70210 SK 51813
SK 51813
APPLICATION
PARTS LIST

PRECEDING PAGE BLANK NOT FILMED

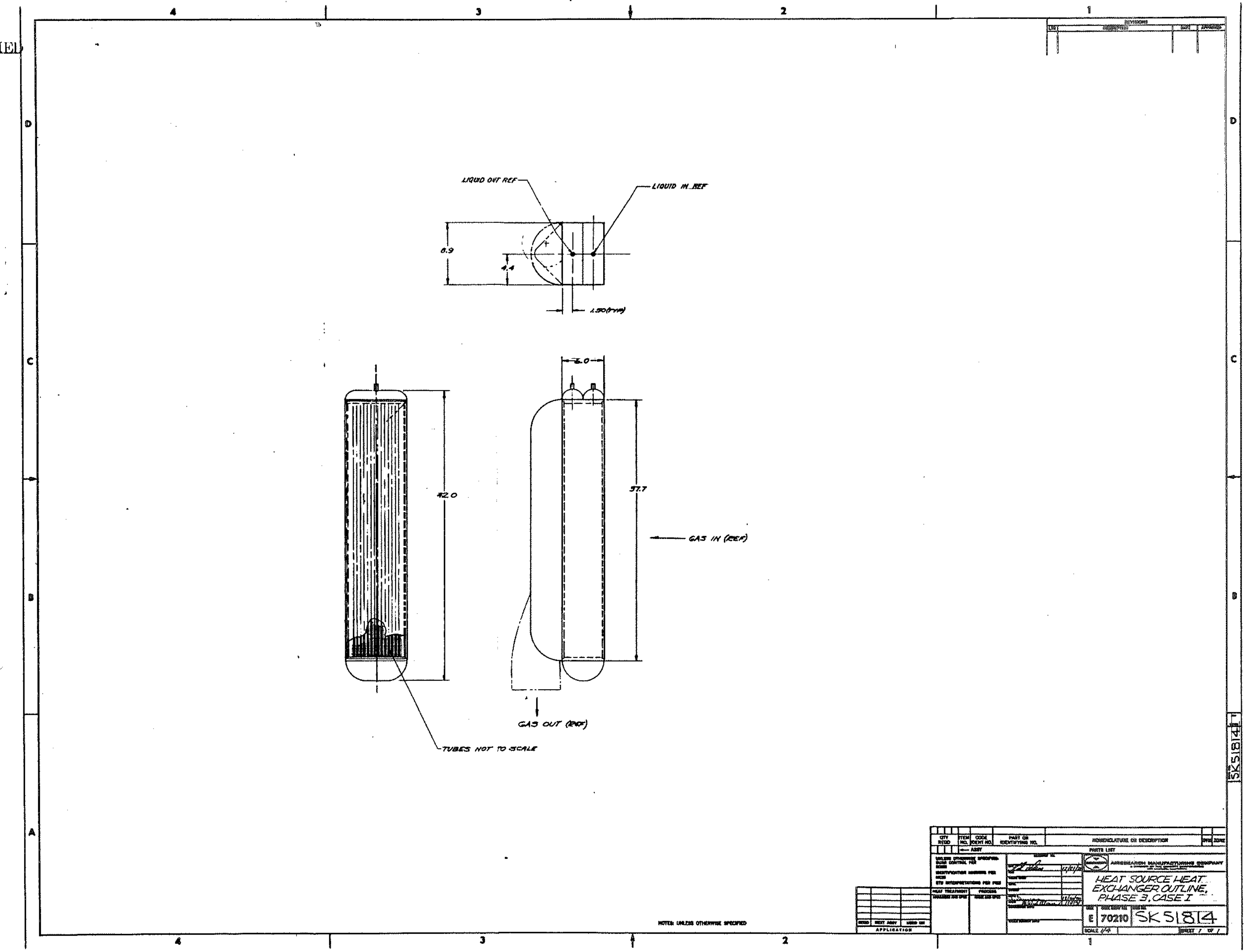

FOLDOUT FRAME 1

AIRESEARCH MANUFACTURING COMPANY
Los Angeles, California

FOLDOUT FRAME 2

PRECEDING PAGE BLANK NOT FILMED

Listed in Table 3-7 are manifold and duct sizes and weights. Ducting material is Hastelloy X for all manifolds and ducts, with the exception of the heat source heat exchanger outlet manifold and turbine inlet duct, which are constructed of Haynes 25. Wall thicknesses are based on structural pressure (Table 3-1), with a minimum allowable thickness of 0.032 in. (8.1×10^{-4}m). Total weights for the ducting system are 147 lb (66.8 kg) for the triangular-end recuperator case and 203 lb (92.2 kg) for the rectangular-end recuperator case.

Frame

Design of a mounting frame for the HXDA is discussed in Section 6. The overall HXDA system is shown with mounting frame attached in Drawing SK51811. Estimated weight of the frame is 120 lb (54 kg).

SYSTEMS COMPARISON

A summary of the four HXDA designs obtained for Case I is presented in Table 3-8. The penalty incurred by matching heat exchanger faces is 70 lb (31.8 kg) in total heat exchanger weight for the system with the triangular-end recuperator and 110 lb (50.0 kg) in total heat exchanger weight for the rectangular-end case. Weights associated with structural reinforcement of the connecting ducts or transition sections required for nonmatched heat exchangers would reduce or reverse this weight penalty.

The triangular-end recuperator configuration is 177 lb (80.5 kg) lighter in total HXDA weight than the rectangular-end recuperator configuration. For this reason, the triangular-end recuperator is preferred for the HXDA Case I design.

TABLE 3-7

CASE I DUCTS AND MANIFOLDS

Item		Triangular-End Recuperator System			Rectangular-End Recuperator System		
		Diameter, in. (m)	Wall Thickness, in. ($m \times 10^4$)	Weight, lb (kg)	Diameter, in. (m)	Wall Thickness, in. ($m \times 10^4$)	Weight, lb (kg)
Duct	Compressor outlet	5.85 (0.149)	0.032 (8.1)	5 (2)	6.50 (0.165)	0.032 (8.1)	6 (3)
	Turbine inlet	7.00 (0.178)	0.111 (28.2)	39 (18)	7.80 (0.198)	0.124 (31.5)	48 (22)
	Turbine outlet	7.70 (0.195)	0.068 (17.2)	22 (10)	8.60 (0.218)	0.076 (19.3)	33 (15)
	Compressor inlet	6.30 (0.160)	0.032 (8.1)	15 (7)	7.00 (0.178)	0.032 (8.1)	17 (8)
Manifold	Recuperator high pressure in	8.43 (0.214	0.032 (8.1)	5 (2)	6.50 (0.165)	0.032 (8.1)	5 (2)
	HSHX out	8.90 (0.226)	0.140 (35.6)	24 (11)	7.80 (0.198)	0.123 (31.2)	24 (11)
	Recuperator low pressure in	13.3 (0.338)	0.117 (29.8)	30 (14)	18.4 (0.467)	0.162 (41.2)	58 (26)
	WHX out	11.8 (0.300)	0.032 (8.1)	7 (3)	18.6 (0.472)	0.033 (8.5)	12 (5)
	Total	———	———	147 (67)	———	———	203 (92)

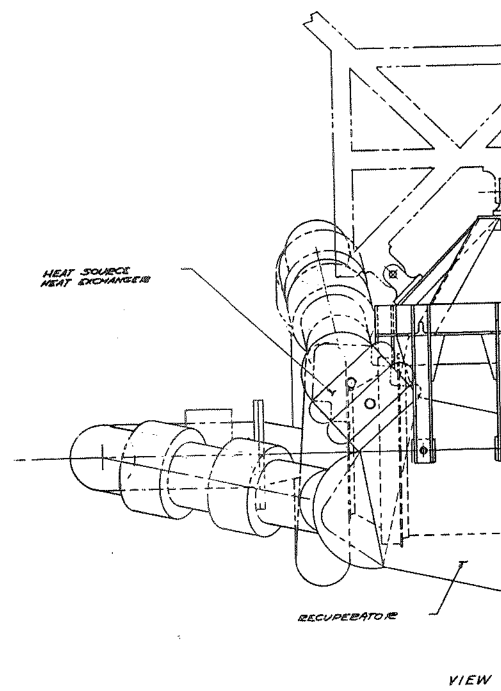

AIRESEARCH MANUFACTURING COMPANY Los Angeles, California FOLDOUT FRAME

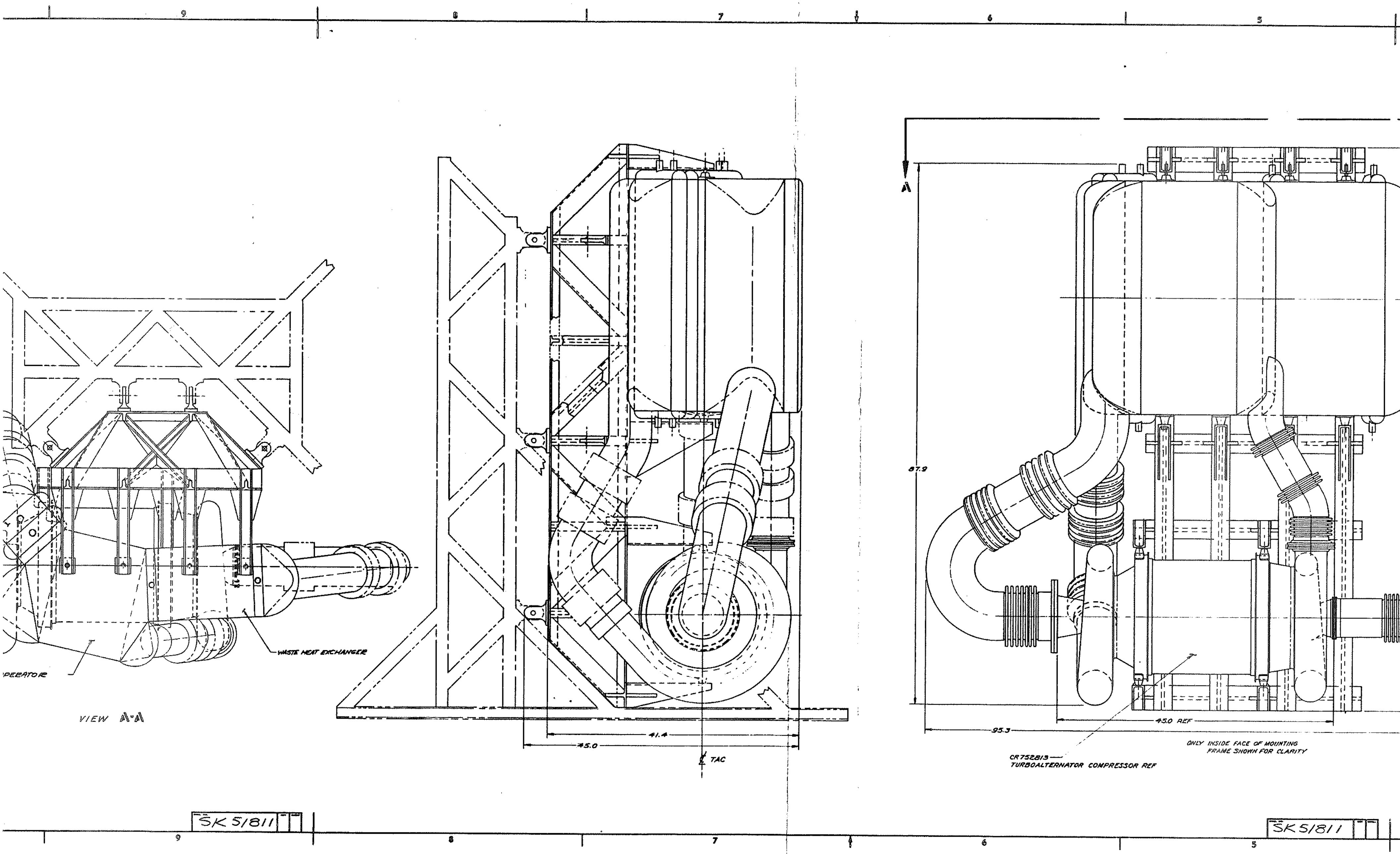

FOLDOUT FRAME 2

FOLDOUT FRAME 3

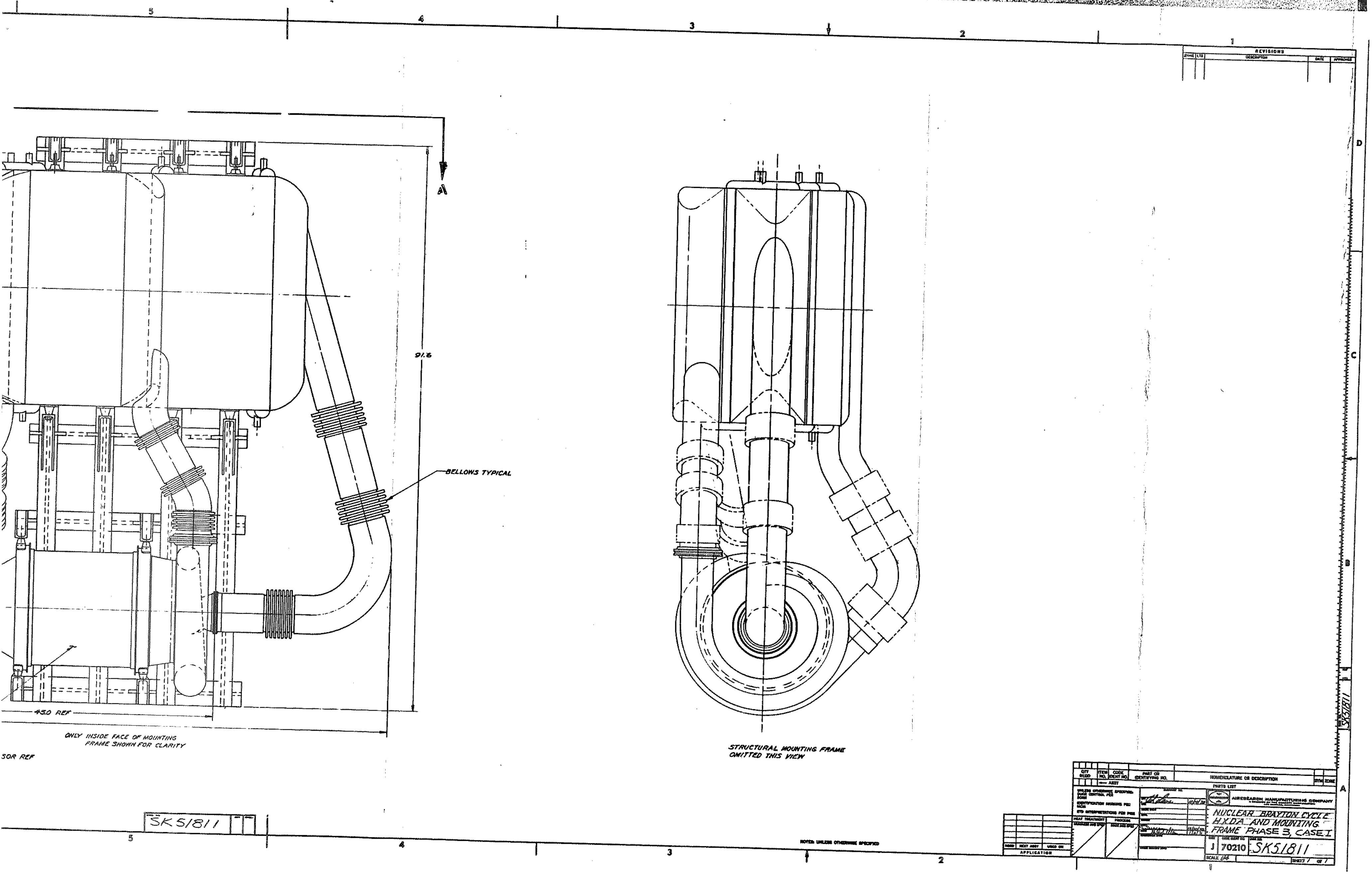

FRAME 3

FOLDOUT FRAME 4

FOLDOUT FRAME 5

TABLE 3-8

CASE I SYSTEMS SUMMARY

Item	Rectangular-End Recuperator		Triangular-End Recuperator	
	Matched Faces	Minimum Weight	Matched Faces	Minimum Weight
Weight, lb (kg)				
HSHX	136 (62)	145 (66)	135 (61)	145 (66)
Recuperator	772 (351)	681 (310)	732 (332)	600 (272)
WHX	623 (283)	595 (270)	543 (247)	595 (270)
Total HX	1531 (696)	1421 (646)	1410 (640)	1340 (608)
Manifolds and Ducts	203 (92)	———	147 (67)	———
Total HXDA	1734 (788)	———	1557 (707)	———
Insulation*	342 (155)	———	310 (141)	———
Frame	———	———	120 (54)	———
HSHX Liquid ΔP, psi (kN/m^2)	1.3 (8.96)	0.5 (3.45)	1.0 (6.89)	0.5 (3.45)
WHX Liquid ΔP, psi (kN/m^2)	10.9 (75.1)	9.8 (67.6)	13.5 (93.1)	8.5 (58.6)

*Based on 2.0 in. (0.0508 m) of insulation at 20 lb per cu ft (320 kg/m^3) on all heat exhangers and ducts.

SECTION 4

CASE II DESIGN STUDIES

INTRODUCTION

The parametric analyses and preliminary design of the HXDA for the Phase 3, Case II design conditions are presented in this section. The Case II cycle conditions, shown in Table 4-1 and in the system schematic (Figure 4-1), define a system operating at a 1600°F (1144°K) turbine inlet temperature, but with additional structural capability to provide system flexibility and growth potential to higher temperatures and pressures. Thus, the heat exchangers and ducts are designed structurally for 105 and 200 psi (724 and 1380 kN/m^2), respectively, at compressor inlet and outlet, and for a set of system temperatures approximately consistent with a 1700°F (1200°K) turbine inlet. The 1700°F (1200°K) temperature level was established during the study as the maximum that could be achieved without changing the construction material in the recuperator from that used at nominal temperatures and pressures.

Fluids used in the Case II system are NaK-78 in the heat source coolant loop, a xenon-helium mixture with a molecular weight of 39.94 as the cycle working fluid, and either monoisopropyl-biphenyl (MIPB) or NaK-78 as the heat rejection fluid. The NaK-78 has a growth potential provided by its high-temperature capability. Design pressure drops are 3.0 percent total for the gas system heat exchangers and ducting, 10.0 psi (68.9 kN/m^2) maximum for the waste heat exchanger liquid side, and 5.0 psi (34.5 kN/m^2) maximum for the heat source heat exchanger liquid side.

COMPONENT DESIGNS

Recuperator

Recuperators were sized as a function of gas fractional pressure drop for the Case II problem statement. Three core fin sets were used to obtain the optimum core geometry. The construction material is Hastelloy X, sized for structural capability in a system operating at 1700°F (1200°K) turbine inlet (corresponding to a high-pressure side recuperator inlet of 1284°F (970°K)) and high- and low-pressure levels of 200 and 105 psi (1380 and 724 kN/m^2). The combination of 1284°F (970°K) and 200 psi (1380 kN/m^2) results in a required fin area density on the high-pressure side of 0.16, which is the maximum that can be fabricated with assurance of good quality fins. Thus, this recuperator temperature level represents the maximum temperature capability of Hastelloy X for this application. The recuperator geometry is pure counterflow, with either triangular or rectangular crossflow end sections.

To obtain the optimum pressure drop split between recuperator core and end sections, a series of end section designs for several end section pressure

TABLE 4-1

CASE II DESIGN CONDITIONS

Thermodynamic	
Gas flow rate	11.27 lb/sec (5.12 kg/sec)
Recuperator effectiveness	0.925
Waste heat exchanger effectiveness	0.95
Capacity-rate ratio (gas ÷ liquid)	0.90
Heat source heat exchanger effectiveness	0.8643
Capacity-rate ratio (gas ÷ liquid)	1.0
Temperatures	see Figure 4-1
Compressor inlet pressure	70 psi (483 kN/m^2)
Compressor outlet pressure	133 psi (917 kN/m^2)
Pressure drops	
Gas system, total HXDA	3.0 percent
Waste heat exchanger liquid, maximum	10.0 psi (68.9 kN/m^2)
Heat source heat exchanger liquid, maximum	5.0 psi (34.5 kN/m^2)
Structural	
Temperatures	
Heat source heat exchanger, maximum	1770°F (1239°K)
Recuperator, maximum	1284°F (970°K)
Waste heat exchanger, maximum	674°F (631°K)
Compressor inlet duct	343°F (446°K)
Compressor outlet duct	624°F (603°K)
Turbine inlet duct	1700°F (1200°K)
Turbine outlet duct	1284°F (970°K)
Pressures	
Compressor inlet	105 psi (724 kN/m^2)
Compressor outlet	200 psi (1380 kN/m^2)
Heat source loop, maximum	30 psi (207 kN/m^2)
Heat rejection loop, maximum	75 psi (517 kN/m^2)

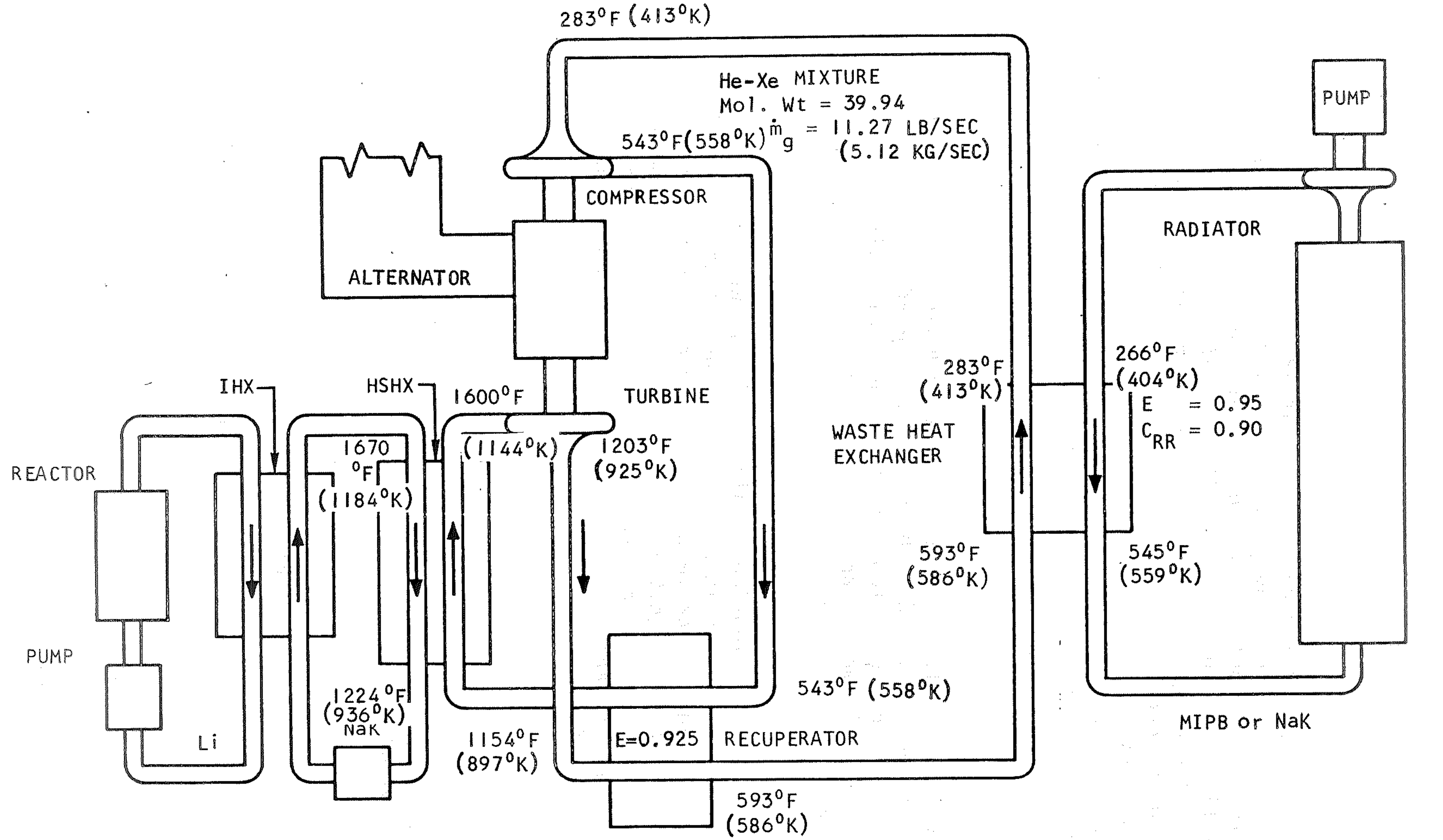

COMPRESSOR INLET PRESSURE = 70 PSI (483 kN/m^2)
COMPRESSOR OUTLET PRESSURE = 133 PSI (917 kN/m^2)
TURBINE OUTLET PRESSURE = 71.5 PSI (493 kN/m^2)

$\left(\frac{\Delta P}{P}\right)_{HXDA}$ = 0.03 (HEAT EXCHANGER AND DUCTS)

MECHANICAL DESIGN PRESSURE = 200/105 PSI
(1380/724 kN/m^2) AT 1700°F (1200°K) TURBINE INLET

S-61080

Figure 4-1. Case II Cycle Conditions

drops was calculated for each of several counterflow core pressure drops and each core fin set. The end section designs were obtained using AiResearch computer program H1440 (see Section 5), which calculates end section geometry combinations that provide uniform core flow distribution.

The combined weights of counterflow and end sections are shown in Figures 4-2 through 4-7. The core fin sets used are shown in Table 4-2. The dashed lines in the figures represent the recuperator weight variations corresponding to optimum pressure drop splits between counterflow and end sections. The optimized weight variations are summarized in Figures 4-8 and 4-9 for the two types of end sections. The weight advantage of triangular end sections in comparison with rectangular ends varies from about 170 lb (77.2 kg) at a total recuperator pressure drop of 3.0 percent to 380 lb (173 kg) at a pressure drop of 1.0 percent. Since this weight advantage is small relative to anticipated total HXDA weights, both recuperator types were included in the detailed studies of HXDA system configurations.

Waste Heat Exchanger

Plate-fin units were sized for the waste heat exchanger design conditions using MIPB as the heat rejection fluid. The units considered are eight-pass, cross-counterflow heat exchangers with two separate liquid circuits in the core. Liquid passages are alternately active and redundant, i.e., the ordering of passages is liquid 1, gas, liquid 2, gas, liquid 1, etc. Materials used are nickel for the fins and 347 stainless steel for the plates and header bars.

Heat exchanger weights and dimensions, calculated for two different liquid-side fin geometries, are shown in Figure 4-10. Use of the 20R-0.075 (788R-0.00190) fin[1] on the liquid side results in the minimum-weight heat exchanger, but use of the 16R-0.100 (630R-0.00254) fin results in a longer liquid flow length for a given liquid pressure drop, which is advantageous for matching the waste heat exchanger to the recuperator. In both cases, the gas-side fin is 20R-0.100 (788R-0.00254).

Heat Source Heat Exchanger

Size and weight for the heat source heat exchanger are shown as a function of gas pressure drop in Figure 4-11. The core matrix for this heat exchanger is the SFT 18 finned tube bundle with 0.500-in. (0.0127-m) OD tubes. The SFT 18 matrix has the following geometry:

Transverse tube spacing	=	1.98 x (tube OD)
Tube row spacing	=	0.99 x (tube OD)
Fin diameter	=	1.27 x (tube OD)

1 The 20R-0.075 (788R-0.00190) designation is 20 fins per inch (788 fins per meter), rectangular fins, 0.075-in. (0.00190-m) plate spacing.

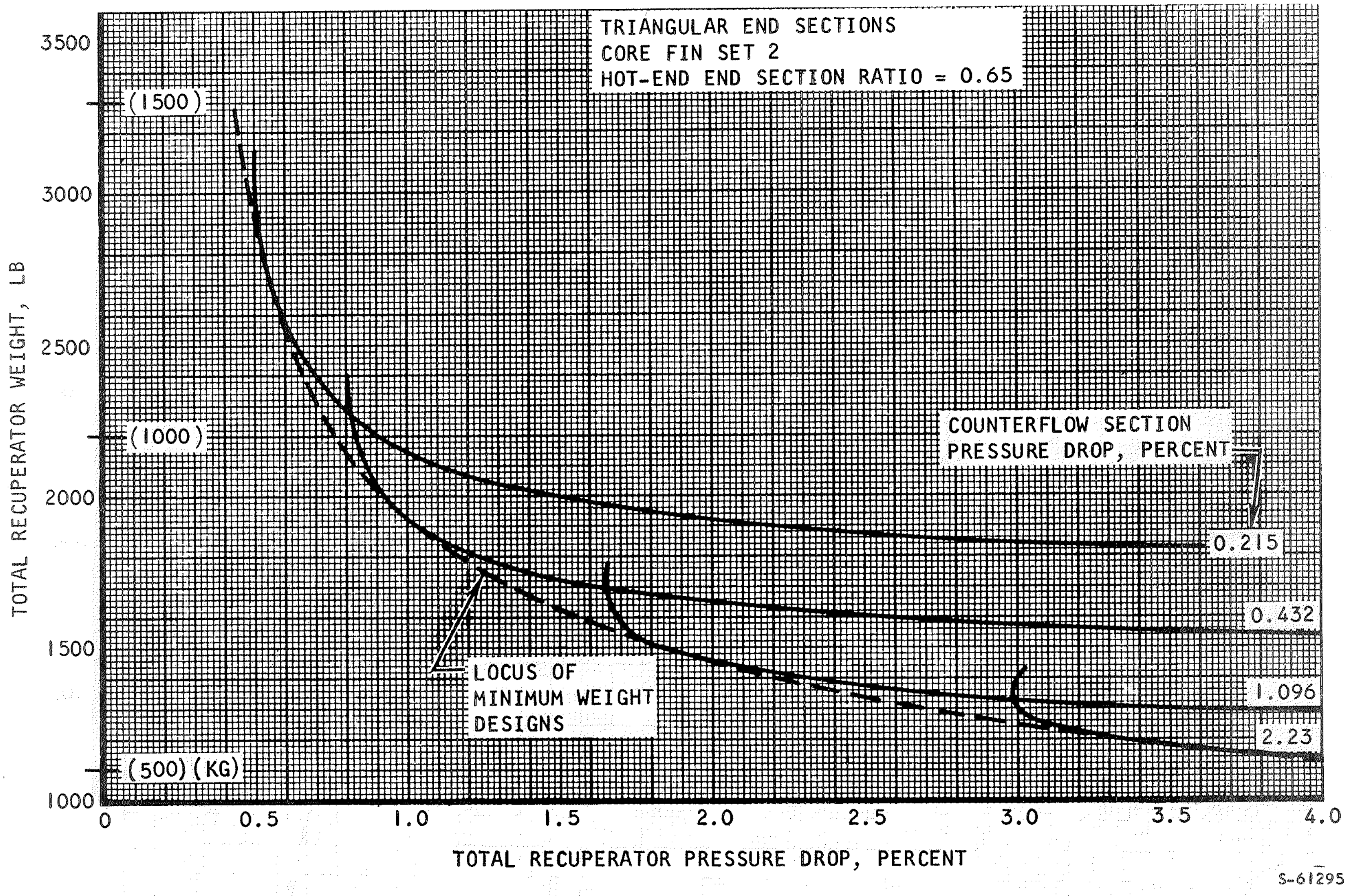

Figure 4-2. Variation of Total Weight with Total Pressure Drop for the Case II Recuperator

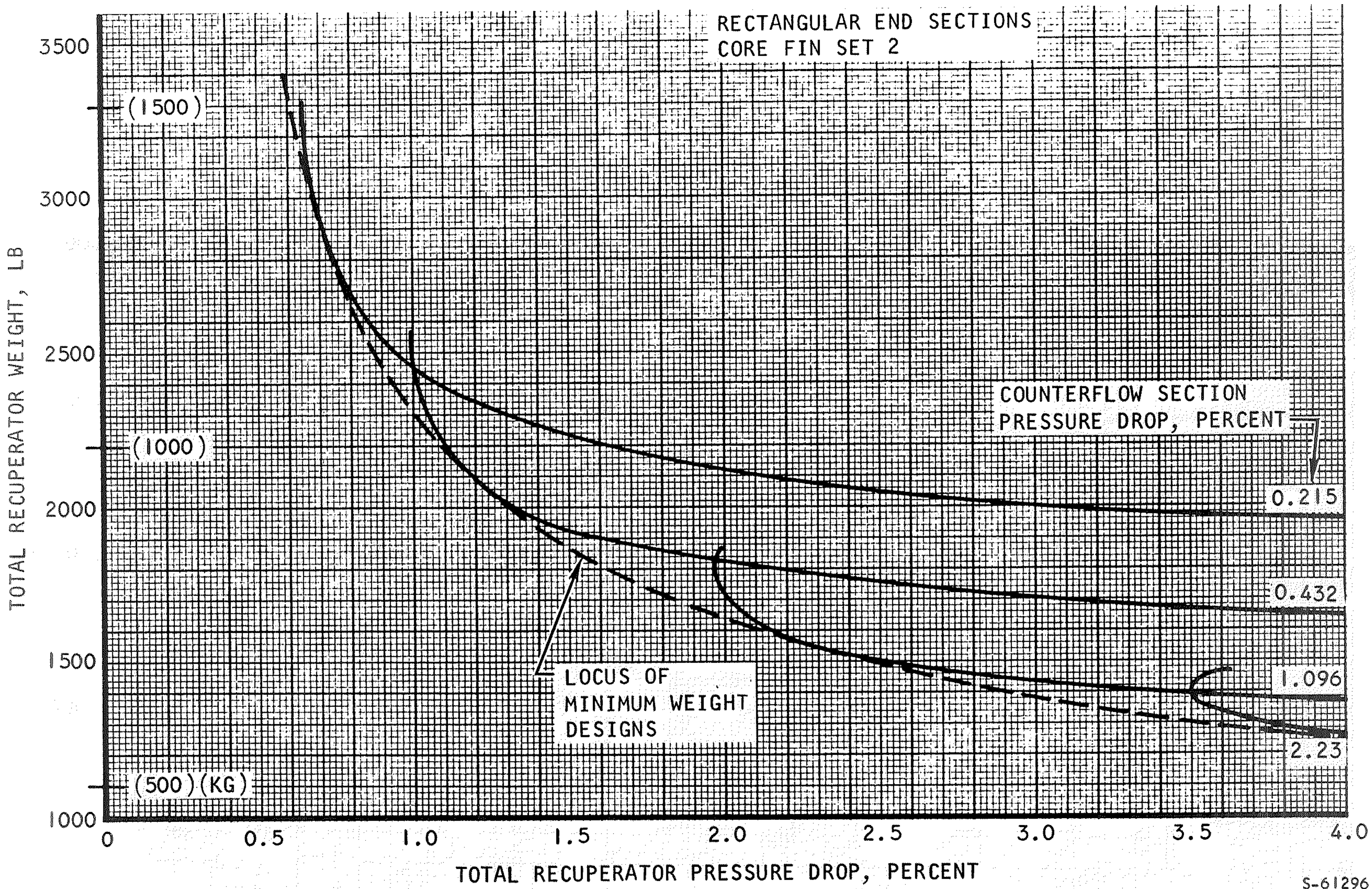

Figure 4-3. Variation of Total Weight with Total Pressure Drop for the Case II Recuperator

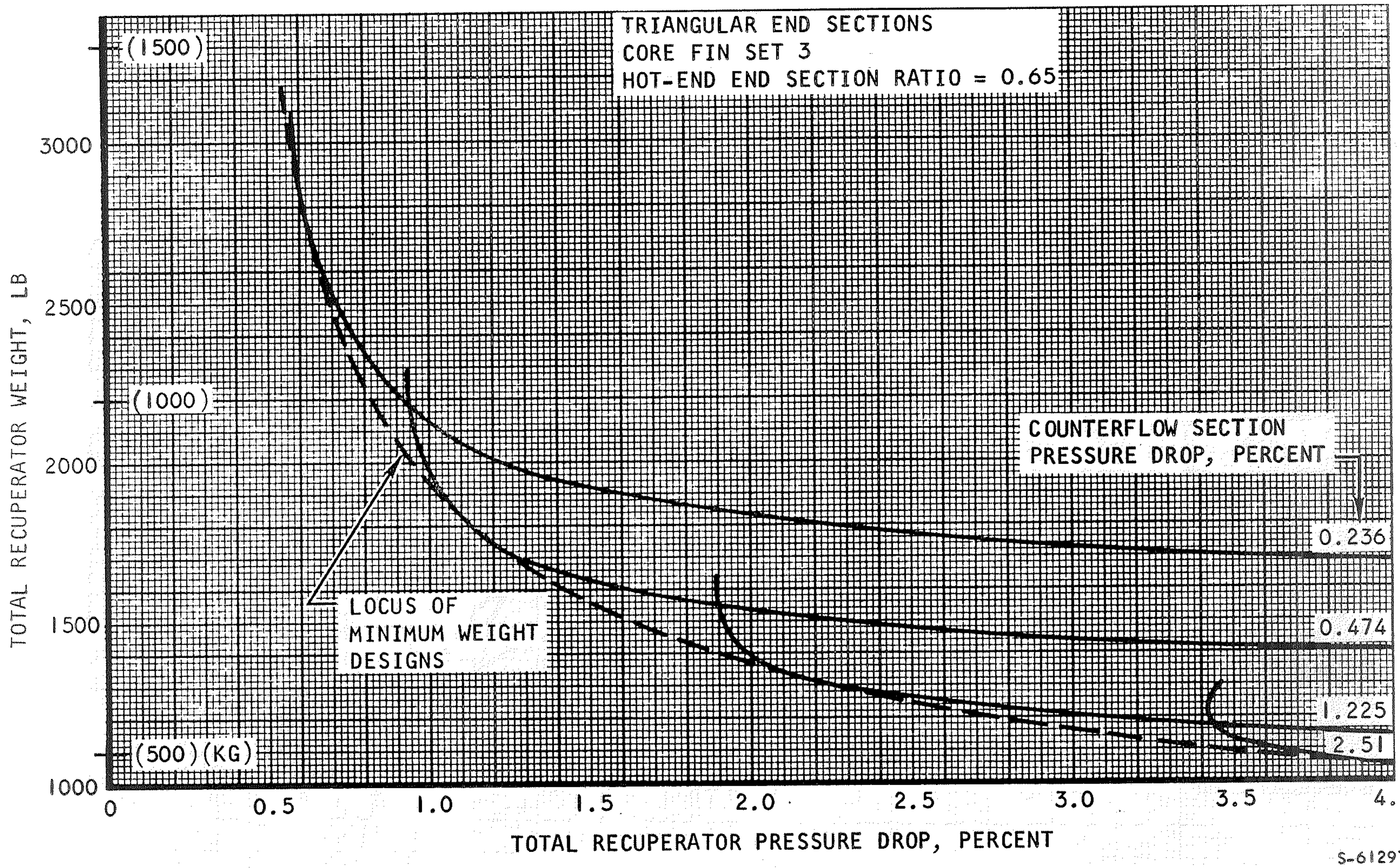

Figure 4-4. Variation of Total Weight with Total Pressure Drop for the Case II Recuperator

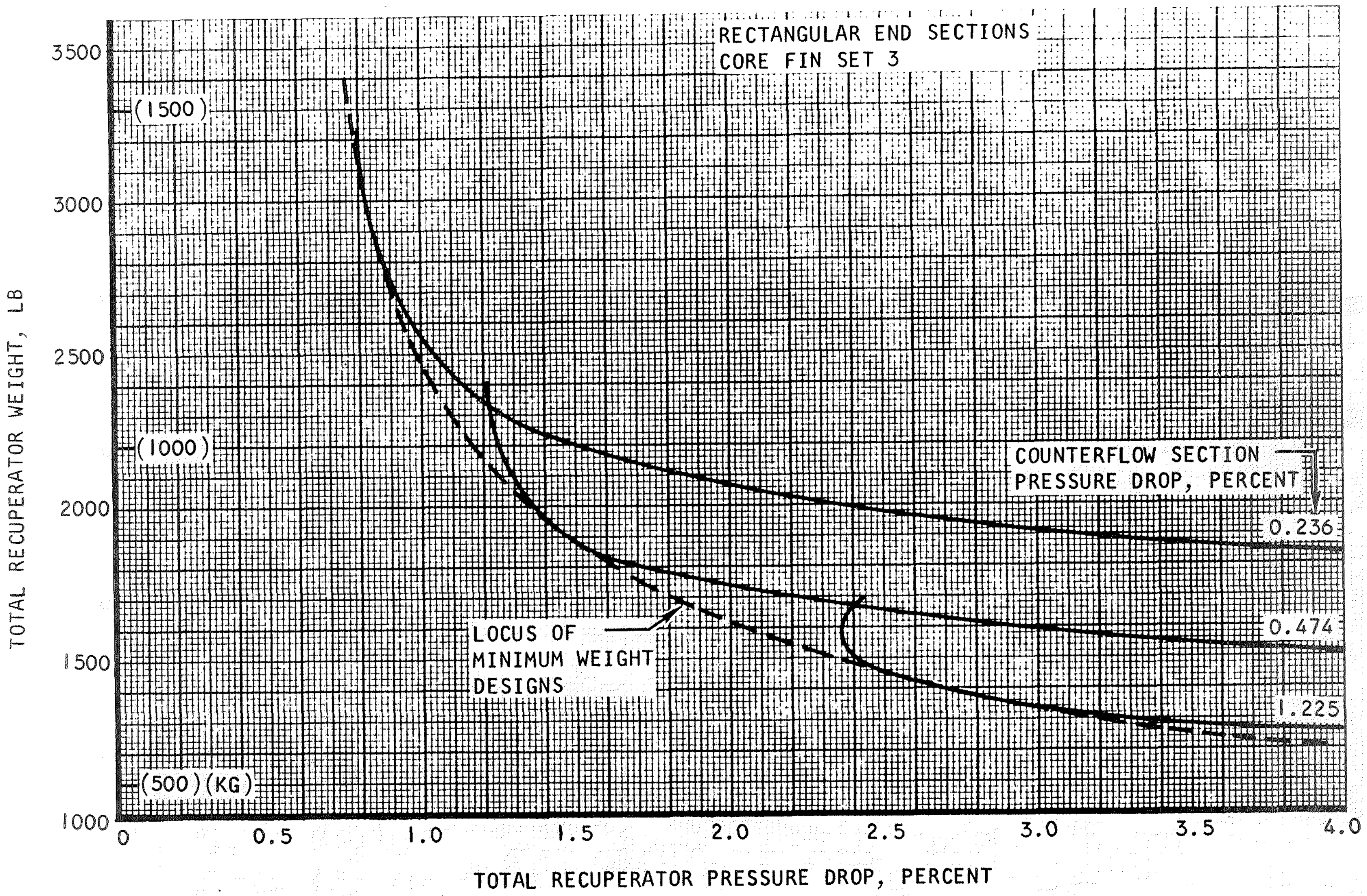

S-61298

Figure 4-5. Variation of Total Weight with Total Pressure Drop for the Case II Recuperator

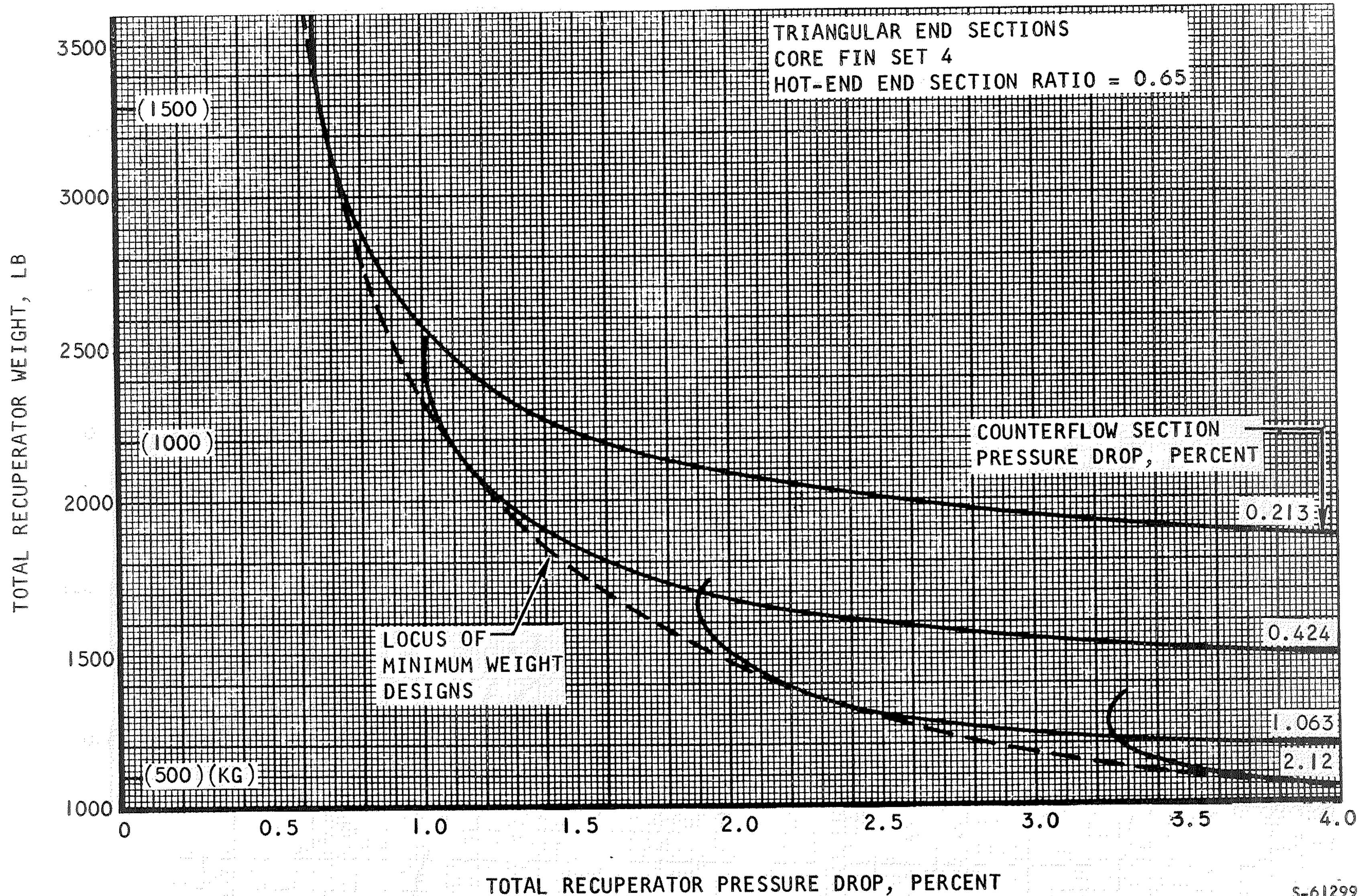

Figure 4-6. Variation of Total Weight with Total Pressure Drop for the Case II Recuperator

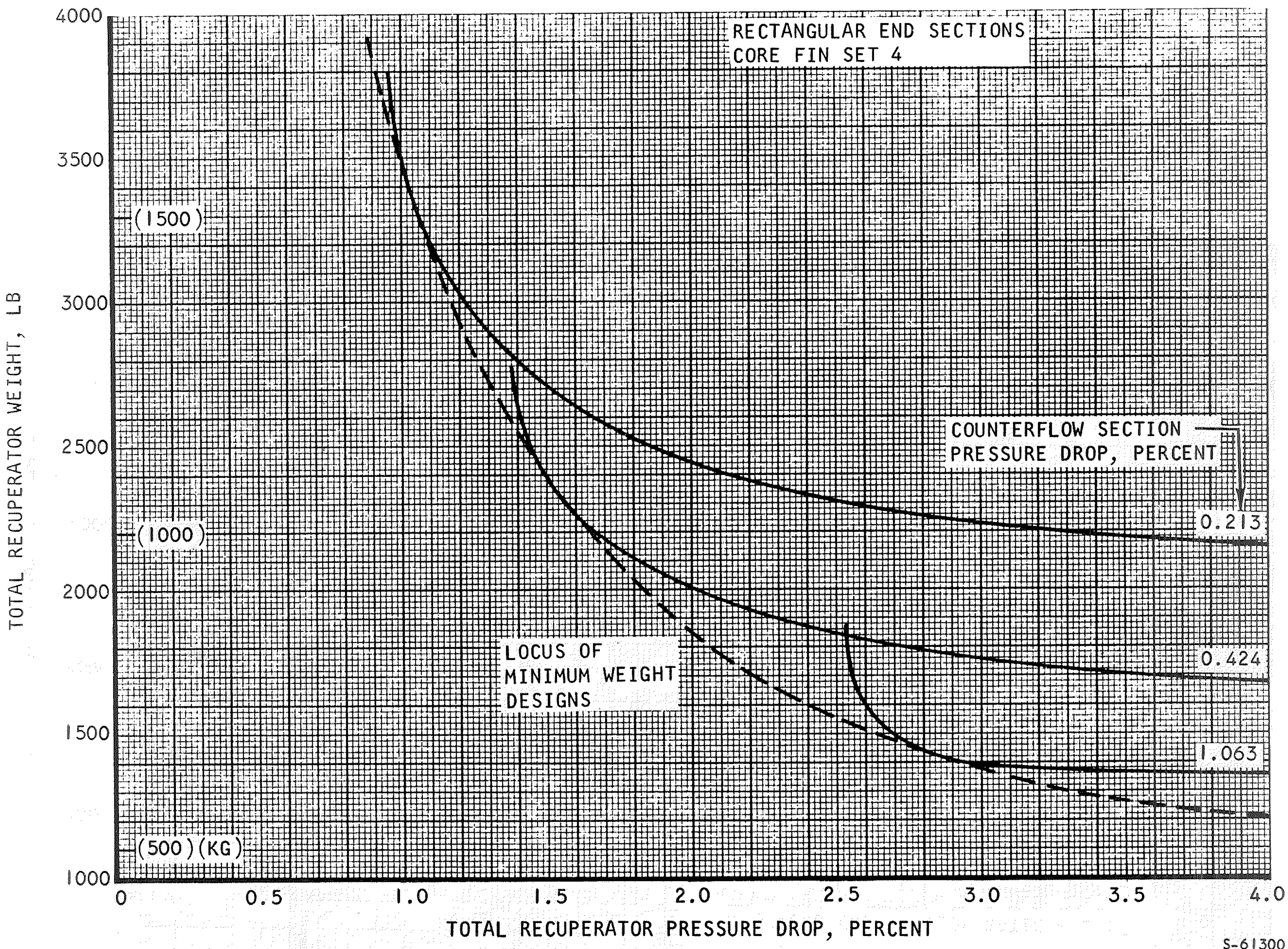

Figure 4-7. Variation of Total Weight with Total Pressure Drop for the Case II Recuperator

TABLE 4-2

RECUPERATOR CORE FIN SETS (CASE II)

Low-Pressure Side			
Fin Set	Fins/In. (fins/m)	Fin Ht, in. (m)	Fin Thick, in. (m)
2	16 (630)	0.153 (0.00388)	0.00569 (1.45×10^{-4})
3	16 (630)	0.125 (0.00317)	0.00569 (1.45×10^{-4})
4	20 (788)	0.100 (0.00254)	0.00455 (1.16×10^{-4})
High-Pressure Side			
Fin Set	Fins/In. (fins/m)	Fin Ht, in. (m)	Fin Thick, in. (m)
2	16 (630)	0.125 (0.00317)	0.0100 (2.54×10^{-4})
3	20 (788)	0.100 (0.00254)	0.0080 (2.03×10^{-4})
4	20 (788)	0.075 (0.00190)	0.0080 (2.03×10^{-4})

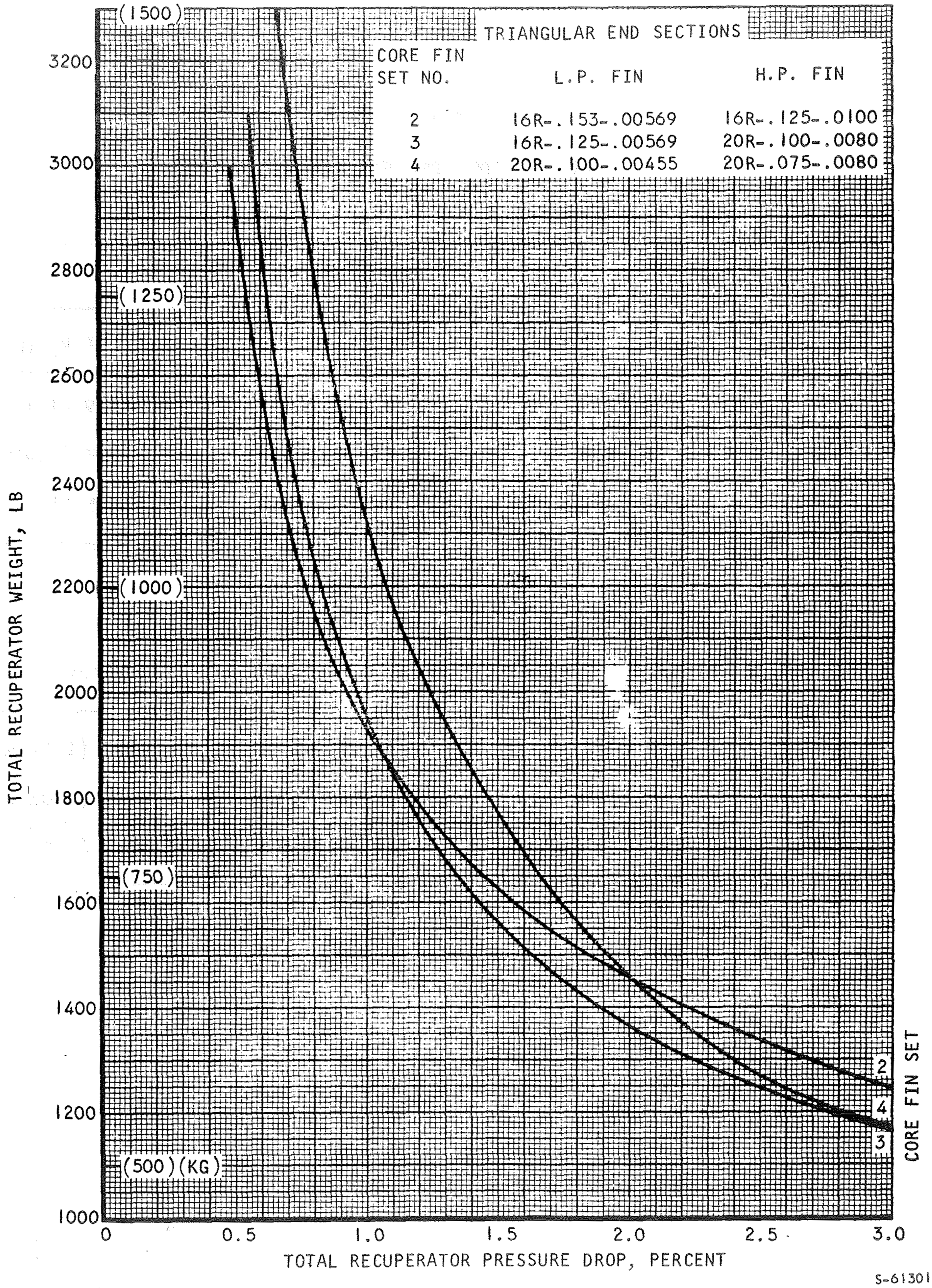

Figure 4-8. Variation of Total Weight with Total Pressure Drop for Case II Recuperator, Minimum-Weight Curves

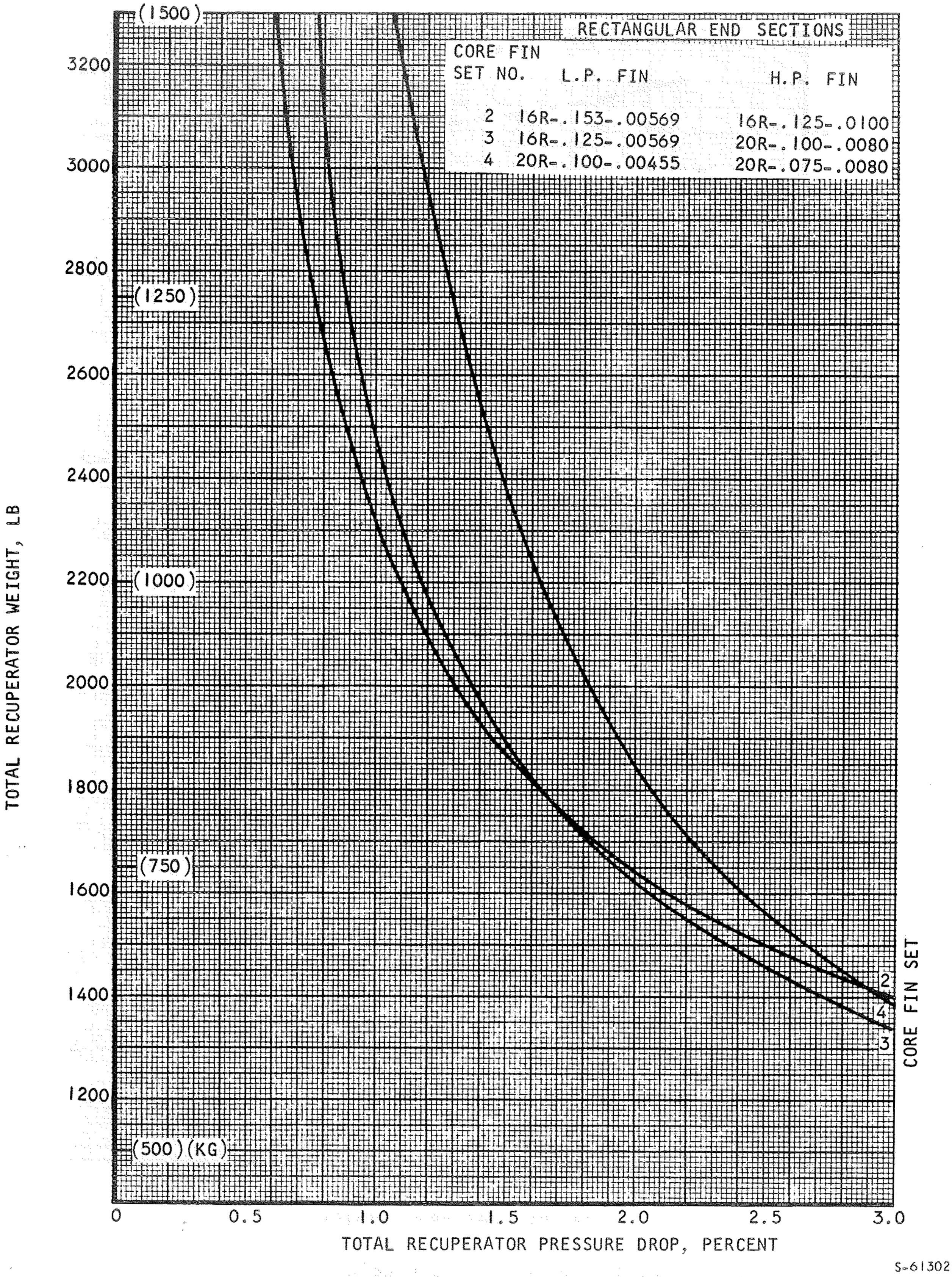

Figure 4-9. Variation of Total Weight with Total Pressure Drop for Case II Recuperator, Minimum-Weight Curves

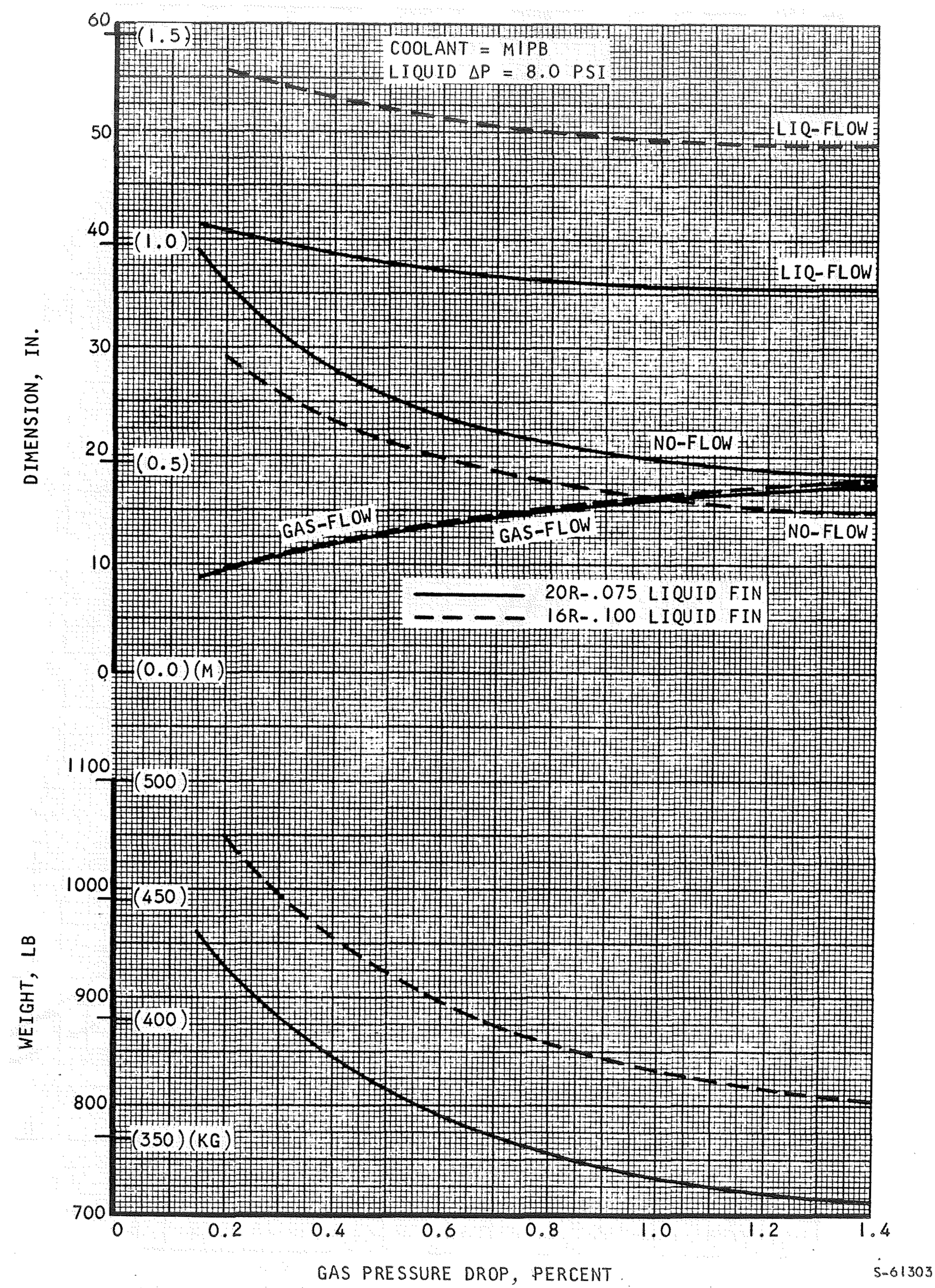

Figure 4-10. Variation of Size and Weight with Gas Pressure Drop for Case II Waste Heat Exchanger

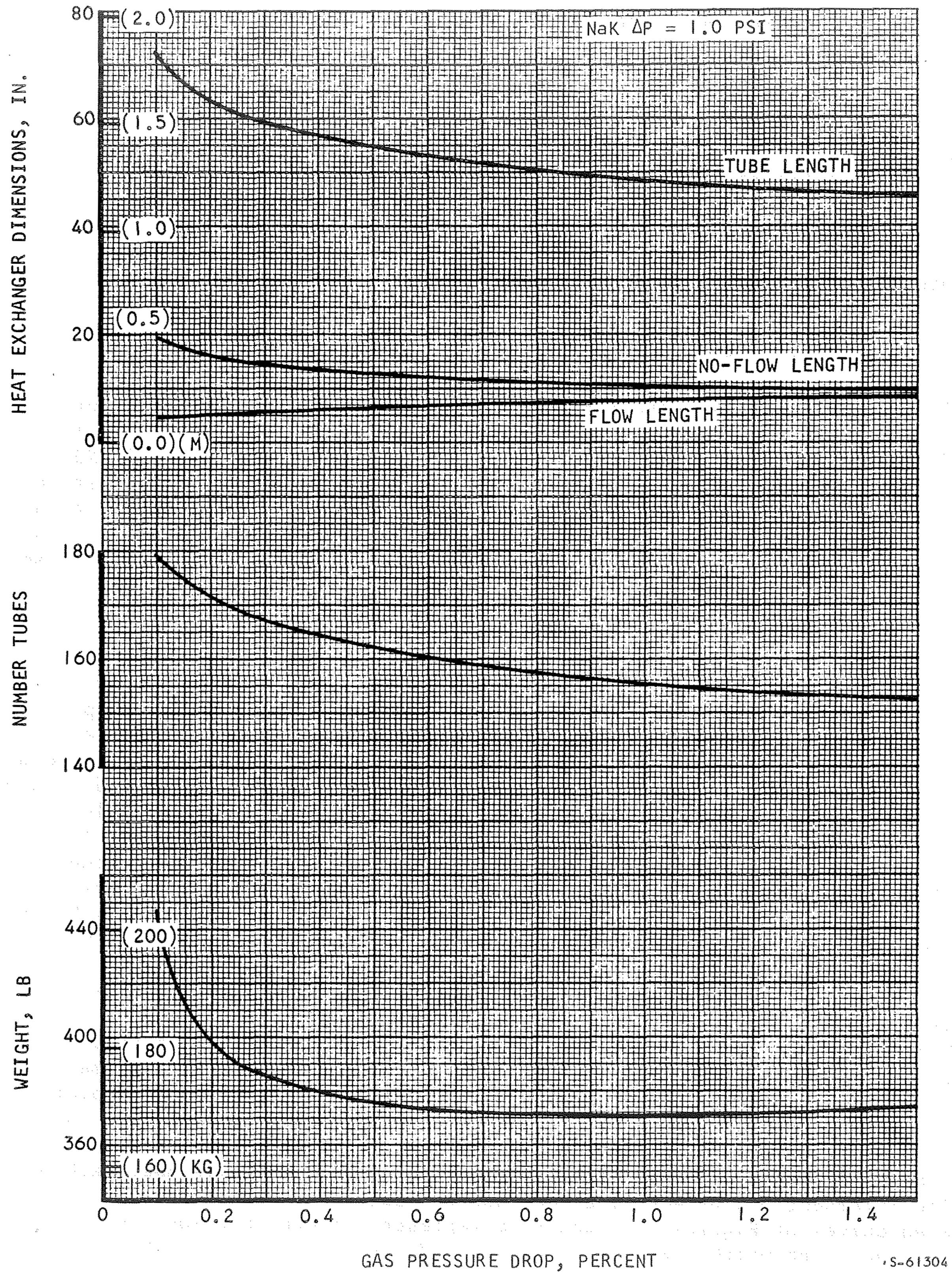

Figure 4-11. Case II Heat Source Heat Exchanger

Fins per inch = 30 (fins per meter = 1180)

Staggered tubes

Cb-1 percent Zr is used both as the fin material and the material of construction throughout the core. The fin thickness is 0.005 in. (1.27×10^{-4}m). The overall flow configuration is four-pass cross-counterflow.

DESIGN POINT SELECTION

Matched Face Area Solutions

Complete HXDA system configurations were obtained based on matched heat exchanger face areas for both triangular- and rectangular-end recuperator designs. In these systems the waste heat exchanger gas face dimensions match the recuperator low-pressure outlet face dimensions, and the heat source heat exchanger gas face dimensions match the recuperator high-pressure outlet face dimensions as closely as possible. For these studies, the overall HXDA gas pressure drop was fixed at 3.0 percent, and a pressure drop of 0.5 percent was reserved for the manifolds and ducts. Thus, the total pressure drop to be apportioned among the three heat exchangers is 2.5 percent. From Figures 4-8 and 4-9, the fins selected for the recuperator counterflow core are fin set 3 and fin set 2, respectively, for the triangular- and rectangular-end recuperators.

Figures 4-12 and 4-13 show the face areas of the waste heat exchanger and recuperator low-pressure outlet plotted as a function of recuperator pressure drop. Since the pressure drop available to the waste heat exchanger for a given value of recuperator pressure drop depends on the pressure drop allotted to the heat source heat exchanger, the waste heat exchanger face area is plotted parametrically for several values of heat source heat exchanger pressure drop. Each intersection between a waste heat exchanger face area curve and a recuperator face area curve represents a design point for the specified value of heat source heat exchanger pressure drop. Since only one such value results in an exact face area match between heat source heat exchanger and the recuperator high-pressure outlet, a unique solution is defined in which both face area matches are obtained. To determine the required heat source heat exchanger pressure drop, recuperator low-pressure outlet face area is plotted as a function of high-pressure outlet face area, as shown in Figure 4-14. For each value of heat source heat exchanger pressure drop used in Figures 4-12 and 4-13, the low-pressure outlet face area corresponding to a recuperator/waste heat exchanger match can be related to the corresponding high-pressure outlet face area through Figure 4-14. Successive points obtained in this manner result in the curves of recuperator high-pressure outlet face area plotted as a function of heat source heat exchanger pressure drop in Figures 4-15 and 4-16. Each point on the recuperator curves in these figures corresponds to a face area match between recuperator low-pressure outlet and waste heat exchanger. The intersections between the heat source heat exchanger and recuperator face area curves of Figures 4-15 and 4-16 represent unique solutions in which the two face-area matches are obtained coincidentally. Since the above procedure was implemented for both rectangular- and triangular-end recuperator designs

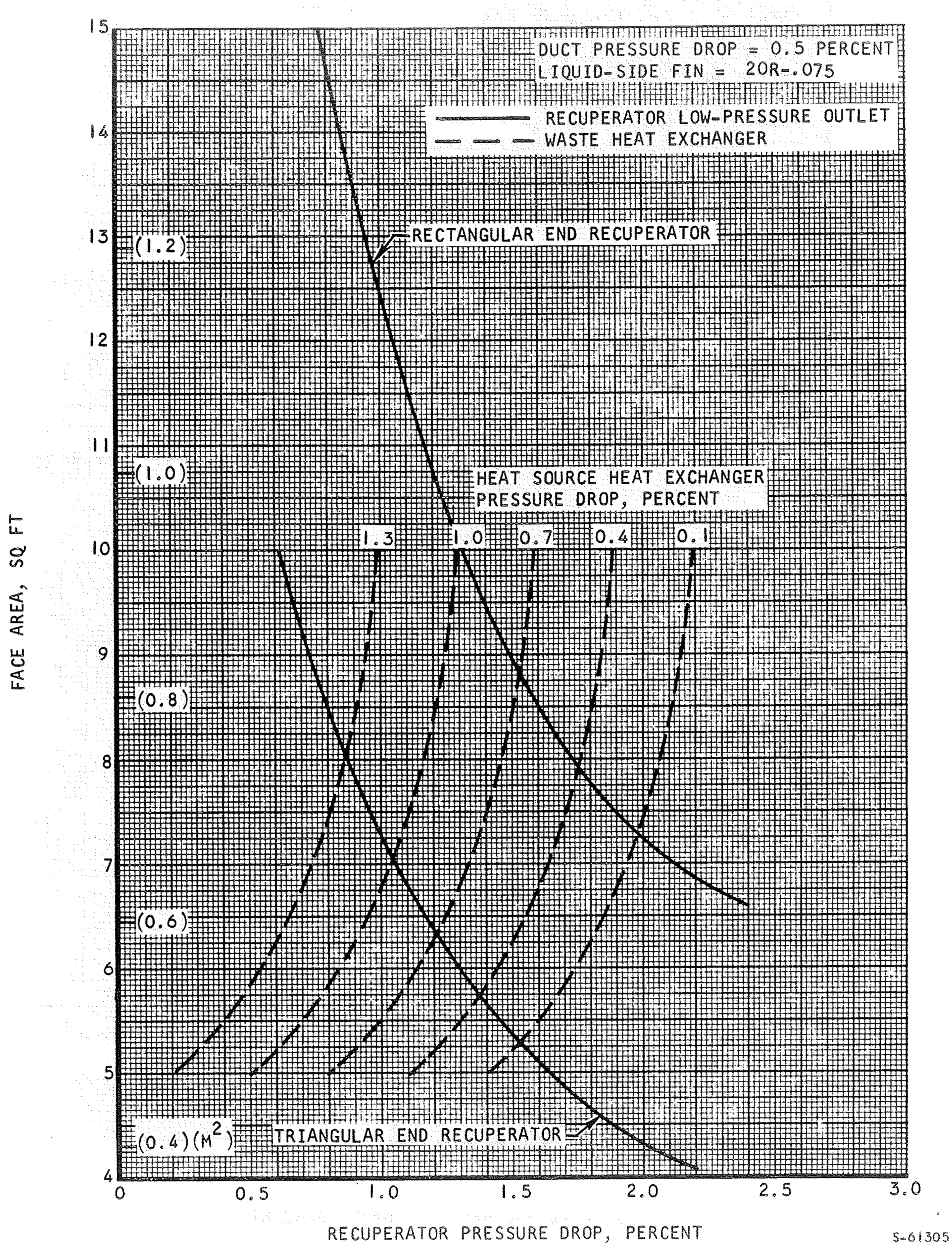

Figure 4-12. Recuperator and Waste Heat Exchanger Face Areas for Case II

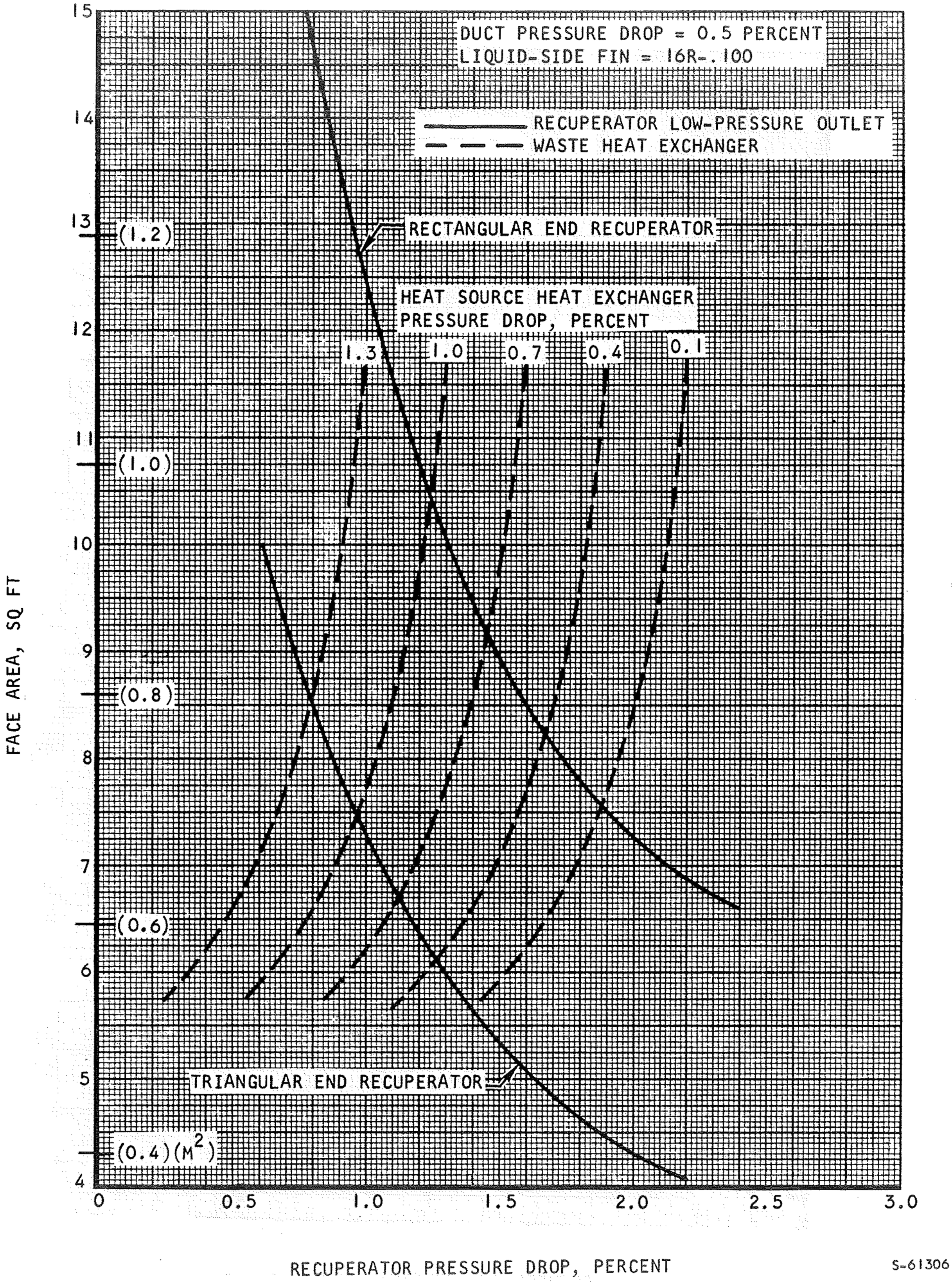

Figure 4-13. Recuperator and Waste Heat Exchanger Face Areas for Case II

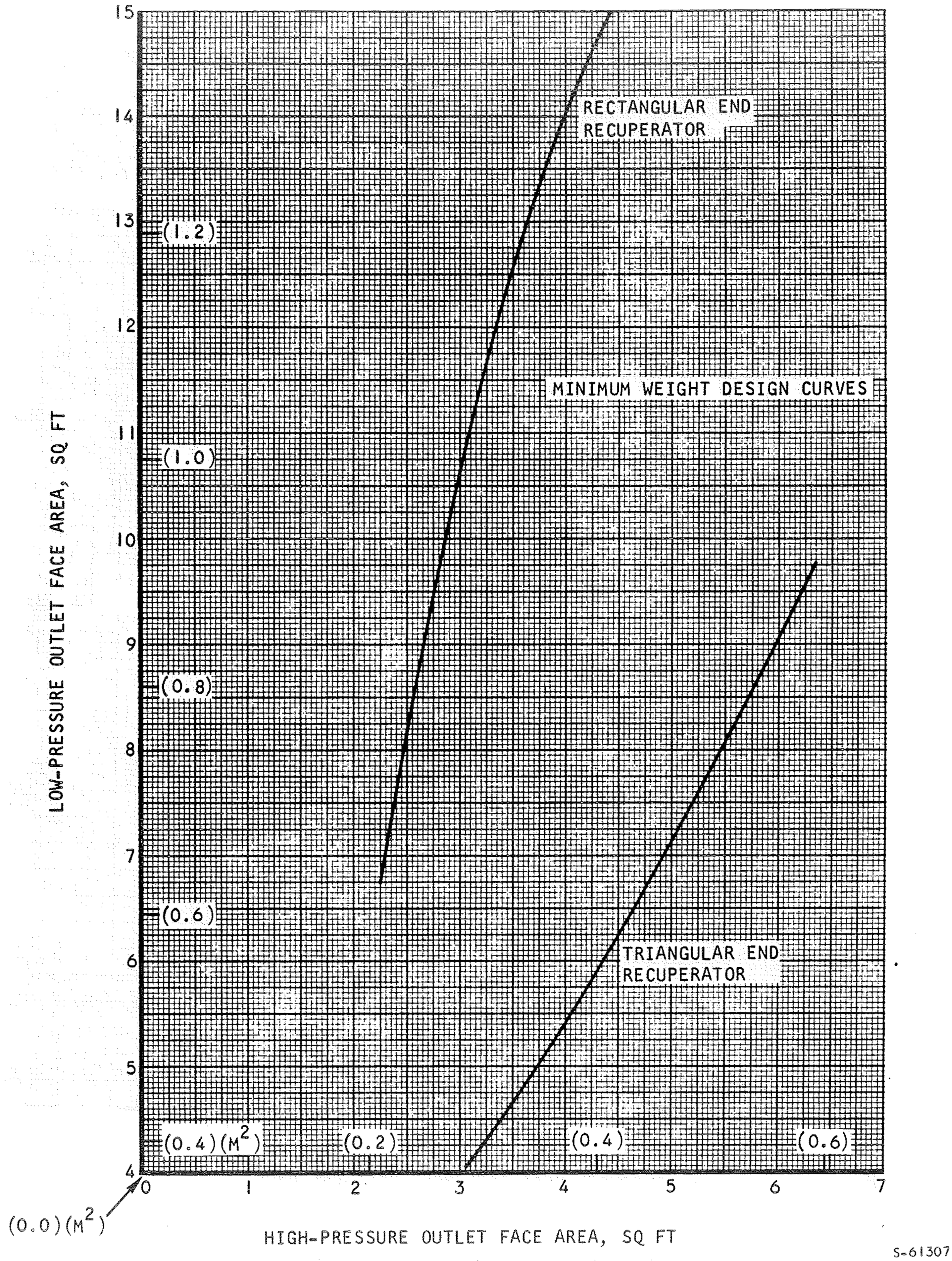

Figure 4-14. Variation of Recuperator Face Areas for Case II

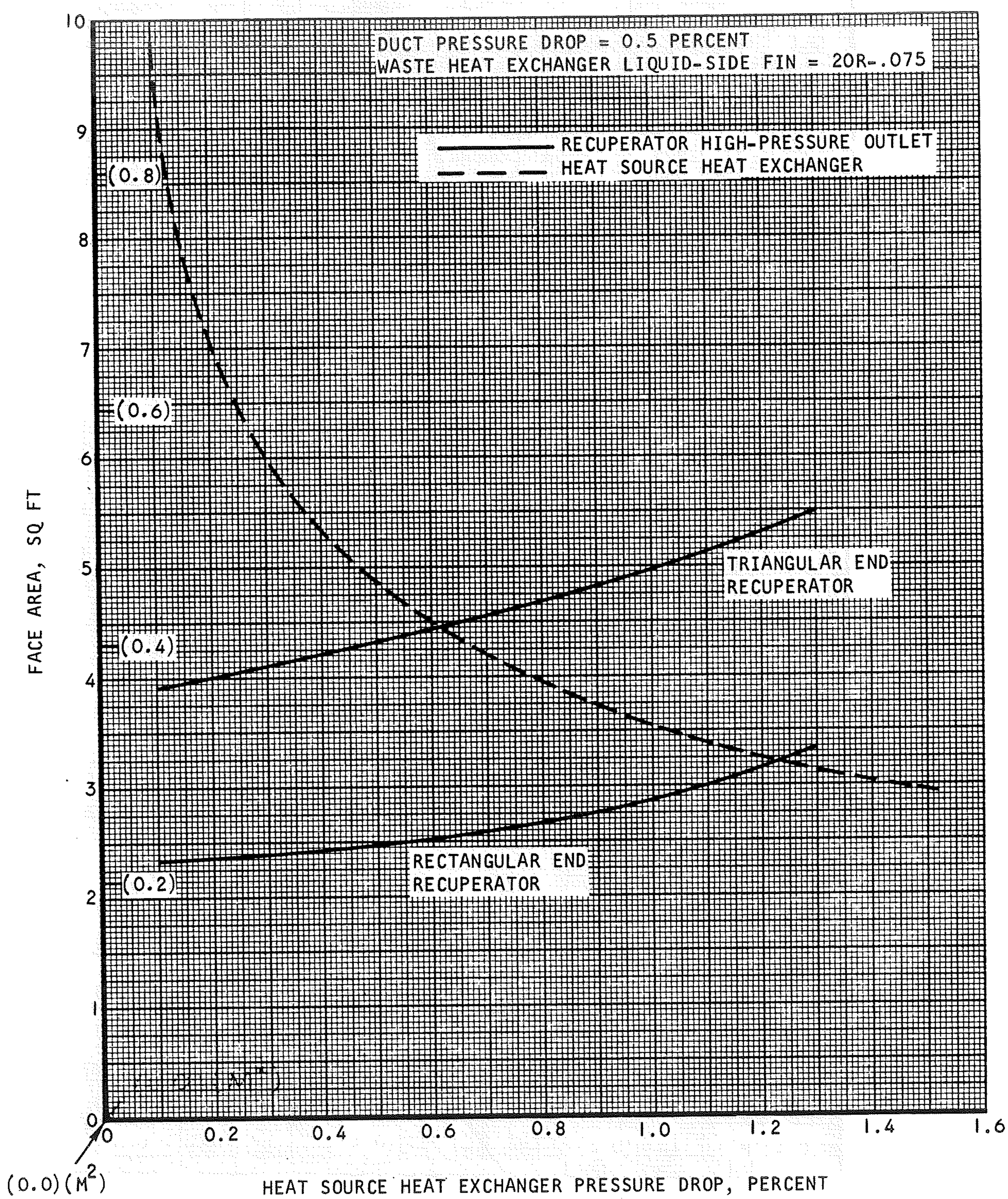

Figure 4-15. Recuperator and Heat Source Heat Exchanger Face Areas for Case II

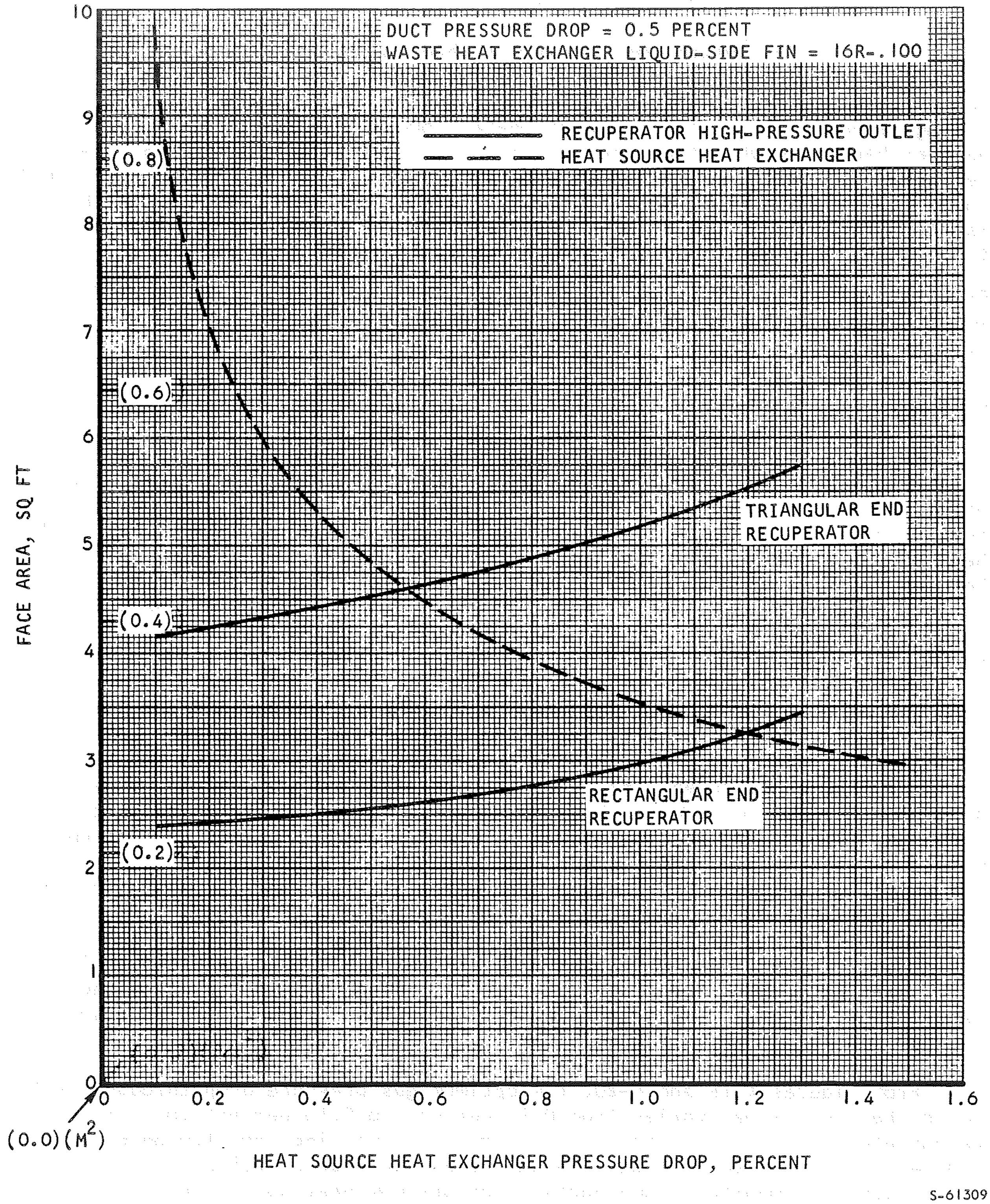

Figure 4-16. Recuperator and Heat Source Heat Exchanger Face Areas for Case II

and two different waste heat exchanger liquid fins, four distinct system design points are obtained.

The four HXDA system configurations obtained by the foregoing face area matching procedure are summarized in Tables 4-3 through 4-6. For both waste heat exchanger liquid fin geometries, the system configuration utilizing the triangular-end recuperator is approximately 600 lb (272 kg) lighter (in total heat exchanger weight) than the configuration utilizing the rectangular-end recuperator. Using the triangular-end recuperator, the 20R-0.075 (788R-0.00190) waste heat exchanger liquid fin results in a total heat exchanger weight that is 140 lb (63.6 kg) less than is obtained with the 16R-0.100 (630R-0/00254) fin. However, dimensional matching of the waste heat exchanger to the recuperator results in a liquid pressure drop of 22 psi (152 kN/m^2) for the 20R-0.075 (788R-0.00190) case, whereas the liquid pressure drop for the 16R-0.100 (630R-0.00254) case is 10 psi (68.9 kN/m^2).

Minimum Weight Solutions

Minimum-weight solutions were obtained for systems incorporating both triangular-end and rectangular-end recuperators. In these solutions, the pressure drops allocated to recuperator, recuperator end sections, heat source heat exchanger, and waste heat exchanger were optimized to obtain minimum total heat exchanger weight without regard to the degree of face area mismatch between recuperator and adjoining heat exchangers. The recuperator weight variation used for this optimization is based on the minimum of the weight curves in Figures 4-8 and 4-9, i.e., fin set 2 at low-pressure drop and fin set 3 at high-pressure drop.

The optimization curves for these two cases are shown in Figures 4-17 through 4-20. In Figures 4-17 and 4-19, the optimum pressure drop split between recuperator and waste heat exchanger is determined. The solid curves in these figures represent the variations of total weight with total gas pressure drop for the two heat exchangers at fixed values of the waste heat exchanger pressure drop. The dashed curves represent the loci of minimum-weight designs. Using the dashed curves of Figures 4-17 and 4-19 to represent the weight variation of the recuperator/waste heat exchanger combination, the optimum pressure drop allocation among all three heat exchangers is obtained in Figures 4-18 and 4-20. The solid curves in these figures represent the variations of total heat exchanger weight with total gas pressure drop in the three heat exchangers for fixed values of pressure drop in the optimized recuperator/waste heat exchanger combination. The dashed curves represent the loci of minimum weight system designs.

From Figures 4-18 and 4-20, the optimum gas pressure drop through the heat source heat exchanger varies from 0.11 percent to 0.16 percent for combined recuperator/waste heat exchanger pressure drops varying from 1.0 percent to 3.0 percent. At a total heat exchanger pressure drop of 2.5 percent (reserving 0.5 percent for manifolds and ducts), the optimum heat source heat exchanger pressure drop is approximately 0.15 percent for both systems. Using a value of 0.15 percent for the heat source heat exchanger, Figures 4-17 and 4-19 indicate an optimum waste heat exchanger pressure drop of 0.40 percent for the triangular-end recuperator system and 0.35 percent for the rectangular-end recuperator system.

TABLE 4-3

CASE II HXDA
TRIANGULAR-END RECUPERATOR/20R-0.075 (788R-0.00190) WHX LIQUID FIN
MATCHED FACE AREA SOLUTION

Recuperator	
Gas pressure drop	1.25 percent
Weight	1720 lb (781 kg)
Core length	10.2 in. (0.259 m)
End section height, hot end	7.1 in. (0.180 m)
cold end	4.1 in. (0.104 m)
End section ratio, hot end	0.65
cold end	0.58
Width	27.3 in. (0.694 m)
Stack height	54.6 in. (1.39 m)
Waste Heat Exchanger	
Gas pressure drop	0.63 percent
Weight	785 lb (356 kg)
Liquid pressure drop	22 psi (152 kN/m^2)
Gas-flow length	13.8 in. (0.351 m)
Liquid-flow length	54.6 in. (1.39 m)
Stack height	16.0 in. (0.406 m)
Heat Source Heat Exchanger	
Gas pressure drop	0.62 percent
Weight	373 lb (169 kg)
Liquid pressure drop	1.1 psi (7.59 kN/m^2)
Gas-flow length	7.1 in. (0.180 m)
Tube length	54.9 in. (1.39 m)
No-flow length	11.1 in. (0.282 m)
Number of tubes	154
Number of tube rows	14
Number of passes	4

TABLE 4-4

CASE II HXDA
TRIANGULAR-END RECUPERATOR/16R-0.100 (630R-0.00254) WHX LIQUID
FIN MATCHED FACE AREA SOLUTION

Recuperator	
Gas pressure drop	1.18 percent
Weight	1778 lb (807 kg)
Core length	10.0 in. (0.254 m)
End section height, hot end	7.1 in. (0.180 m)
cold end	4.1 in. (0.104 m)
End section ratio, hot end	0.65
cold end	0.58
Width	27.8 in. (0.706 m)
Stack height	55.6 in. (1.41 m)
Waste Heat Exchanger	
Gas pressure drop	0.75 percent
Weight	866 lb (393 kg)
Liquid pressure drop	10 psi (68.9 kN/m^2)
Gas-flow length	15.0 in. (0.318 m)
Liquid-flow length	55.6 in. (1.41 m)
Stack height	16.4 in. (0.416 m)
Heat Source Heat Exchanger	
Gas pressure drop	0.57 percent
Weight	374 lb (170 kg)
Liquid pressure drop	1.1 psi (7.59 kN/m^2)
Gas-flow length	7.1 in. (0.180 m)
Tube length	56.2 in. (1.43 m)
No-flow length	11.1 in. (0.282 m)
Number of tubes	154
Number of tube rows	14
Number of passes	4

TABLE 4-5

CASE II HXDA
RECTANGULAR-END RECUPERATOR/20R-0.075 (788R-0.00190) WHX LIQUID FIN
MATCHED FACE AREA SOLUTION

Recuperator	
Gas pressure drop	1.12 percent
Weight	2174 lb (988 kg)
Core length	11.8 in. (0.300 m)
End section height, hot end	8.3 in. (0.211 m)
cold end	6.0 in. (0.152 m)
Total length	19.0 in. (0.482 m)
Width	28.7 in. (0.729 m)
Stack height	57.4 in. (1.46 m)
Waste Heat Exchanger	
Gas pressure drop	0.16 percent
Weight	955 lb (434 kg)
Liquid pressure drop	18 psi (124 kN/m^2)
Gas-flow length	8.9 in. (0.226 m)
Liquid-flow length	57.4 in. (1.46 m)
Stack height	28.2 in. (0.716 m)
Heat Source Heat Exchanger	
Gas pressure drop	1.22 percent
Weight	371 lb (169 kg)
Liquid pressure drop	1.6 psi (11.0 kN/m^2)
Gas-flow length	8.1 in. (0.206 m)
Tube length	56.3 in. (0.143 m)
No-flow length	8.1 in. (0.206 m)
Number of tubes	128
Number of tube rows	16
Number of passes	4

TABLE 4-6

CASE II HXDA
RECTANGULAR-END RECUPERATOR/16R-0.100 (630R-0.00254) WHX LIQUID FIN
MATCHED FACE AREA SOLUTION

Recuperator	
Gas pressure drop	1.10 percent
Weight	2195 lb (997 kg)
Core length	11.7 in. (0.297 m)
End section height, hot end	8.4 in. (0.213 m)
cold end	6.1 in. (0.155 m)
Total length	19.0 in. (0.483 m)
Width	29.1 in. (0.740 m)
Stack height	58.1 in. (1.48 m)
Waste Heat Exchanger	
Gas pressure drop	0.20 percent
Weight	1049 lb (476 kg)
Liquid pressure drop	8.2 psi (56.5 kN/m^2)
Gas-flow length	9.7 in. (0.246 m)
Liquid-flow length	58.1 in. (1.48 m)
Stack height	29.0 in. (0.736 m)
Heat Source Heat Exchanger	
Gas pressure drop	1.20 percent
Weight	371 lb (169 kg)
Liquid pressure drop	1.6 psi (11.0 kN/m^2)
Gas-flow length	8.1 in. (0.206 m)
Tube length	56.4 in. (1.43 m)
No-flow length	8.1 in. (0.206 m)
Number of tubes	128
Number of tube rows	16
Number of passes	4

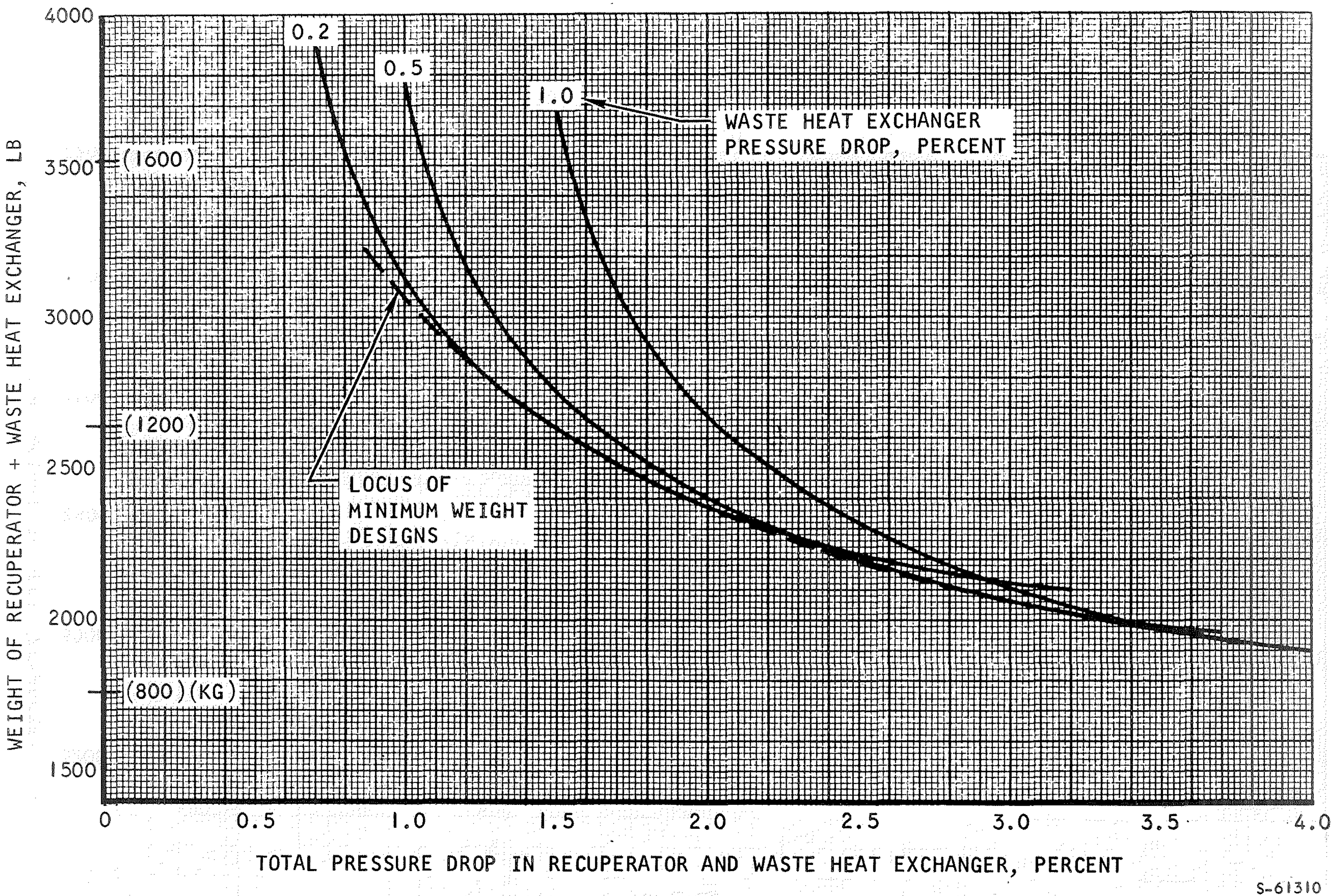

Figure 4-17. Waste Heat Exchanger/Recuperator Optimization for Case II with Triangular-End Recuperator

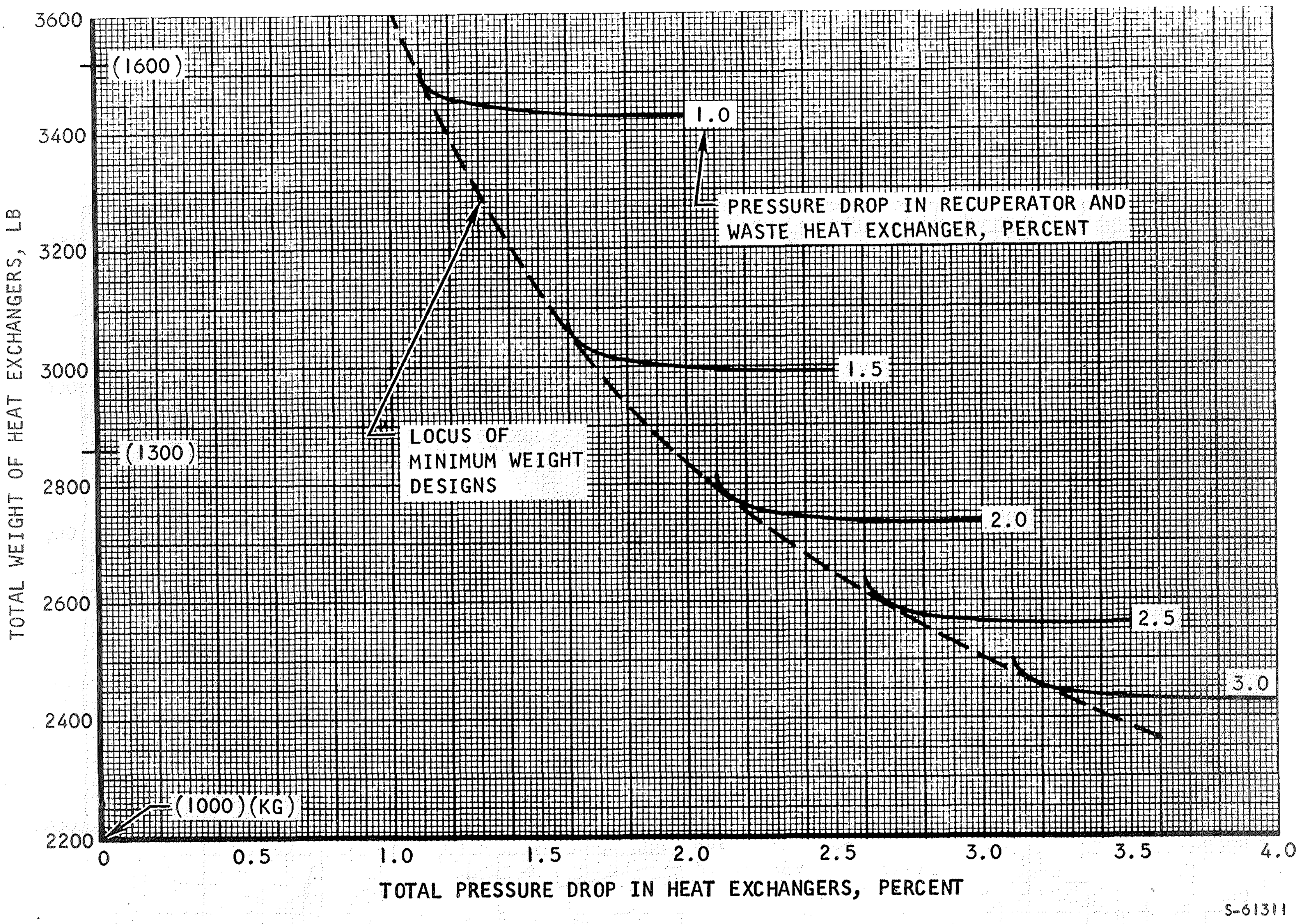

Figure 4-18. System Optimization for Case II with Triangular-End Recuperator

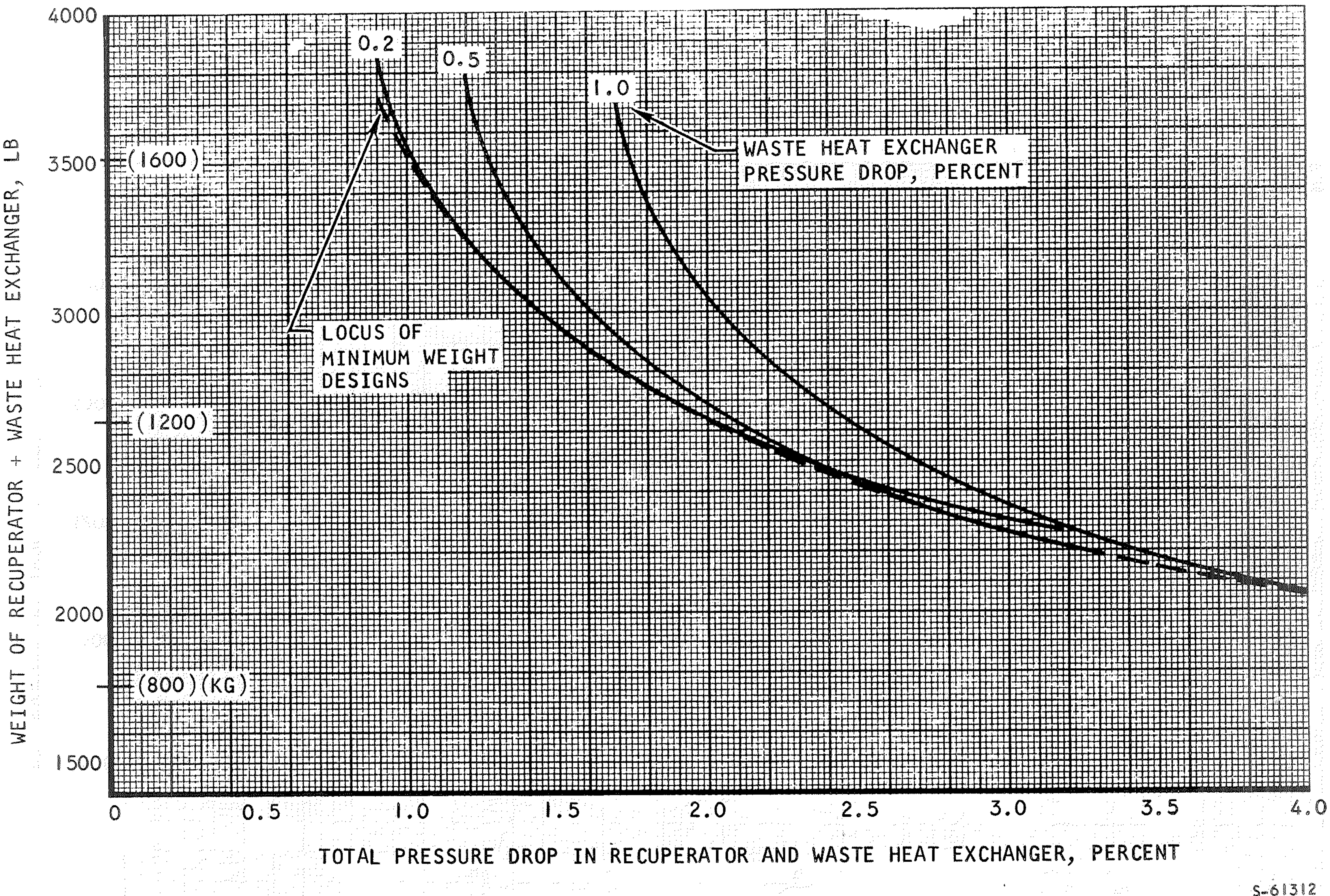

Figure 4-19. Waste Heat Exchanger/Recuperator Optimization for Case II with Rectangular-End Recuperator

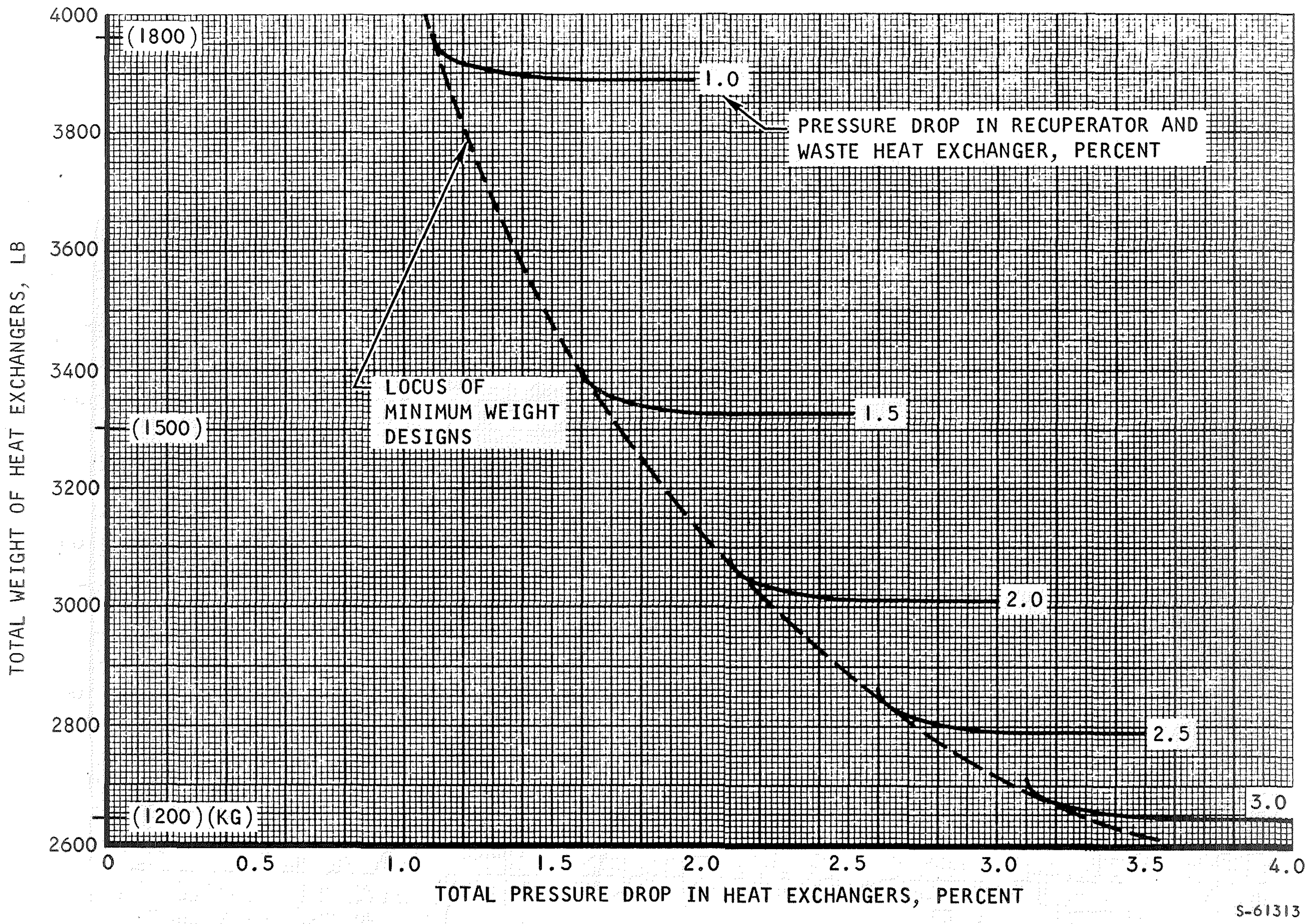

Figure 4-20. System Optimization for Case II with Rectangular-End Recuperator

Using the optimum pressure drop allocations, the heat exchanger designs for the two minimum-weight systems are summarized in Tables 4-7 and 4-8. Total heat exchanger weight for the triangular-end recuperator system is 2640 lb (1200 kg) and total weight for the rectangular-end recuperator system is 2895 lb (1310 kg). In both system designs, the heat source heat exchanger tube length has been set approximately equal to the recuperator stack height, which limits the mismatch in face areas between these two heat exchangers to one dimension only. Similarly, the waste heat exchanger liquid flow length was increased to match the recuperator stack height as nearly as possible within the restriction of a maximum liquid pressure drop of 10.0 psi ($68.9\ kN/m^2$). Exact matches in this one dimension could be obtained with waste heat exchanger liquid pressure drops of approximately 12.9 and 13.5 psi (88.9 and $93.1\ kN/m^2$), respectively, for triangular- and rectangular-end section systems.

PACKAGING

Package Configuration

The selected system configuration for Case II is shown in Drawing SK51815. The packaging configuration is similar to that used for the Case I HXDA, and the factors leading to this arrangement of components and ducts are discussed in Section 3. The system incorporates heat exchangers with matched face areas, a triangular-end recuperator, and a waste heat exchanger with the 16R-0.100 (630R-0.00254) liquid-side fin (Table 4-4). The triangular-end recuperator is used in preference to the rectangular-end recuperator because of the associated weight advantage of approximately 600 lb (272 kg) total for the three heat exchangers in the HXDA system.

The individual heat exchangers in the Case II HXDA are shown in Drawings SK51816, SK51817, and SK51818.

Ducting

Gas duct and manifold sizes were calculated for the packaging configuration of Drawing SK51815. Duct diameters were established to maintain a constant gas velocity head in all four ducts while meeting the manifold/ducting pressure drop allocation of 0.5 percent. Full-radius manifolds are used throughout the system.

Listed in Table 4-9 are manifold and duct sizes and weights. Ducting material is Hastelloy X for all manifolds and ducts with the exception of the heat source heat exchanger outlet manifold and the turbine inlet duct, which are constructed of Cb-1 percent Zr. Wall thicknesses are based on structural pressure (Table 4-1), with a minimum allowable thickness of 0.032 in. (8.1×10^{-4}m). Total weight of the ducting system is 556 lb (252 kg).

TABLE 4-7

CASE II HXDA
TRIANGULAR-END RECUPERATOR
MINIMUM WEIGHT SOLUTION

Recuperator	
Gas pressure drop	1.95 percent
Weight	1382 lb (628 kg)
Core length	12.3 in. (0.312 m)
End section height, hot end	6.7 in. (0.170 m)
cold end	4.1 in. (0.104 m)
End section ratio, hot end	0.65
cold end	0.58
Width	23.5 in. (0.597 m)
Stack height	46.9 in. (1.19 m)
Waste Heat Exchanger	
Gas pressure drop	0.40 percent
Weight	845 lb (384 kg)
Liquid pressure drop	10.0 psi (68.9 kN/m^2)
Gas-flow length	11.9 in. (0.302 m)
Liquid-flow length	42.4 in. (1.08 m)
Stack height	25.8 in. (0.655 m)
Heat Source Heat Exchanger	
Gas pressure drop	0.15 percent
Weight	413 lb (188 kg)
Liquid pressure drop	0.4 psi (2.76 kN/m^2)
Gas-flow length	5.1 in. (0.130 m)
Tube length	46.9 in. (1.19 m)
No-flow length	24.9 in. (0.632 m)
Number of tubes	250
Number of tube rows	10
Number of passes	4

TABLE 4-8

CASE II HXDA
RECTANGULAR-END RECUPERATOR
MINIMUM WEIGHT SOLUTION

Recuperator	
Gas pressure drop	2.0 percent
Weight	1620 lb (736 kg)
Core length	11.6 in. (0.295 m)
End section height, hot end	7.9 in. (0.201 m)
cold end	6.0 in. (0.152 m)
Total length	18.6 in. (0.472 m)
Width	24.2 in. (0.615 m)
Stack height	48.3 in. (1.23 m)
Waste Heat Exchanger	
Gas pressure drop	0.35 percent
Weight	862 lb (392 kg)
Liquid pressure drop	10.0 psi (68.9 kN/m^2)
Gas-flow length	11.3 in. (0.287 m)
Liquid-flow length	42.8 in. (1.09 m)
Stack height	27.2 in. (0.691 m)
Heat Source Heat Exchanger	
Gas pressure drop	0.15 percent
Weight	413 lb (188 kg)
Liquid pressure drop	0.4 psi (2.76 kN/m^2)
Gas-flow length	5.1 in. (0.130 m)
Tube length	47.9 in. (1.22 m)
No-flow length	24.4 in. (0.620 m)
Number of tubes	245
Number of tube rows	10
Number of passes	4

TABLE 4-9

CASE II DUCTS AND MANIFOLDS

Duct/Manifold Component		Diameter, in. (m)	Wall Thickness, in. (m x 10^4)	Weight, lb (kg)
Duct	Compressor outlet	7.90 (0.201)	0.032 (8.1)	12 (5)
	Turbine inlet	9.50 (0.241)	0.272 (69.1)	159 (72)
	Turbine outlet	10.50 (0.267)	0.131 (33.3)	94 (43)
	Compressor inlet	8.60 (0.218)	0.032 (8.1)	26 (12)
Manifold	Recuperator High Pressure in	12.40 (0.315)	0.044 (11.2)	15 (7)
	HSHX out	11.10 (0.282)	0.317 (80.5)	101 (46)
	Recuperator Low Pressure in	19.40 (0.493)	0.243 (61.7)	134 (61)
	WHX out	16.40 (0.416)	0.032 (8.1)	15 (7)
Total		———	———	556 (253)

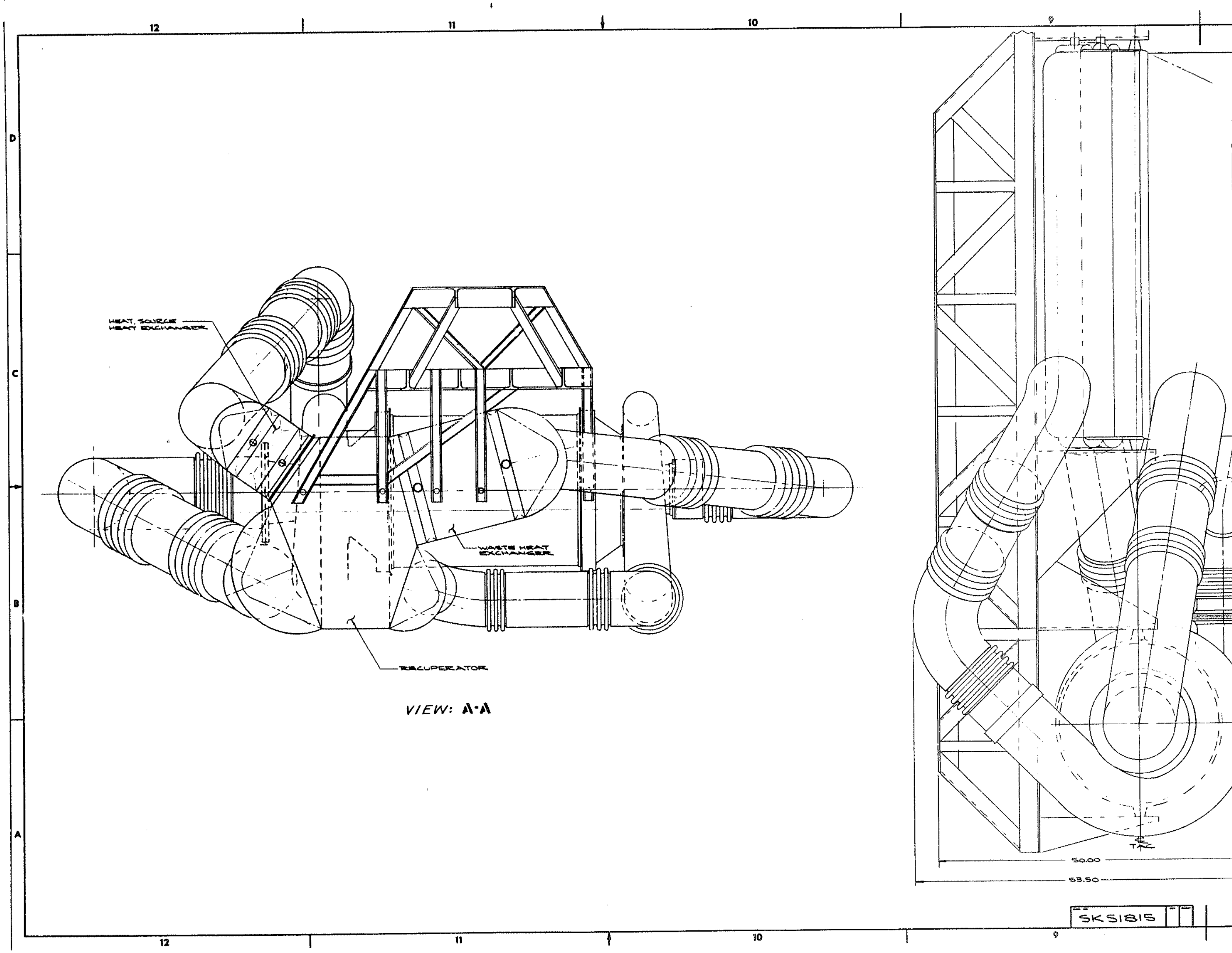

AIRESEARCH MANUFACTURING COMPANY
Los Angeles, California

FOLDOUT FRAME 1

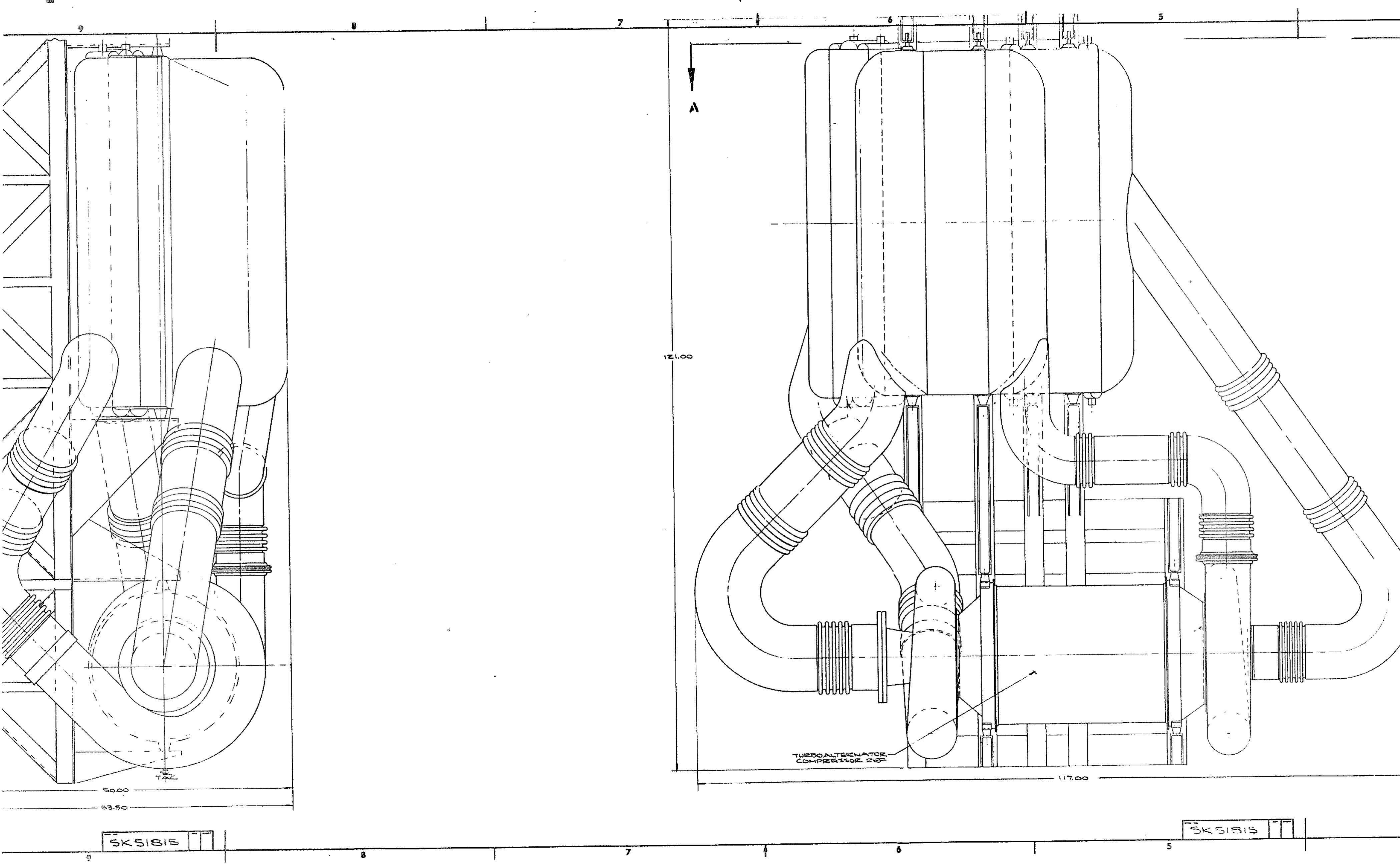

FOLDOUT FRAME 2

FOLDOUT FRAME 3

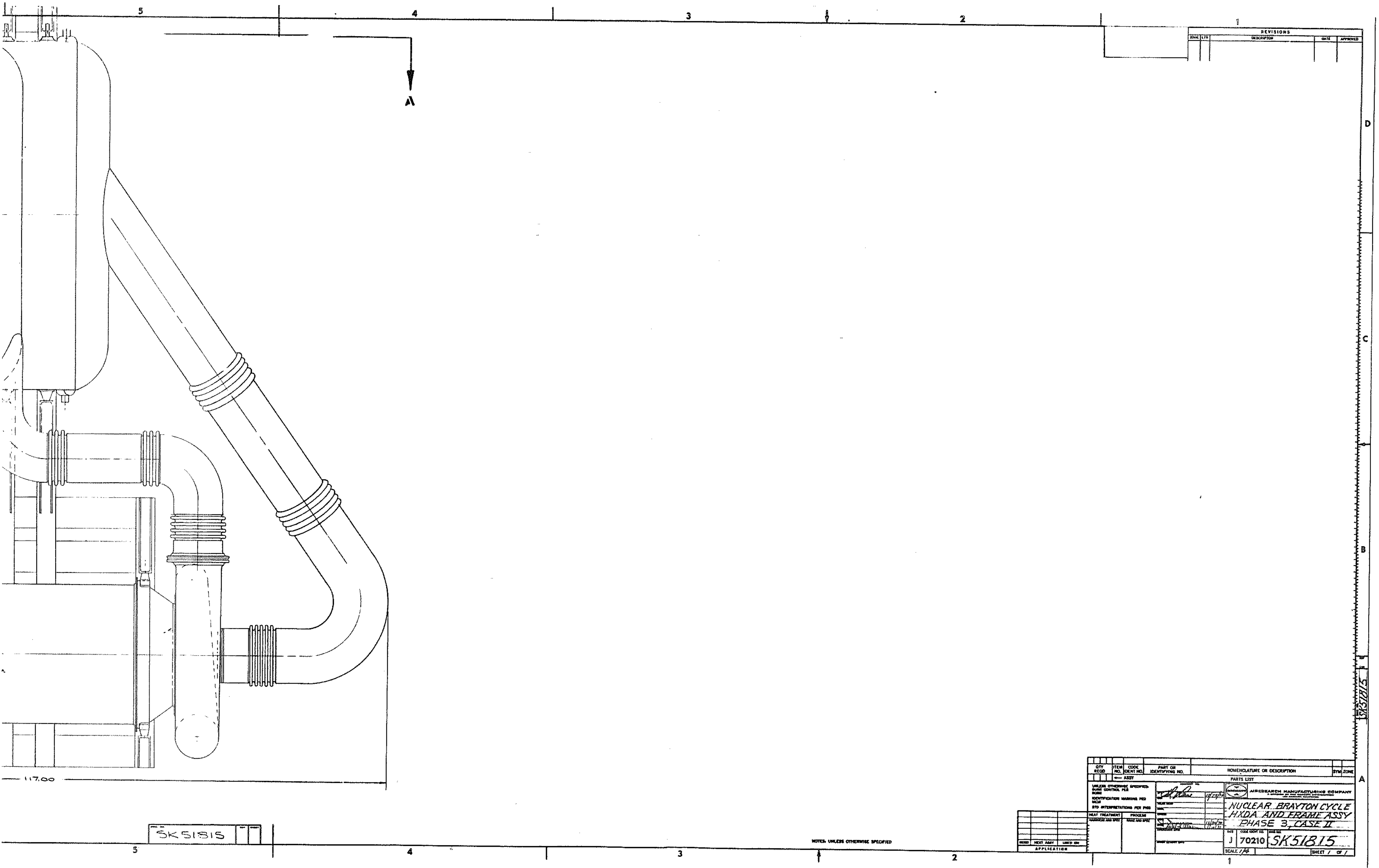

FOLDOUT FRAME 3

FRAME 4

FRAME 5

PRECEDING PAGE BLANK NOT FILMED

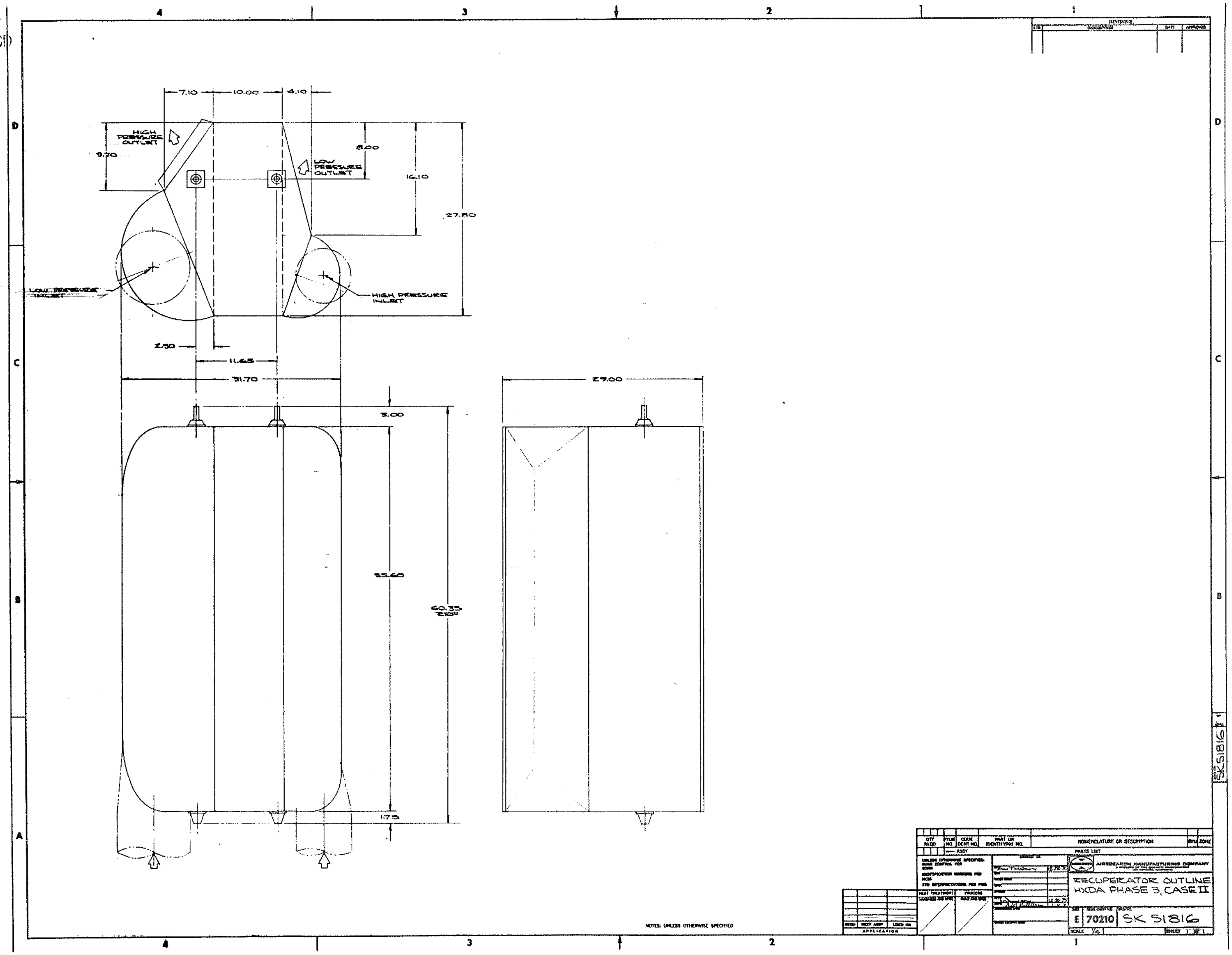

PRECEDING PAGE BLANK NOT FILMED

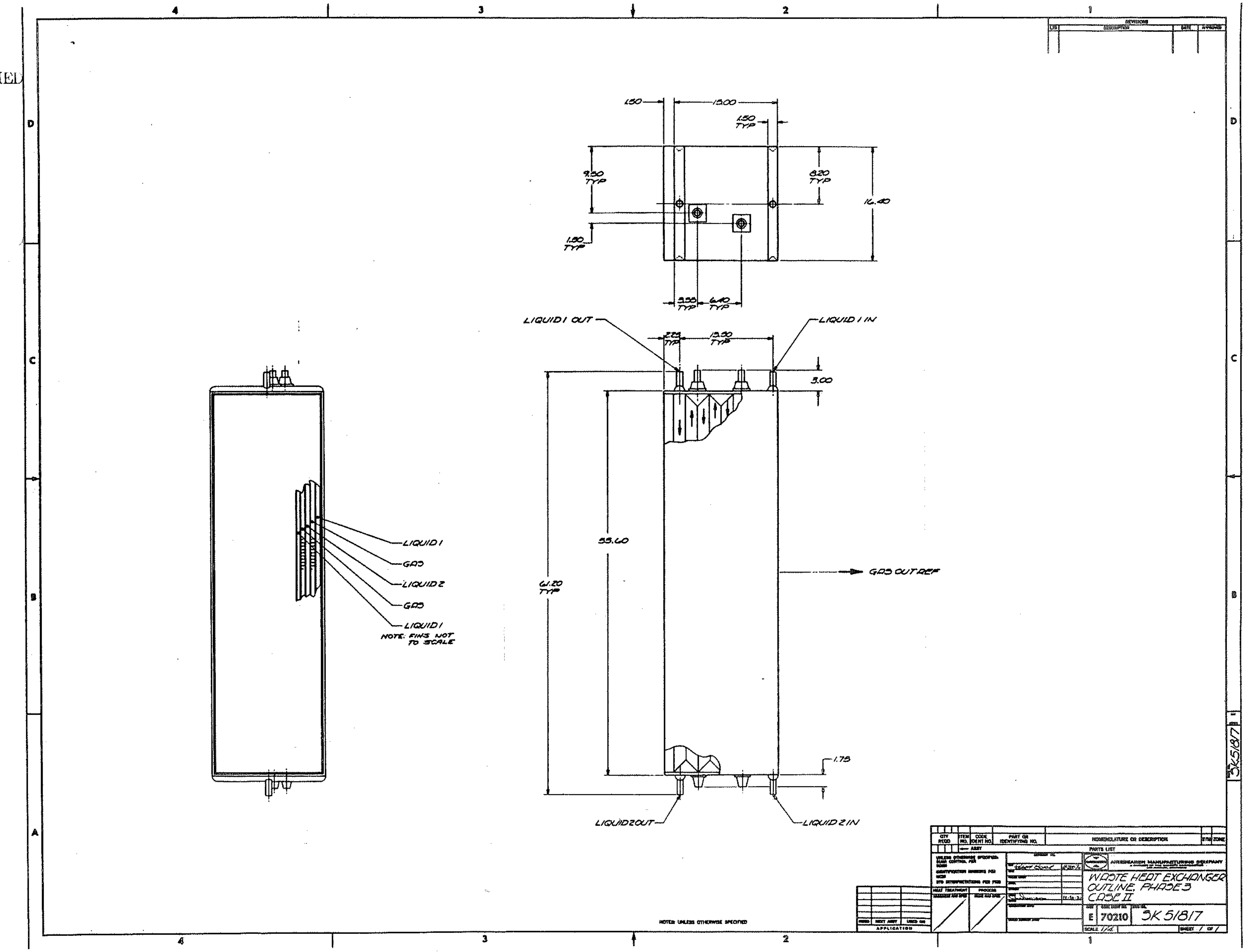

FOLDOUT FRAME 1

FOLDOUT FRAME 2

AIRESEARCH MANUFACTURING COMPANY
Los Angeles, California

ECEDING PAGE BLANK NOT FILMED

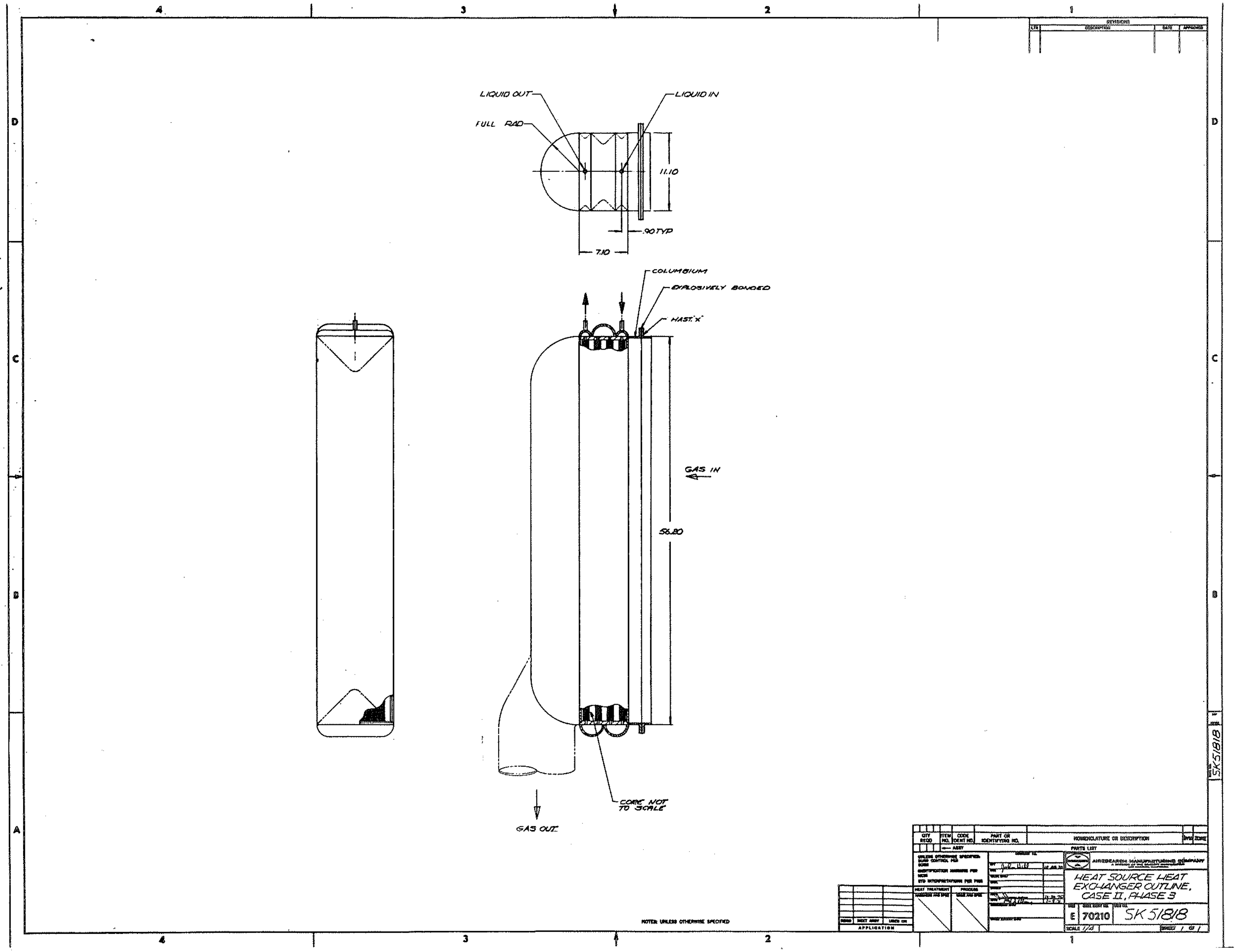

FOLDOUT FRAME 1

FOLDOUT FRAME 2

Frame

Design of a mounting frame for the HXDA is discussed in Section 6. Estimated weight of the frame shown in Drawing SK51815 is 300 lb (136 kg).

SYSTEMS COMPARISON

A summary of the six HXDA designs obtained for Case II is presented in Table 4-10. The penalty associated with face area matching while maintaining a waste heat exchanger liquid pressure drop of 10.0 psi (68.9 kN/m^2) or less is 380 lb (173 kg) in total heat exchanger weight for the system with the triangular-end recuperator and 720 lb (327 kg) in total heat exchanger weight for the rectangular-end case. However, weights associated with structural reinforcement of the connecting ducts or transition sections required for nonmatched heat exchangers would reduce this weight penalty.

Comparing the two recuperator types analyzed, the system incorporating the triangular-end recuperator is about 600 lb (270 kg) lighter than the one with the rectangular-end recuperator. For this reason, the triangular-end recuperator is preferred for this case. Total weight of the HXDA using the preferred recuperator geometry is 3574 lb (1623 kg).

2100°F (1421°K) GROWTH SYSTEM

A brief analysis was made of the effect of structually sizing the HXDA design for capability in a system operating at 2100°F (1421°K) turbine inlet temperature. The thermodynamic design point used is based on the 1600°F (1144°K) turbine inlet conditions. Thus, this growth system would have the capability of operating anywhere in the range of 1600°F (1144°K) to 2100°F (1421°K). The material changes required to provide this high-temperature capability are (1) a change from Hastelloy X to Cb-1 percent Zr in the recuperator, (2) a change from Cb-1 percent Zr to T-111 for the heat source heat exchanger tubes (Cb-1 percent Zr is still assumed for the fins), and (3) the use of NaK as the heat rejection fluid, resulting in a finned-tubular waste heat exchanger with Haynes 25 tubing and copper fins.

Estimated heat exchanger weights for the 2100°F (1421°K) temperature level are compared with the corresponding weights for the 1700°F (1200°K) structural requirement in Figure 4-21. Recuperator weight is less in the 2100°F (1421°K) system because the Cb-1 percent Zr fins are thinner than the Hastelloy X fins required at 1700°F (1200°K). Heat source heat exchanger and waste heat exchanger weights are higher for the 2100°F (1421°K) system because of the additional structure required for gas containment at the higher temperature levels.

TABLE 4-10

CASE II SYSTEMS SUMMARY

Item	Rectangular-End Recuperator			Triangular-End Recuperator		
	Matched Faces			Matched Faces		
	16R-0.100 (630R-0.00254) WHX Liquid Fin	20R-0.075 (788R-0.00190) WHX Liquid Fin	Minimum Weight	16R-0.100 (630R-0.00254) WHX Liquid Fin	20R-0.075 (788R-0.00190) WHX Liquid Fin	Minimum Weight
Weight, lb (kg)						
HSHX	371 (168)	371 (169)	413 (188)	374 (170)	373 (169)	413 (188)
Recuperator	2195 (996)	2174 (987)	1620 (736)	1778 (807)	1720 (781)	1382 (628)
WHX	1049 (476)	955 (434)	862 (392)	866 (393)	785 (356)	845 (384)
Total HX	3615 (1640)	3500 (1590)	2895 (1316)	3018 (1370)	2878 (1306)	2640 (1200)
Manifolds and ducts	-	-	-	556 (253)	-	-
Total HXDA	-	-	-	3574 (1623)	-	-
Insulation*	-	-	-	509 (231)	-	-
Frame	-	-	-	300 (136)	-	-
HSHX liquid ΔP, (kN/m^2)	1.6 (11.0)	1.6 (11.0)	0.4 (2.76)	1.1 (7.59)	1.1 (759)	0.4 (2.76)
WHX liquid ΔP, (kN/m^2)	8.2 (56.5)	18.0 (124)	10.0 (68.9)	10.0 (68.9)	22.0 (152)	10.0 (68.9)

*Based on 2.0 in. (0.0508 m) of insulation at 20 lb per cu ft (320 kg/m^3) on all heat exchangers and ducts.

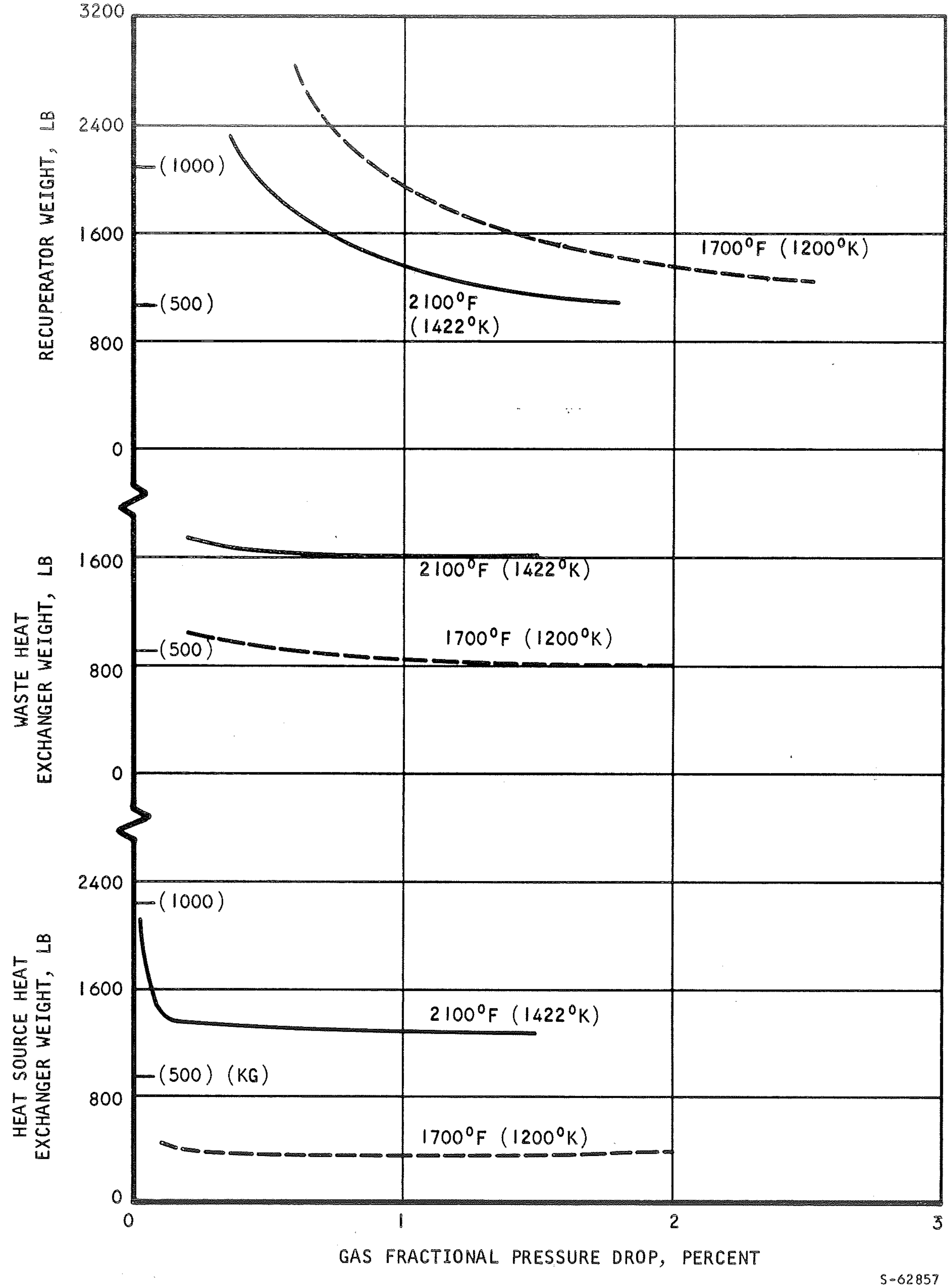

Figure 4-21. Comparison of 1700°F (1200°K) and 2100°F (1421°K) Structural Designs for Case II Heat Exchanger

SECTION 5

RECUPERATOR END SECTION DESIGN

DESIGN PROCEDURE

Triangular Ends

The end sections utilized in the HXDA recuperator designs are sized to provide uniform flow distribution in the counterflow cores. Sizing for uniform flow results in asymmetrical, unequal end section geometries at the two recuperator ends. Use of the same geometry at each end would result in poor gas flow distribution because, although all gas flow paths through equally sized ends would be of equal length, they would not result in equal pressure drops for given mass velocities. The nonuniformity in pressure drops for equal flows along parallel flow paths is due to the large change in gas density (and a smaller change in gas viscosity) that occurs from the inlet to the outlet end of the recuperator.

Figure 5-1 shows a single low-pressure-side fin sandwich of a triangular-end recuperator. Three parallel gas flow paths through the heat exchanger are identified by dashed lines. For uniform core flow distribution, the total (inlet-to-outlet) pressure drop along each flow path should be the same for a constant value of the gas mass velocity. Since the entrance, exit, and turn losses are equal for all three flow paths, regardless of end section geometry, this requirement reduces to a requirement for equal frictional losses, i.e.,

$$\Delta P_{f\ 1A} + \Delta P_{f\ 1B} = \Delta P_{f\ 2A} + \Delta P_{f\ 2B} = \Delta P_{f\ 3A} + \Delta P_{f\ 3B}$$

where ΔP_f = friction pressure drop.

Since $\Delta P_{f\ 1B} = \Delta P_{f\ 3A}$, this is equivalent to the condition

$$\Delta P_{f\ 1A} = \Delta P_{f\ 3B}, \text{ or } \Delta P_{f\ 2A} = \Delta P_{f\ 2B} .$$

That is, for uniform flow distribution, the average frictional pressure loss in the inlet end should be equal to the average frictional pressure loss in the outlet end. This is not equivalent to requiring the average total pressure drops to be equal because kinetic losses at opposite ends are not equal.

Figure 5-1b shows the high-pressure-side fin sandwich for the same recuperator. Similar considerations as those discussed for flow distribution on the low-pressure side apply to the high-pressure side. Thus, to obtain uniform flow distribution throughout the heat exchanger, the end section geometries must be such that the inlet frictional loss equals the outlet frictional loss on each side of the exchanger. Within this requirement, a number of design solutions exist, because for each geometry selected at one end of

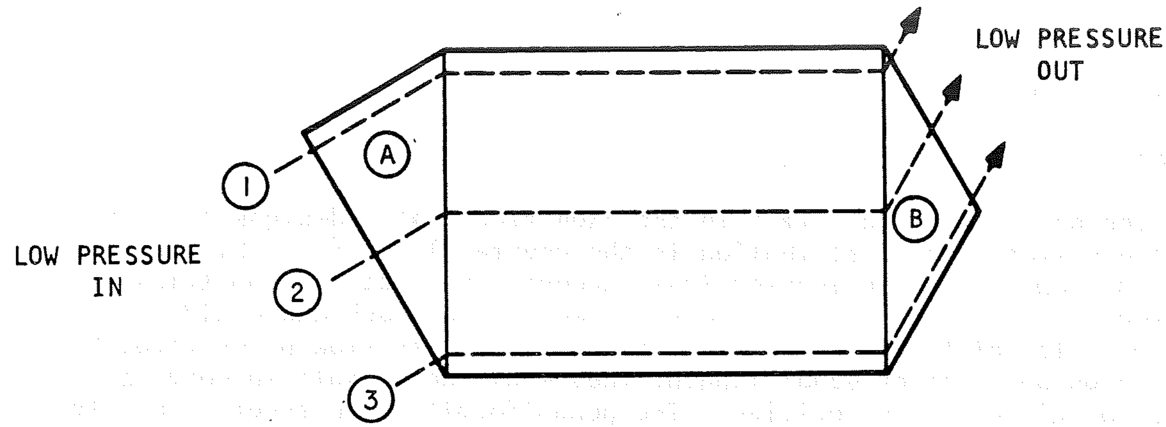

a. Low-Pressure Side Fin Sandwich

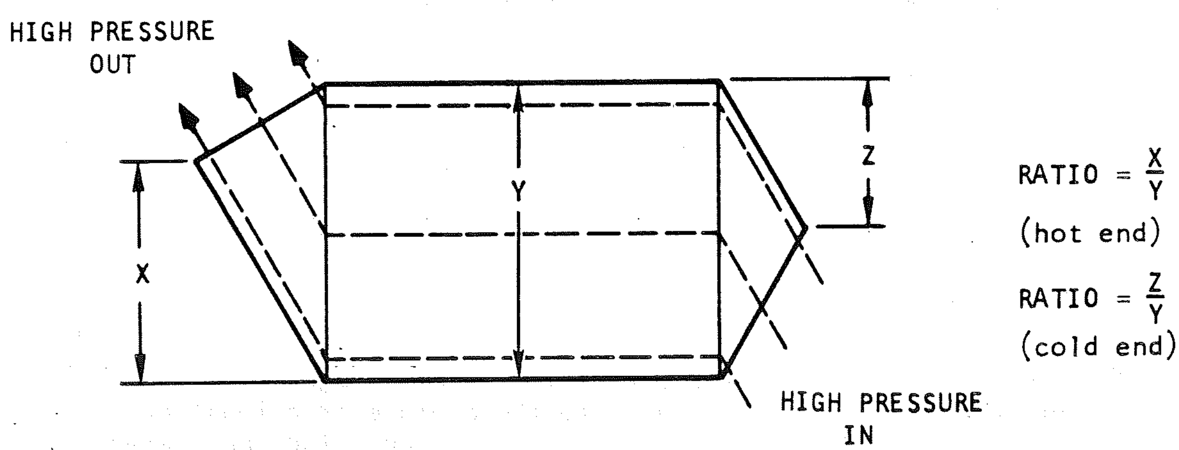

b. High-Pressure Side Fin Sandwich

S-62855

Figure 5-1. Triangular-End Recuperator Geometry the exchanger, there is in general a geometry at the other end (obtained by varying end section RATIO and height) that results in balanced pressure drops on both sides. Solutions can be obtained graphically, as was done in Phase I of this study, or by iteration. The iterative procedure was programmed on the IBM 360 for use in the Phase III design studies.

Rectangular Ends

A typical high-pressure-side passage for the rectangular-end recuperator is shown in Figure 5-2a. Following the same reasoning that was applied to the triangular-end design, uniform flow distribution is obtained by requiring that the frictional pressure drop along path 1 equal the frictional pressure drop along path 3 for equal gas mass velocities in these two paths. Since the unequal end sections result in unequal core flow lengths, core pressure drops must be included in the analysis for this recuperator. Thus, for uniform flow,

$$\Delta P_{f\ A1} + \Delta P_{f\ C1} = \Delta P_{f\ B3} + \Delta P_{f\ C3}$$

This is equivalent to

$$\Delta P_{f\ B2} - \Delta P_{f\ A2} = \frac{1}{2} \Delta P_c \ (L_{c1} - L_{c3})$$

where ΔP_c = counterflow core (high-pressure side) pressure drop per unit length

and L_{c1} and L_{c3} are core lengths as defined in Figure 5-2.

On the low-pressure side of the recuperator (Figure 5-2b), the gas makes a straight pass, and uniform flow distribution is obtained for any end section geometry. Thus, to obtain uniform flow distribution throughout the heat exchanger, the two end section heights are selected to obtain the pressure drop relationship derived above for the high-pressure passage. A number of design solutions exist because for each end-section height selected at one end of the recuperator, there is in general a corresponding height at the opposite end that results in uniform flow. An iterative calculation procedure for determining the required end-section designs was programmed for the Phase III design studies.

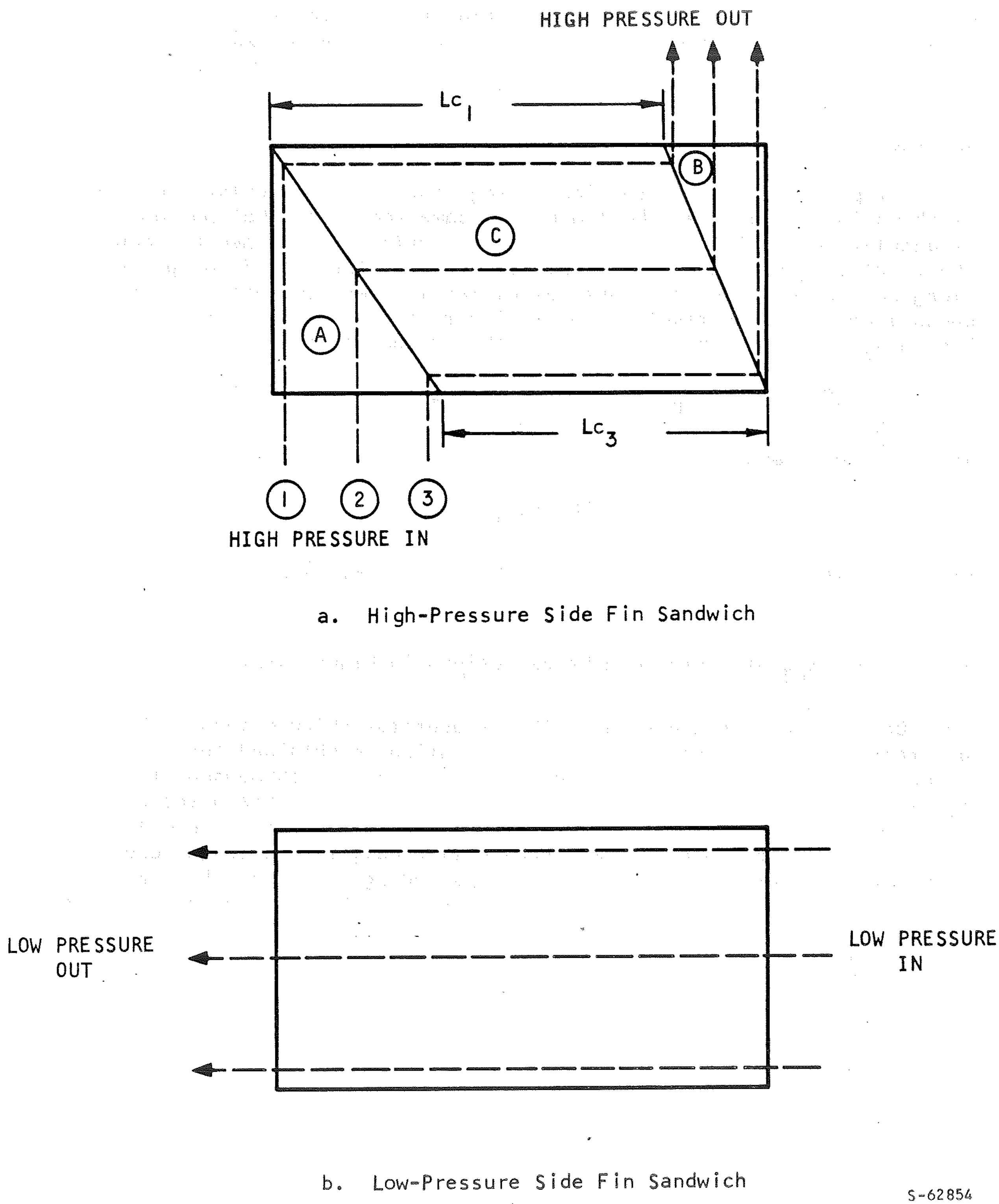

Figure 5-2. Rectangular-End Recuperator Geometry

COMPUTER PROGRAM

Computer program H1440 was written to calculate recuperator end section configurations (either triangular or rectangular) that result in uniform core flow distribution. The end-section geometries considered are those shown schematically in Figures 5-1 and 5-2. The program utilizes an iterative procedure to determine the required end section geometry at the high-pressure inlet end of the recuperator for a given geometry at the low-pressure inlet end. Thus, the program iterates on high-pressure inlet end section height when the specified geometry is rectangular and on both height and RATIO (see Figure 5-1) when the specified geometry is triangular. For each set of end sections determined in this manner, the total end section pressure drops (including entrance, exit, turning, and friction losses) are calculated. Total end section weight, based on volume and an input weight factor, also is calculated

Input to the program includes recuperator counterflow section geometry; counterflow section pressure drop per unit length (only required for rectangular-end-section designs); flow rates, temperatures, and pressures on both sides at both ends; the gas density factor (a number proportional to gas molecular weight) on both sides; and the series of end-section geometries at the low-pressure inlet end for which solutions are desired. The end-section geometry specification includes end-section height, RATIO, fin thickness (each side), and number of fins per inch (each side). Plain, rectangular fins are used in the end sections. Fluid viscosities, friction factors, expansion and contraction coefficients, and turning loss coefficients are input in tabular form.

A typical solution in the computer printout is shown in Figure 5-3. The first three lines of output give input values of pressure, temperature, flow, end section geometry, and counterflow core geometry. In addition, the calculated high-pressure-inlet end section geometry, as required for uniform flow distribution, is given on the second line. Line 4 gives total pressure drop for each end, expressed both in lb per sq in. and as a percentage of the inlet pressure. Line 5 gives the corresponding frictional pressure drops. Line 6 gives additional end section data, including volume and weight (total for both ends) and flow Reynolds numbers. The seventh line of output gives the total of the percentage pressure losses in each end section.

A complete listing of H1440 is given in the Appendix.

```
                    LOW  PRESSURE  SIDE                                                   HIGH  PRESSURE  SIDE
  FLOW      INLET TEMP  OUTLET TEMP  PRESS IN  PRES OUT              FLOW     INLET TEMP  OUTLET TEMP  PRESS IN  PRES OUT
 LB/SEC         R            R         PSIA      PSIA               LB/SEC        R             R         PSIA      PSIA
  7.1000   1325.000      846.000      71.500    70.500              7.1000     807.000      1286.000    126.000   125.000

 LOW PRESSURE IN      HIGH PRESSURE IN
HEIGHT,IN    RATIO     HEIGHT,IN    RATIO    TESTI  RECT.TURN CON  NO.FIN LP   NO.FIN HP   FIN THICK LP,IN  FIN THICK HP,IN
  8.000      0.700       4.136      0.587    0.0         0.0         10.00       10.00         0.0062            0.0099

WIDTH,IN 13.4000     NO.FLOW,IN  27.000     PASSAGE HT. LP  .153     PASSAGE HT. HP  .125

        LOW PRESSURE SIDE,PRESSURE DROPS                                  HIGH PRESSURE SIDE,PRESSURE DROPS
INLET,PSIA   OUTLET,PSIA   INLET,PERCENT   OUTLET,PERCENT    INLET,PSIA  OUTLET,PSIA  INLET,PERCENT  OUTLET,PERCENT
  0.0522       0.1011         0.0731          0.1415           0.2026      0.1683       0.1608          0.1336
  0.0374       0.0361         0.0523          0.0506           0.0867      0.0894       0.0688          0.0709  FRICT DP
VOLUME,CU.IN  WEIGHT,LB    DIMENSIONS,IN   L.P. RH,FT  H.P. RH,FT  IN RE  LP   OUT RE  LP   IN RE  HP   OUT RE  HP
 2195.4180    117.2353     8.893   6.904   0.002385    0.002106   1917.22      3951.26      6190.61      3161.11

 TOTAL PRESSURE DROP=   0.5089 PERCENT
```

Figure 5-3. Typical Output, End-Section Design Program

SECTION 6

STRUCTURAL DESIGN CONSIDERATIONS

INTRODUCTION

Preliminary structural design and analysis was performed for the two HXDA systems, Case I with a maximum design temperature of 1300°F (980°K) and Case II with a maximum temperature of 1770°F (1240°K). The above temperatures are associated with the liquid inlet to the heat source heat exchanger. Since this unit has the most severe operating conditions in the HXDA, the heat exchanger structural design effort was directed toward determining the feasibility of the HSHX tubular design and its mounting location on the recuperator. The preliminary analysis showed that the Haynes 25 unit for Case I was satisfactory; however, for the Case II design the heat exchanger and structural concept becomes marginal at the higher temperatures.

The mounting system established for the HXDA and TAC includes provisions for thermal expansion and support of vehicle launch loads. Preliminary frame designs had an estimated weight of 120 lb (54 kg) for Case I and 300 lb (136 kg) for Case II. Three link-type convoluted bellows in each of the four ducts in the HXDA package provide the required flexibility to accommodate differential thermal expansion between the TAC and HXDA. Preliminary bellows geometry was established for the high temperature duct connecting the HSHX and TAC in the Case I design. However, analysis indicated that the Case II high temperature bellows may require use of a material such as the tantalum T-111 or some external cooling of the convolutes. Since the other bellows in the two systems operate at lower temperatures, there are no design difficulties.

DESIGN CRITERIA

The operating requirements of the system include a 50,000-hr service life and inertia loads during vehicle operation. The inertia loads were based on the use of an isolation system which limits the load to 24 g in any direction. The natural frequencies of the components will be greater than 50 Hz to avoid the isolation system frequencies. In addition, the components must withstand a minimum of 100 complete operating cycles (i.e., startup and shutdown).

A variety of load conditions, stress conditions, and types of failure mode possibilities will be experienced by the components during their service life. Although the emphasis in this study was on pressure and inertia loads, a comprehensive set of design criteria was used to accommodate pressure loads, inertia loads, and thermal stresses.

The standard design practice employed by AiResearch is to design the pressure carrying structure for proof pressures of 1.5 times the working pressures and for burst pressures of 2.5 times the working pressures. The structure must not yield at proof pressure or rupture at burst pressure. This implies that the proof pressure is the governing design condition if the ratio of yield stress to ultimate stress is less than 0.6 and that the burst pressure will govern if the ratio is greater than 0.6. The allowable stress at working pressure is, therefore, the lesser of the following:

$$\sigma_{all} = (\sigma_{ult})/2.5 \tag{6-1a}$$

$$\sigma_{all} = (\sigma_{y})/1.5 \tag{6-1b}$$

At elevated temperature for extended operating times, the above condition must be satisfied and, in addition, the component must be satisfactory for creep effects. A set of criteria for creep must be comparable to those for the short time loading. Accordingly, limitations based upon stress-to-rupture and stress-to-one-percent creep must be established. The rated design life of the unit is five years; it will be designed for sustained pressure operation at maximum operating temperature throughout the entire design life. Allowable stresses at working pressure must be the lesser of the following.

$$\sigma_{all} = \left[(\text{1-percent creep stress})_{50,000\ hr}\right]/1.2 \tag{6-2a}$$

$$\sigma_{all} = \left[(\text{creep-rupture stress})_{50,000\ hr}\right]/1.5 \tag{6-2b}$$

Material properties at elevated temperatures are very sensitive to temperature. For the candidate materials, an increase in temperature of $100^{o}F$ ($56^{o}K$) typically leads to a decrease of approximately 33 percent in creep and stress rupture strengths. Therefore, an allowance must be made to account for the possibility of overtemperature. The design temperature used to establish allowable stresses is taken to be the maximum operating temperature plus $100^{o}F$ ($56^{o}K$). The $100^{o}F$ ($56^{o}K$) overtemperature criteria results in an effective safety factor greater than those shown in Equation 6-2.

The above criteria were used for direct stresses; however, when the limiting stress is due to bending, a small amount of yielding can be allowed in the outermost fibers, which leads to a modified stress distribution through the thickness. Accordingly, the allowable indicated elastic stresses due to bending were taken to be 1.5 times the allowable values shown above. Inertia load allowables were the same as pressure stress allowables. The 24-g maximum load derivation is discussed below.

Thermal stresses (strains) were considered in the heat source heat exchanger and bellows designs. Low temperature allowable strains, where creep is not a factor, would be determined from the standard low-cycle fatigue relation where the number of cycles to failure N is related to the plastic strain range ϵ_{ρ} by

$$N = (C/\epsilon_{\rho})^{0.6} \tag{6-3}$$

Equation 6-3, by Manson, relates the cycle life to the material reduction-in-area properties RA by

$$C = \left[\ell n \frac{100}{100-RA}\right]^{0.6} \tag{6-4}$$

A safety factor of 2 would be used on the computed strain to achieve the desired 100 cycle life.

At elevated temperatures, where creep damage adds to the fatigue damage, a more restrictive criteria was used. It was assumed that repeated sustained thermal strains that lead to stress relaxation must be avoided. The elevated temperature thermal strains were therefore limited to the yield strain (stress) of the material to prevent repeating relaxation damage.

MATERIAL SELECTION AND PROPERTIES

Material choices for the various HXDA components were established during the conceptual design study (NASA CR-72783). The selections were primarily a function of component operating temperature. In the order of decreasing temperature, these components are (1) heat source heat exchanger, (2) recuperator, and (3) waste heat exchanger. The HSHX materials were Haynes 25 for Case I and Columbium-1Zr for Case II. In both cases the recuperator was Hastelloy X and the WHX was 347 stainless steel with nickel fins. Duct and bellows material selections were consistent with the heat exchanger materials. Allowable direct stresses versus maximum operating temperature, based on the above stress criteria, are shown in Figures 6-1 through 6-4 for 347 steel, Hastelloy X, Haynes 25, and Cb-1Zr, respectively.

HEAT SOURCE HEAT EXCHANGER DESIGN

The NaK-to-gas HSHX will be a tubular heat exchanger which is directly attached to the high-pressure gas outlet face of the recuperator. This heat exchanger is one of the critical components in the HXDA because it has the highest operating temperatures. In addition, it would be desirable to mount the HSHX directly on the recuperator; however, the resulting thermal stresses between the tubular and plate-fin heat exchanger types must be acceptable. For these reasons, the HSHX was analyzed in greater detail than the recuperator and WHX. The results indicate that the Haynes 25 heat exchanger at 1300°F (980°K) will be an acceptable Case I design; however, the Case II design with Cb-1Zr at 1770°F (1240°K) will require a more complex structure.

The HSHX design shown in Figure 6-5 includes details such as baffles, tie rods, and the recuperator joint area. The liquid flow, gas flow, and no-flow lengths shown in the figure provide a matching HSHX and recuperator face area design in the Case I Haynes 25 unit. The resulting material gauges and component weights for a 200-psi (1380-kN/m^2) gas pressure, 80-psi (550-kN/m^2) liquid pressure, 24-g inertia load and 50-Hz minimum material frequency requirement are summarized in Table I for the Haynes 25 unit. The total weight of 175 lb (80 kg) includes about 30 lb (14 kg) for the gas outlet manifold and transition structure between cores.

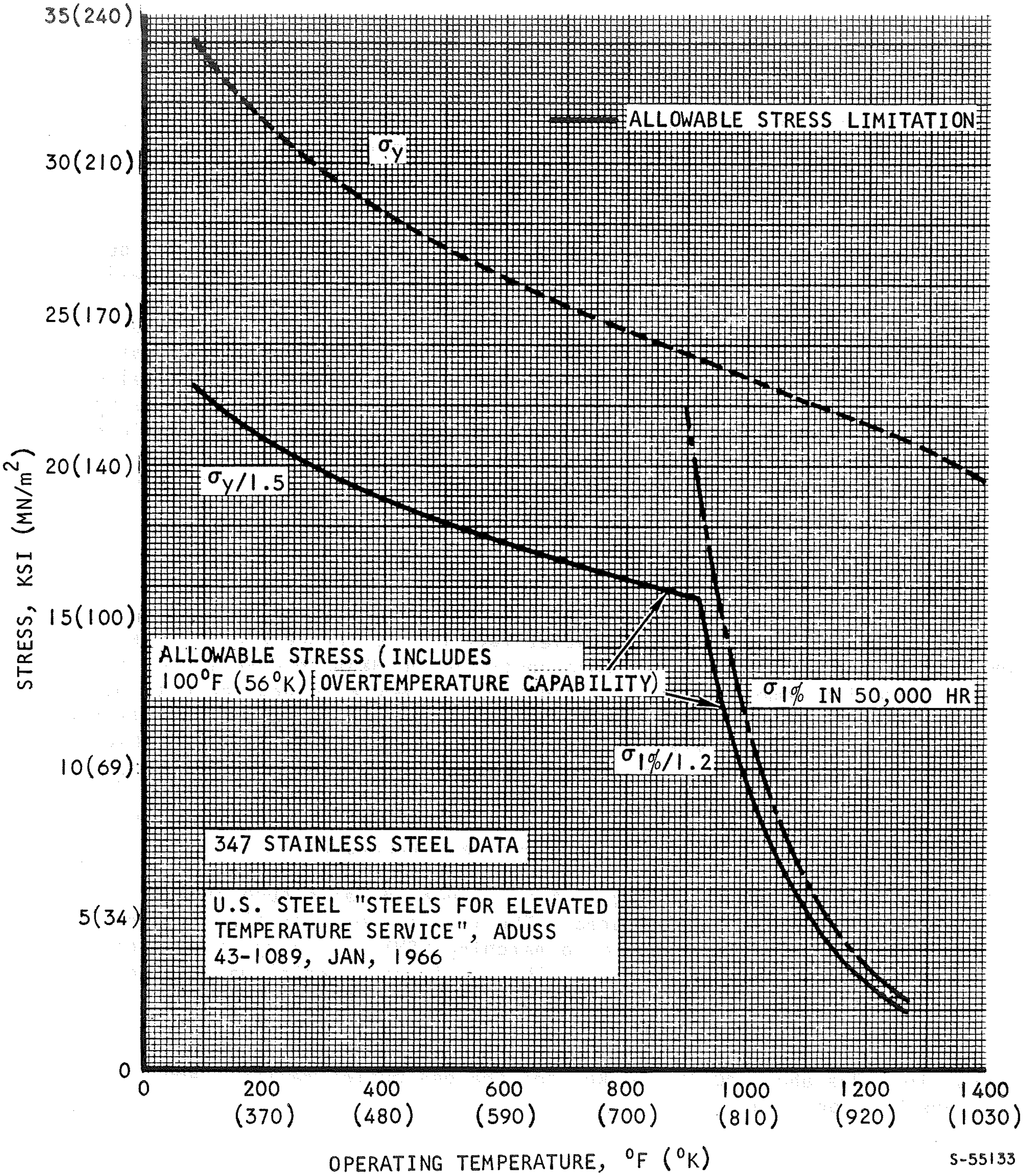

Figure 6-1. 347 Stainless Steel Allowable Stress vs Operating Temperature for 50,000 Hr Operation

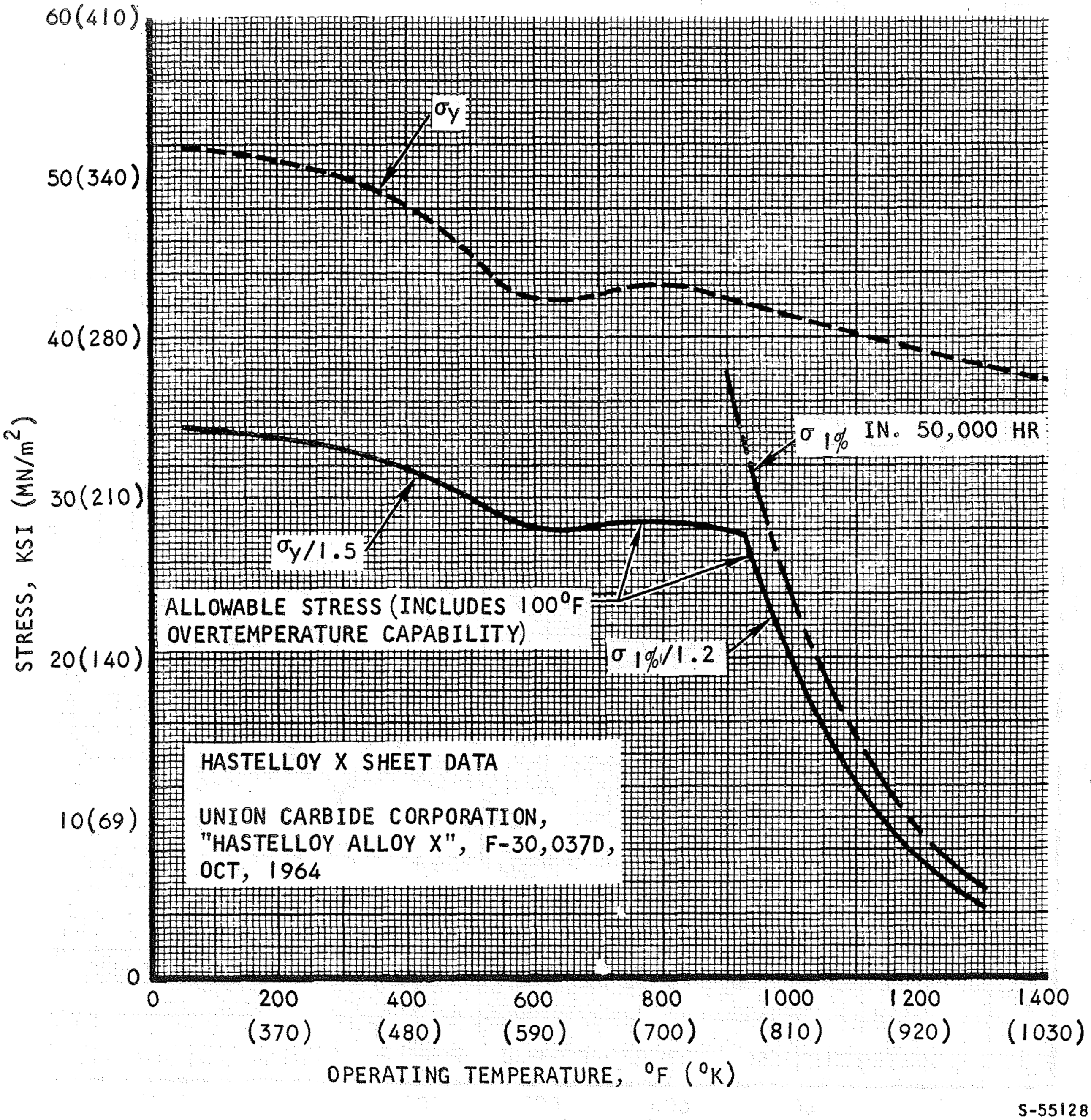

Figure 6-2. Hastelloy X Allowable Stress vs Operating Temperature for 50,000 Hour Operation.

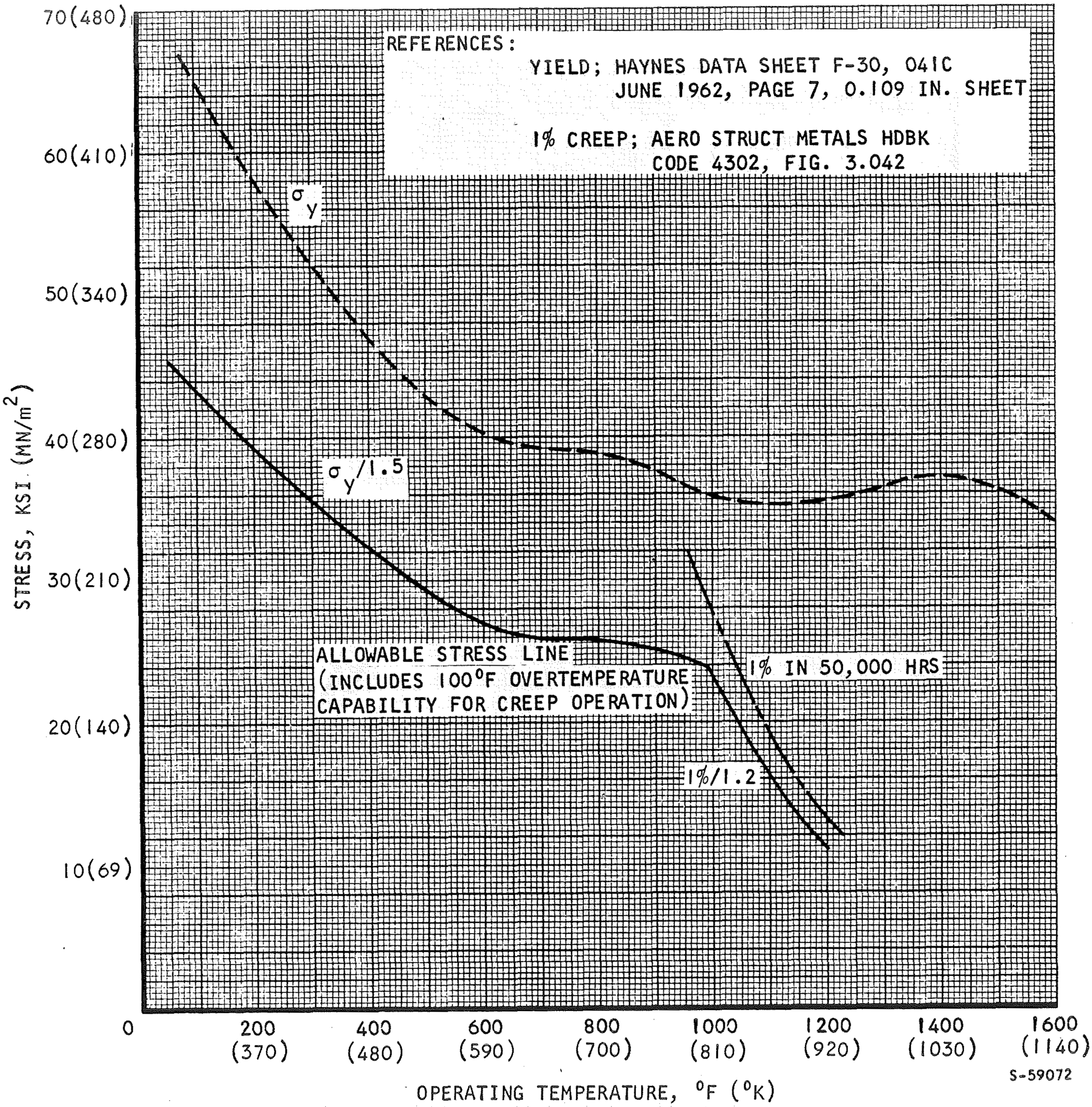

Figure 6-3. Haynes 25 Allowable Stress vs Operating Temperature for 50,000 hr Operation

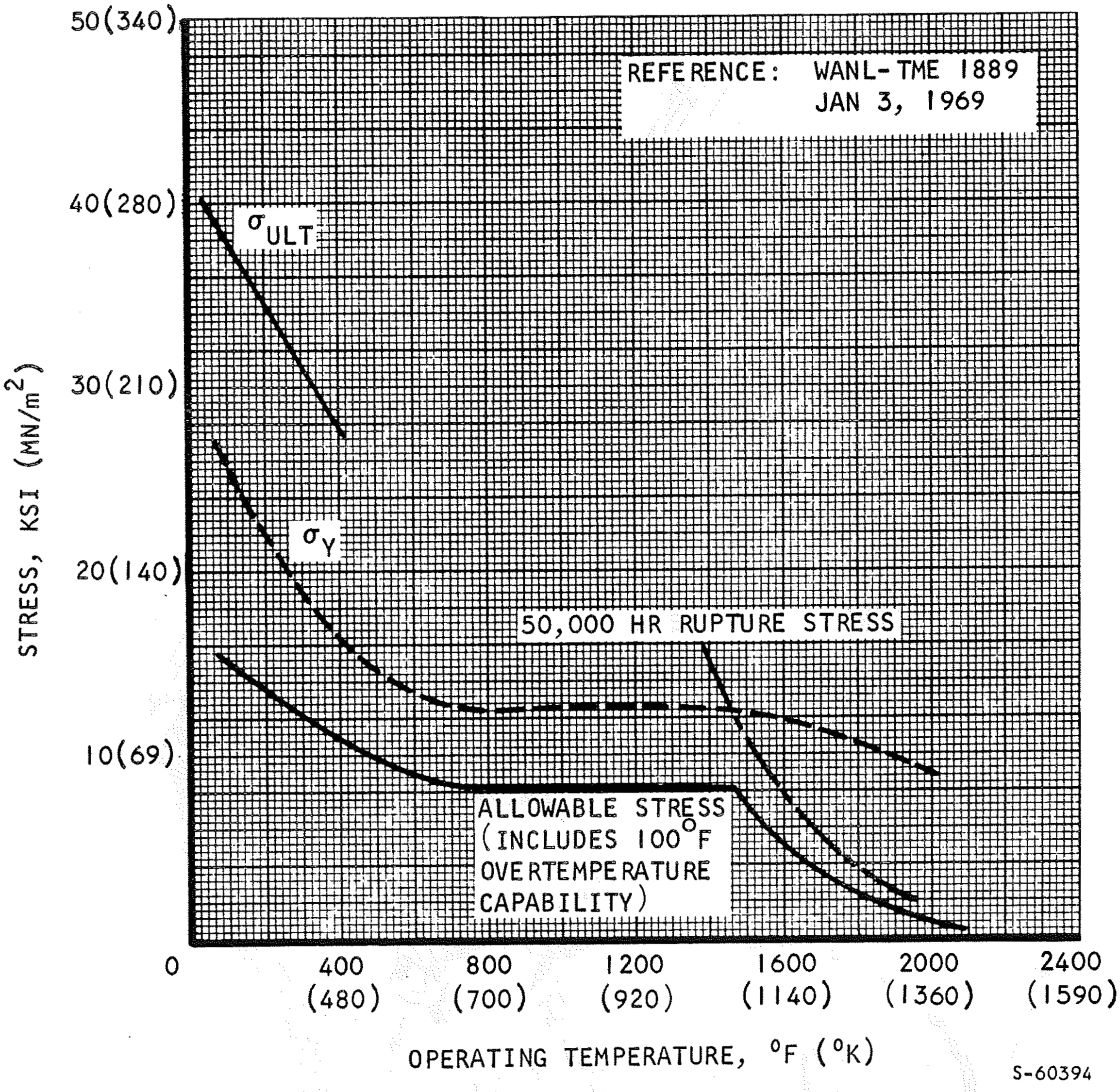

Figure 6-4. Columbium-1Zr Allowable Stress vs Operating Temperature for 50,000 hr Operation

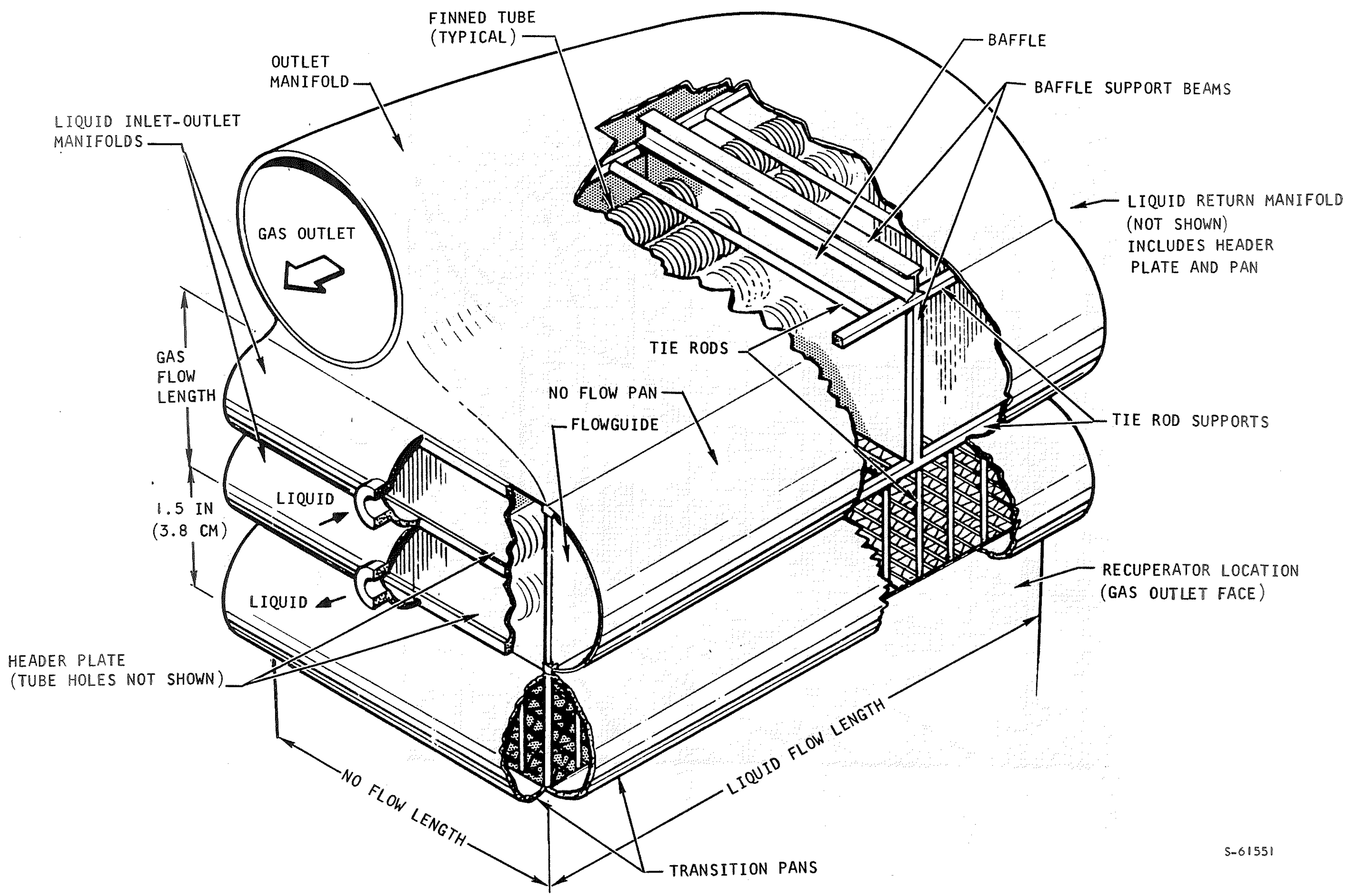

Figure 6-5. Heat Source Heat Exchanger Design

TABLE 6-1

HAYNES 25 HSHX WEIGHT SUMMARY

Component		Design Temperature, °F (°K)	Thickness, in. (cm)	Weight, lb (kg)
Type	Location			
Tubes and liquid		1300 (980)	0.02 (0.05)	74.0 (33.6)
Liquid manifolds	Inlet-outlet	1300 (980)	0.33 (0.84)	9.8 (4.5)
	Return	1300 (980)	0.08 (0.20)	2.8 (1.3)
Gas manifold	Outlet	1300 (980)	0.14 (0.36)	24.2 (11.0)
No-flow pan	-	1300 (980)	0.05 (0.15)	15.2 (6.9)
Flow guide	-	1300 (980)	0.17 (0.43)	25.4 (11.5)
Baffle and baffle supports	Tube center span	1300 (980)	0.03 (0.08)(1)	1.2 (0.5)
Transition pan and tie rods	Extends around perimeter of gas inlet face	1235 (940)	0.03 (0.08)(2)	5.6 (2.5)
Tie rods	No-flow pan edge	1300 (980)	-	12.8 (5.8)
Tie rod supports	No-flow pan edge	1300 (980)	-	4.0 (1.8)
		Total weight = 175 lb (80 kg)		

NOTES: (1) Baffle plate thickness
(2) Pan thickness

At 1770°F (1240°K), the Cb-1Zr HSHX had considerably thicker material gauges than those shown in Table 6-1. This was due to the lower allowable stress, 2.6 ksi (18 MN/m^2) for Cb-1Zr compared to 9.6 ksi (66 MN/m^2) for Haynes 25 at their respective maximum operating temperatures, and the increased core dimensions of the Columbium unit. For example, the gas outlet manifold thickness for the Columbium unit would be 0.32 in. (0.81 cm) compared to 0.14 in. (0.36 cm) for Haynes 25. This Cb-1Zr pan thickness may not be desirable from a fabrication standpoint, and a more complex manifolding arrangement than that shown in Figure 6-5 might be considered to permit use of smaller thicknesses (for example, segmenting the manifold would reduce the membrane load).

The following discussions of thermal, pressure, and inertia stresses outline some of the design considerations and acceptable approaches to HSHX design. The Haynes 25 Case I design is used as an example, although the comments are also generally applicable to Case II.

Thermal Stresses

The tubes are one of the critical heat exchanger components since liquid-to-gas leakage cannot be tolerated. Restraint of tube thermal expansion, which causes thermal stresses and which may result in unacceptably low cycle life, must therefore be avoided. Axial restraint was minimized by fixing the tubes at the liquid inlet-outlet headers and providing sliding support at the intermediate baffle (required for inertia loads) and the header plate at the liquid return pan. This eliminates loads due to differential growth between the tubes and the surrounding manifold structure; however, some tube bending arises due to the difference in temperature between the two lengths of tube connected by the U-tube in the return pan. Figure 6-6a is a sketch of tube movement due to the different tube temperatures. An estimate of tube bending moment was obtained from the loading assumed in Figure 6-6b. The rotation required at the return header causes a maximum bending stress of about 17 ksi (120 MN/m^2). This is less than the material yield stress, so the life will be considerably in excess of the required life of 100 cycles, indicating that this approach to supporting the tubes will be satisfactory.

Thermal stresses must be a consideration for all of the heat exchanger components; however, the general approach used in this preliminary structural effort was to minimize material thickness to reduce undesirable temperature gradiants within the structure. These preliminary component geometries and sizes can be used to determine thermal responses in the structure, and thermal stress calculations will be performed during the final detailed structural design.

Pressure Stresses

Pressure loads were generally supported by direct rather than bending stresses to achieve minimum thickness, lightest weight, and minimum temperature gradiants. The external pressure carrying envelope therefore consisted of

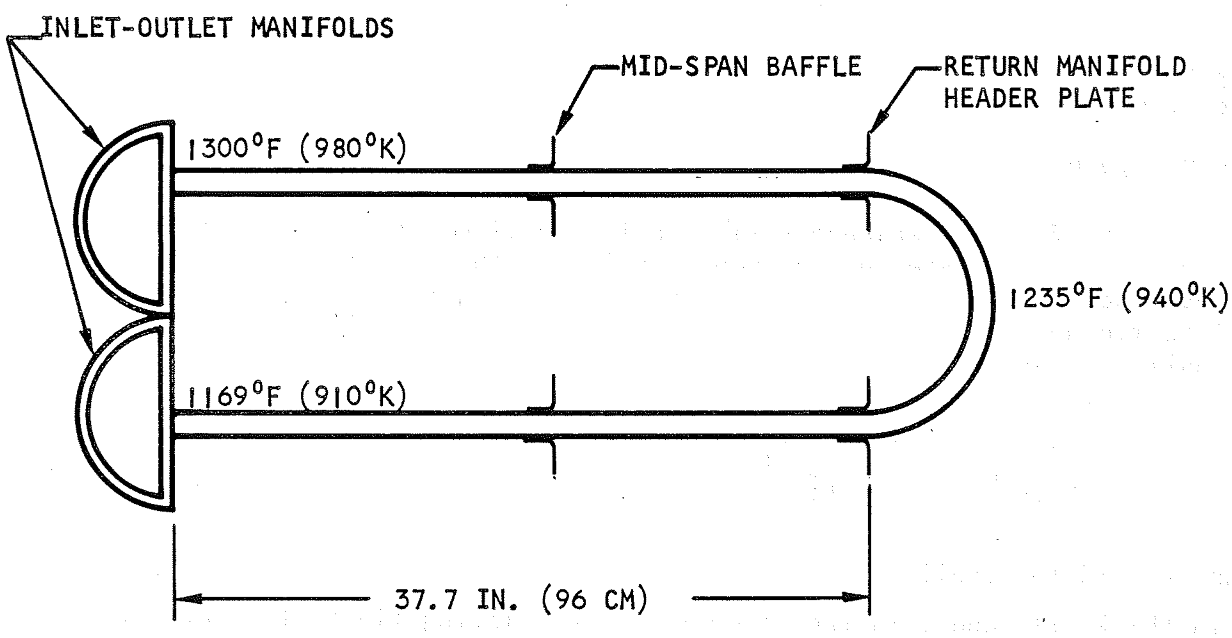

a. Tube Geometry

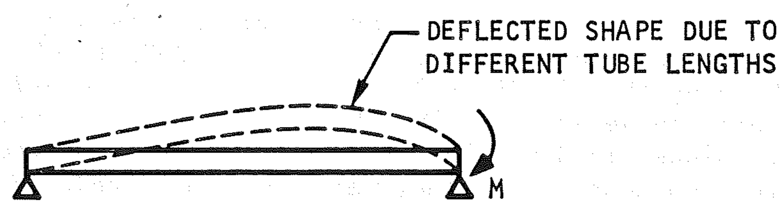

b. Assumed Tube Loading

S-62851

Figure 6-6. Tube Thermal Expansion Provisions and Loading membrane pan geometries with edge loads supported by tension members such as tie rods. The liquid manifolds were an exception to this because shear and bending loads will be transmitted to the flow guide using the section provided by the header plates and semicircular pans.

Inertia Stresses

The 50-Hz minimum frequency requirement established a maximum allowable unsupported tube span of 25 in. (64 cm). A singe baffle and its support beams will therefore carry tube inertia loads at mid-span to give a 19-in. (48-cm) unsupported length. Inertia loads in the tube axis direction will be supported by the liquid inlet-outlet header in a manner similar to the gas pressure force mentioned above.

PLATE-FIN PRESSURE CAPABILITY

Plate-fin heat exchanger fin density requirements were determined for the recuperator and waste heat exchanger prior to the heat transfer calculations. Thus, the fin densities used in the analyses are reflected in the weight of the plate-fin heat exchangers. Fin area density requirements were based on fin tensile stress as given by

$$\sigma_{fin} = \frac{p}{f} \quad \frac{b_{fin} - t_{fin}}{t_{fin}} \tag{6-5}$$

where p is the applied internal pressure, b_{fin} is the fin spacing, t_{fin} is fin thickness, and f is the strength ratio relating fin tested performance to theoretical tensile strength based on this equation. Equation 6-5 can be rewritten to express the required fin area density as a function of pressure, allowable stress, and strength ratio, which gives

$$\frac{t_{fin}}{b_{fin}} = \frac{p}{f\sigma_{all} + p} \tag{6-6}$$

Typical recuperator fin areas versus pressure is shown for Hastelloy X at operating temperatures of 1000° and 1200°F (810° and 920°K) in Figure 6-7. As shown by the 1200°F (920°K) results in Figure 6-7, plate-fin designs for pressures above 400 psi (280 kN/m²) require fin densities greater than 20 percent. Since fin densities of about 18 percent or greater would require improved fabrication techniques, they were not considered. Fin designs for Cases I and II were based on curves similar to Figure 6-7 for the design operating temperatures and pressures previously discussed.

MOUNT SYSTEM DESIGN

A mounting frame will be required for the HXDA and TAC components. This frame will provide inertia load support while permitting relative thermal expansion between the frame and attached components. Although lateral loads

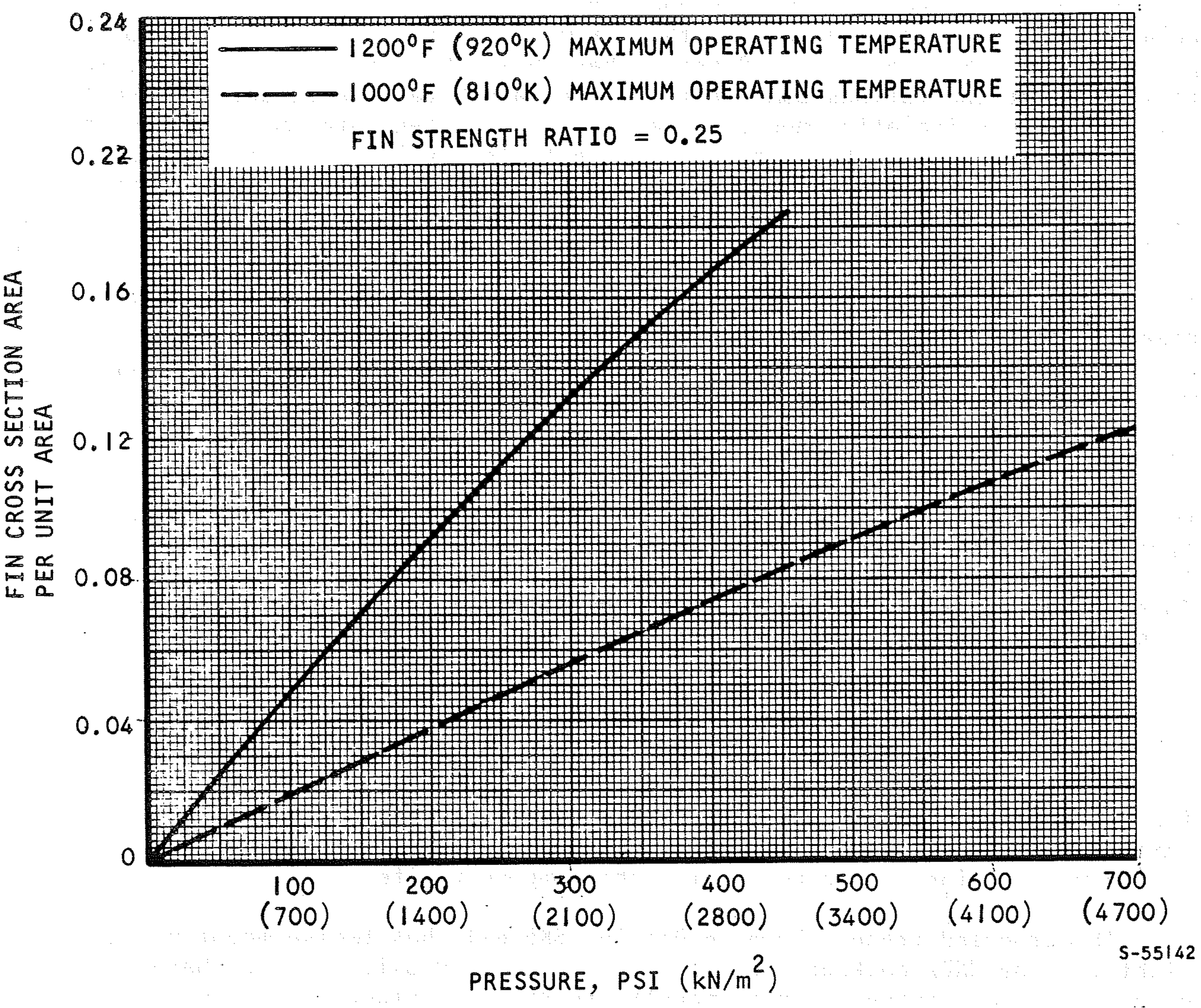

Figure 6-7. Maximum Estimated Fin Area Density Requirements for Hastelloy X at Two Recuperator Operating Temperatures

will be lower, preliminary frame design will be based on 24-g inertia loads applied separately in any direction. Since the mounting direction in a spacecraft has not been defined, use of the maximum load will give a conservative frame design. In addition to the load requirement, the frame component internal frequencies must be greater than 50 Hz to avoid resonance with an assumed isolation system (isolator resonance assumed to be about 15 Hz).

The Brayton-cycle subsystems and components environmental specification P2241-1 will be used to determine the maximum applied loadings at the mount points. Past experience at AiResearch has shown that it is not feasible to rigidly mount the various components to the launch vehicle structure, and that a low-frequency isolation mounting was needed to attentuate the combined shock, vibration, and acceleration forces to acceptable levels. From Specification P2241-1, the vibratory input level from 5 to 33 Hz is 0.14 in. double amplitude displacement, and at 10 Hz this corresponds to a 0.72-g input level. The specification also indicates that there will be low frequency oscillations (1 to 10 Hz) that will persist for several seconds during the boost phase of flight. The amplitudes of the later oscillations is 3-g longitudinal and 2-g lateral; however, these loads can be avoided by employing a mount system with a frequency greater than 10 Hz. Assuming that a mount system frequency of 15 Hz would be selected, the vibratory input level due to the 0.14-in. double amplitude displacement would be 1.6 g in all directions. A damping coefficient equal to 10 percent of critical damping will limit the amplification factor to 5.0 at isolator resonance, and this would produce 8-g vibratory loading at the mount points. This mounting system will also provide shock isolation from the 20-g half-sine pulse of 10-msec time duration. The shock isolation factor would be 0.5, and the shock load factor would be approximately 10 g. These loads combine with the constant longitudinal and lateral accelerations of 6 and 2 g, respectively, to produce the following load factors.

$$\text{Longitudinal} = 8 + 10 + 6 = 24 \text{ g}$$

$$\text{Lateral} = 8 + 10 + 2 = 20 \text{ g}$$

Therefore, even with a highly efficient mounting system for the package, the maximum load factors are substantial. The above launch loads are expected to be the maximum inertia forces during the component life.

The proposed frame, shown in Drawing SK51811, has twelve mount points, eight for the HXDA package and four for the TAC. Provisions for thermal expansion in the plane of these mounts are shown in Figure 6-8, whereas thermal expansion out-of-plane must be minimized (a typical tolerance might be +0.005 in. (0.013 cm)). The basic approach illustrated in Figure 6-8 is to fix one point on both the HXDA and TAC and to provide in-plane load capability at the other points where possible without preventing expansion (arrows indicate load carrying capability in the plane). The fixed points are placed as close to each other as feasible to minimize relative growths that must be accommodated by the bellows. Additional mounting provisions, not shown in Drawing SK51811, may be required to support some of the ducts and bellows if vibration frequencies of these components are below 50 Hz. Such mounts would support relatively small loads if they are required and would not have a significant effect on the overall frame design.

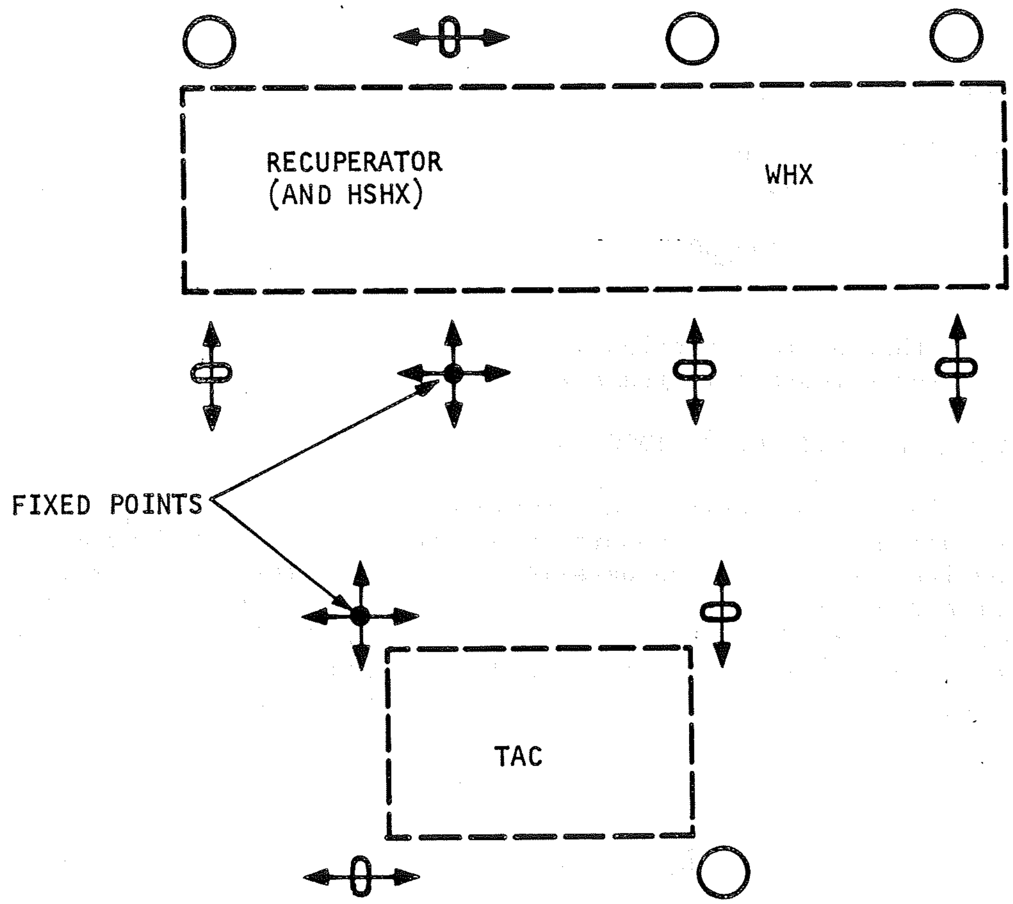

NOTES: (1) ARROWS INDICATE DIRECTION OF MOUNT LOAD CAPABILITY IN THE MOUNT PLANE
(2) ALL MOUNTS HAVE CAPABILITY FOR SUPPORTING LOADS NORMAL TO THE MOUNT PLANE

S-62850

Figure 6-8. Plane of Bolt Hole Locations on the HXDA and TAC

The frame shown in Drawing SK51811 was estimated to have a weight of 120 lb (54 kg). This was based on using Inconel 718 with an allowable stress of 50 ksi (340 MN/m^2), and about 1000 in. (25 m) of tube or beam members (the equivalent of about 10 members with the 92-in. (2.3 m) length shown in the drawing). The required cross sectional area of the members can be estimated from the cantilever load case shown in Figure 6-9 using the recuperator weight of 732 lb (330 kg). The required cross-sectional area of the outer members can be computed from the standard bending equation

$$\sigma_{all} = M/Z \tag{6-7}$$

The section modulus Z is the product of the member area A and their separation h of 12 in. (30 cm). The required area is therefore

$$A = M/h\sigma_{all} = \frac{100,000}{12(50,000)} = 0.2 \text{ in.}^2 \ (1.3 \text{ cm}^2)$$

This indicates that a cross-sectional area of 0.4 sq in. (2.6 sq cm) will be conservative, and a reasonable frame weight estimate is

$$W = \rho AL = 0.3\ (0.4)\ (1000) = 120 \text{ lb } (54 \text{ kg})$$

For the final frame design, the complete load system would be considered to size the various members. Computer programs (available at AiResearch) would be required to perform the detailed analysis of the frame, TAC, and HXDA system. For a space system, isolators would attach the frame to the launch vehicle to provide the design load levels discussed above. Isolator locations would be determined by vehicle and frame design requirements. Their location would be selected to avoid weight penalties in either the frame, TAC, HXDA, or the vehicle.

DUCTING

The ducts, exclusive of bellows sections, connecting the various components will be designed primarily for internal pressure loads. Duct diameters are determined by heat transfer requirements, and the required wall thicknesses were based on pressure forces (see Tables 3-7 and 4-9).

BELLOWS

Expansion joints will be required in the ducts connecting the components in the package. The recommended approach to accommodate the thermal movement between components is to incorporate three link-type convolute bellows in each section (a total of twelve, as shown in Drawing SK51811). The use of link-type bellows, shown in Figure 6-10a, provides pressure balance in the piping system; this avoids unbalance forces on the components and simplifies the package support system (the piping system may be more complicated with the link-type bellows since they must be out-of-line to provide three directional thermal expansion capability). In addition, a combination of link- or rotation-type bellows provides the desired movement capability without applying excessive forces to the heat exchanger and TAC manifolds. This is particularly important for the elevated temperature bellows in the system because pressure containment

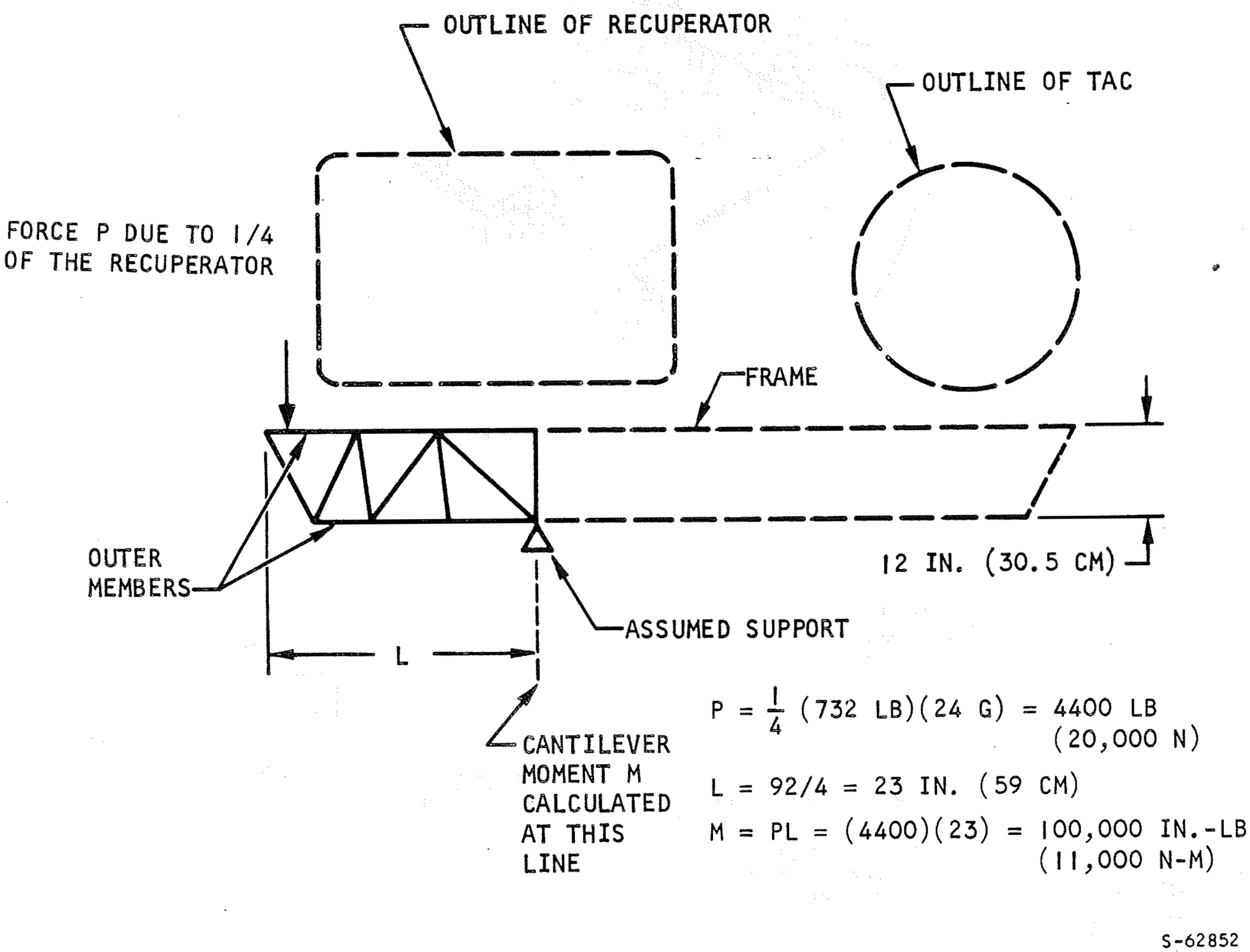

Figure 6-9. Frame Loading for Weight Estimate

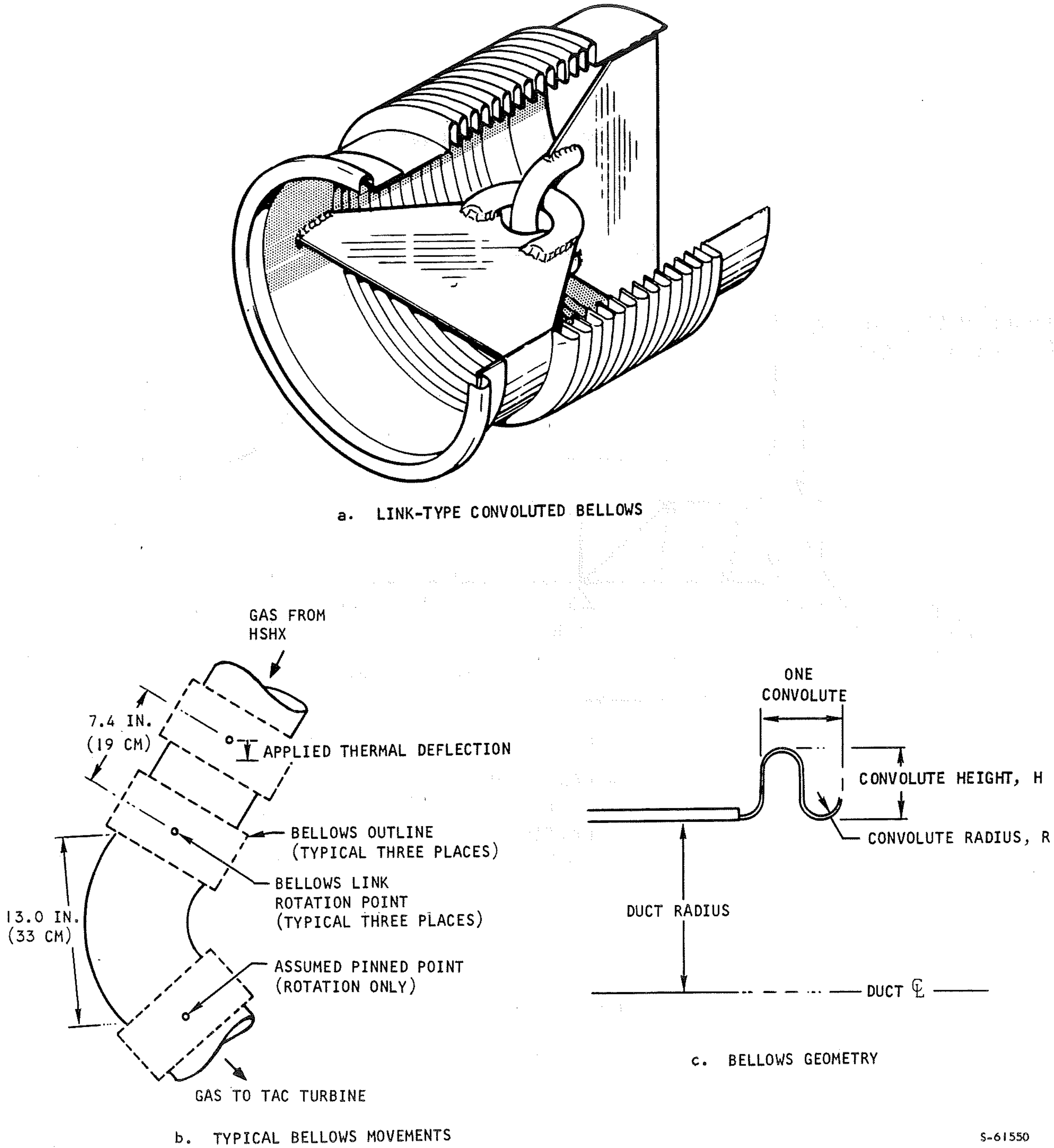

a. LINK-TYPE CONVOLUTED BELLOWS

b. TYPICAL BELLOWS MOVEMENTS (TAKEN FROM SK51811, HAYNES 25)

c. BELLOWS GEOMETRY

Figure 6-10. Bellows Design

strength requirements dictate relatively small convolute heights and large wall thicknesses, which are opposite requirements for thermal stress and load alleviation.

The primary stresses in the bellows convolutes are due to pressure and thermal forces. Pressure stress design can be used to establish an acceptable convolute geometry, and bellows buckling strength establishes the maximum active length of the convolutes (typical designs are discussed below). Allowable segment lengths between bellows can then be determined to avoid excessive thermal stresses and flange loads for the relative thermal expansion of the components. The relative thermal movements that must be accommodated by a set of three bellows is obtained from the mount system geometry and appropriate thermal expansion of component sections.

Preliminary Case I and Case II bellows designs were analyzed for the high temperature heat connecting the HSHX to the TAC turbine inlet. Results for Haynes 25 at 1285°F (970°K) and Cb-1Zr at 1700°F (1200°K) are summarized in Table 6-2. Input values for the calculation include the material properties, internal gas pressure of 200 psi, duct diameters, and an estimated value for thermal deflection that will be accommodated by the bellows system. The thermal deflection requirements are based on (1) a 20-in. spacing between the fixed points on the HXDA and TAC, (2) a duct at the above maximum operating temperatures, and (3) a room temperature frame. For example, the deflection for the Haynes 25 bellows system is

$$\delta = \ell \alpha \Delta T = 20\ (8.38 \times 10^{-6})\ (1285 - 70) = 0.20 \text{ in. } (0.51 \text{ cm})$$

Bellows design outputs for satisfactory pressure containment are included in the table, and the geometry variables are shown in Figure 6-10b. Bellows minimum wall thickness and maximum convolute height and radius are established by internal gas pressure. (Two-ply bellows were used in both cases, and the thickness per ply are given in Table 6-2.) Bellows axial movement is constrained by the internal links, and the allowable number of convolutes was determined for a buckling pressure equal to three times the operating pressure.

With the bellows geometry established by pressure containment, the bellows spacing is adjusted to give acceptable thermal stresses and duct loads. Calculations for the Haynes 25 bellows showed that the link separations would have to be 7.4 and 13 in. (23 and 33 cm) as shown in Figure 6-10b. The link system in Figure 6-10b gives a 0.075-radian rotation at the middle bellows of the three for the 0.020 in. thermal deflection. Duct flange loads due to the bellows movement were not considered in this analysis, although the final designs could be affected by the flange load criteria to be established at a later date.

The Cb1Zr bellows geometry appears to require an excessive thickness, i.e., 0.08-in. (0.20-cm) sheet material. Assuming that the pressure level of 200 psi (1380 kN/m^2) is retained, design solutions to achieve a fabricable geometry include cooling the convolutes to increase material strength properties or changing to a higher strength material. Tantalum T-111, with an allowable

TABLE 6-2

PRELIMINARY HIGH-TEMPERATURE
BELLOWS DESIGNS

Variables		Haynes 25 at 1285°F (970°K)	Cb-1Zr at 1700°F (1200°K)
Inputs	Internal pressure, psi (kN/m^2)	200 (1380)	200 (1380)
	Duct diameter, in. (cm)	7 (18)	9.5 (24)
	Allowable pressure stress, ksi (MN/m^2)	9.8 (68)	3.6 (25)
	Material yield stress, ksi (MN/m^2)	36 (250)	11.8 (81)
	Elastic modulus, ksi (MN/m^2)	25.2×10^3 (170×10^3)	5.8×10^3 40×10^3)
	Thermal deflection, in. (cm)	0.20 (0.51)	0.14 (0.36)
Outputs	Thickness per ply, in. (cm)	0.019 (0.048)	0.084 (0.21)
	Number of ply	2	2
	Convolute radius, in. (cm)	0.077 (0.20)	0.32 (0.81)
	Convolute height, in. (cm)	0.30 (0.76)	0.86 (2.2)
	Number of convolutes	34	18
	Bellows link separations, in.(cm)	9 and 13 (23 and 33)	-(1)

NOTE: (1) not computed

stress of 10.5 ksi (72 MN/m^2) at 1700°F (1200°K), may provide an acceptable geometry, although the convolute wall thicknesses are greater than for the Haynes 25 design at 1300°F (980°K) due to the larger duct diameter.

DISSIMILAR METAL TRANSITION JOINT

A Cb-1Zr to Hastelloy X transition joint is required in the duct between the HSHX and the recuperator in the Case II system. A rather large joint area is required because the duct will have a rectangular cross section of approximately 10 in. by 50 in. The wall thickness of the duct will be approximately 0.050 in.

The explosive bonding process should be capable of producing a reliable leak-tight joint between Cb-1Zr and Hastelloy X. The geometry of the joint is shown in Figure 6-11.

The joint can be produced by the DuPont Deta-clad process. This process consists of bonding two dissimilar metal plates together by the use of explosives. Two metal plates are placed together, separated by a small "standoff" gap. A sheet of explosive material (such as amatol, nitroguanidine, or dynamite) is placed against the cladding material. The explosive is detonated at one edge or corner, and the resultant high-speed high-pressure wave causes mating metal surfaces to impinge at high speed. At the colliding interface, a portion of the surfaces become fluid, which forms a small jet that breaks up unwanted surface films and promotes bonding. Under optimum conditions, a wavy interface is generated, which increases bond area and provides mechanical interlocking between the surfaces in addition to the metallurgical bond.

A typical explosive bond is shown in Figure 6-12. Nickel 200 was bonded to oxygen-free copper for possible application in a hypersonic ramjet engine. Tensile tests with applied stress perpendicular to the bond resulted in failure in the copper and not at the weldment. Low-cycle fatigue tests were conducted at room temperature using push-pull type specimens, again with applied stress perpendicular to the bond. All failures occurred in the copper metal and not at the weldment.

Although there is no prior experience in explosive bonding of Cb-1Zr to Hastelloy X, it is believed that a successful joint will be obtained without difficulty.

Materials bonded by the explosive method include tantalum-to-mild steel, columbium-to-titanium, titanium-to-stainless steel, and titanium-to-mild steel. The DuPont Company has indicated that the current maximum cladding thickness for a Cb-1Zr to Hastelloy X combination is about 3/4 in. With development, the thickness of the cladding material could probably be increased to 1 or 1-1/2 in. A 3/4-in. distance between the explosive bond and the GTA welds, as shown in Figure 6-12, should be adequate.

In practice, therefore, a 3/4-in. plate of Cb-1Zr, approximately 14 by 56 in., will be bonded to a 3/4-in-thick Hastelloy X plate of the same size. The transition joint will then be machined from the two bonded plates. A modification of this procedure can be used to save material. For this procedure,

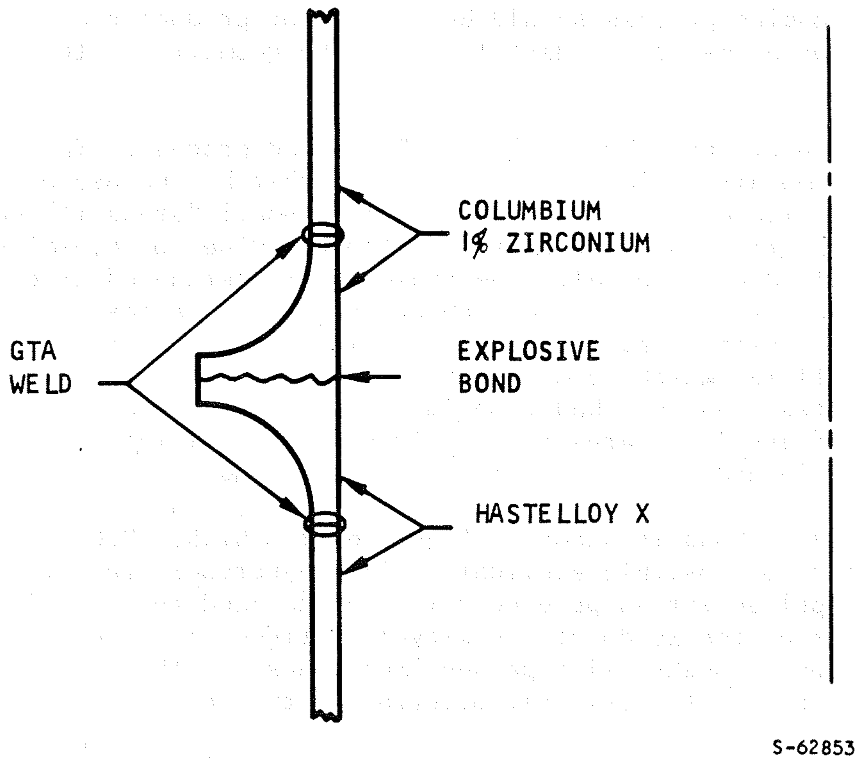

Figure 6-11. Transition Joint in Duct Between HSHX and Recuperator

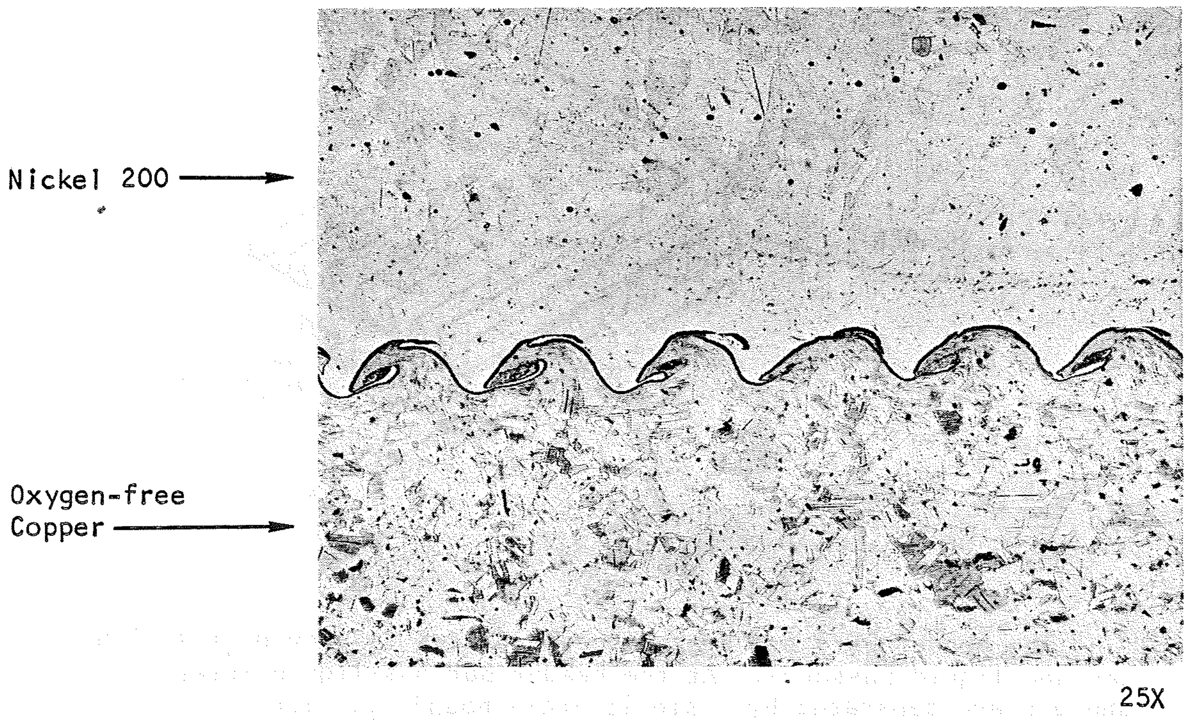

Figure 6-12. Explosive Welded Interface between Nickel 200 and Oxygen-Free Copper

a composite upper plate consisting of a Columbium "picture frame" enclosing a mild steel filler plate is used, and the lower plate consists of a composite assembly of mild steel and Hastelloy X. This scheme was used to produce the copper-nickel transition joint shown in Figure 6-12.

DOUBLE HEADER BARS

The waste heat exchanger designs employ a plate-fin heat transfer matrix. In a plate fin construction, the fluids are separated from each other or contained by plates in one plane and by header bars in the other planes, as illustrated below.

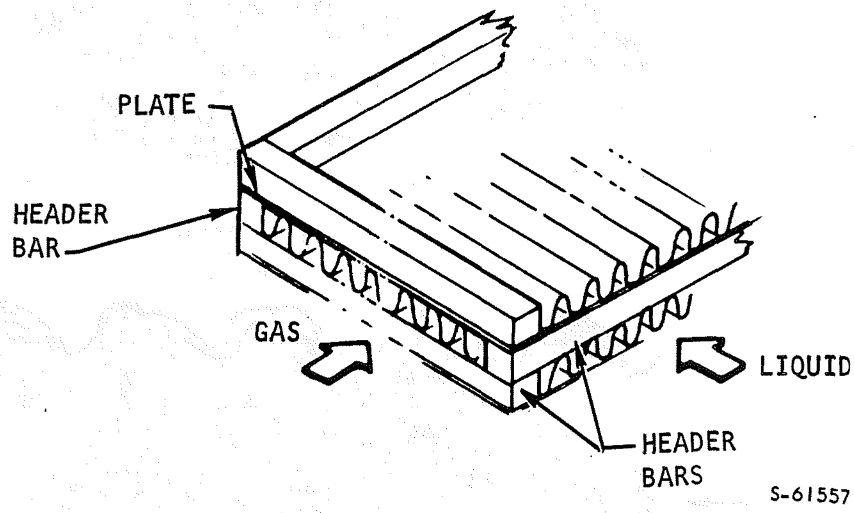

The header bars are brazed to the plates to provide a seal between the gas and liquid passages. At the header bar gas-liquid interface, the fluid and gas are separated by a single braze boundary. Thus, if this braze boundary is violated, it will allow the gas and liquid circuits to intermix. One solution to this problem is to use double header bars along this interface, as illustrated in Figure 6-13. This would require two braze joint failures before any intermixing of the fluids could take place, and no single failure would cause system shutdown. Header bars also form the boundary between the fluid (and gases) and the external vacuum environment. The double header bar approach could also be taken at this boundary, or welded side plates could be used to provide double containment.

One of the problems in using double header bars is in maintaining very close tolerances on the header bars to assure good braze joints on both bars. It is also difficult to maintain appropriate positioning of the header bars during the braze cycle. However, with proper fixtures and tight tolerances, satisfactory double header bar joints can be and have been made. This type of construction has been used successfully in fuel-to-air heat exchangers where it was mandatory that the two fluids never come in contact with each other.

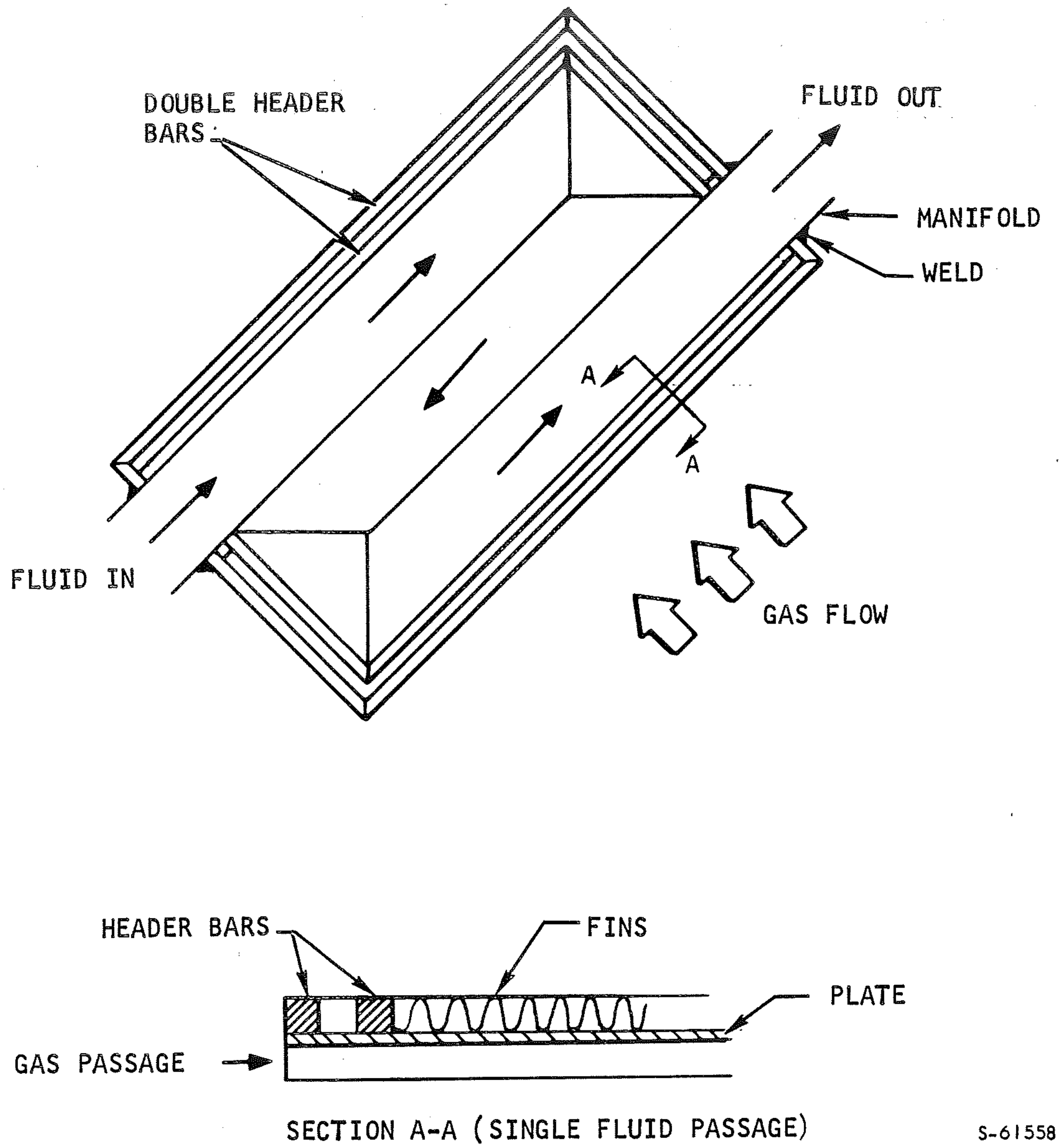

Figure 6-13. Typical Plate-Fin Heat Exchanger With Double Header Bars

A second item of concern is the temperature gradient across the double header joint. Keeping the working fluid away from the outer header bar could produce a large ΔT during the transient startup condition. Before final selection of metal gauges/sizes, a thermal analyzer computer program should be used to define the best core geometry and determine the most severe design conditions.

APPENDIX

END SECTION DESIGN PROGRAM

This appendix presents a complete listing of AiResearch computer program H1440. This program was developed to provide recuperator end section designs for uniform core flow distribution.

```
             C      H1440 PLATE-FIN END SECTION DESIGN PROGRAM
 0001               DIMENSION WLQ(12),WHQ(12)                                        GAR40010
 0002               DIMENSION TINLQ(12),TINHQ(12)                                    GAR40020
 0003               DIMENSION TOUTLQ(12),TOUTHQ(12)                                  GAR40030
 0004               DIMENSION PINLQ(12),PINHQ(12)                                    GAR40040
 0005               DIMENSION POUTLQ(12),POUTHQ(12)                                  GAR40050
 0006               DIMENSION ROELQ(12),ROEHQ(12)                                    GAR40060
 0007               DIMENSION TEMP(30),VIS(30)                                       GAR40070
 0008               DIMENSION TEMPH(30),VISH(30)                                     GAR40080
 0009               DIMENSION RE(30),FF(30)                                          GAR40090
 0010               DIMENSION REH(30),FFH(30)                                        GAR40100
 0011               DIMENSION ARAT1(12),EXL(12)                                      GAR40110
 0012               DIMENSION ARAT2(12),CONL(12)                                     GAR40120
 0013               DIMENSION ARAT3(12),TEX(12)                                      GAR40130
 0014               DIMENSION ARAT4(12),TCON(12)                                     GAR40140
 0015               DIMENSION THETA(12),TURN(12)                                     GAR40150
 0016               DIMENSION HTQ(50),RATIOQ(50)                                     GAR40160
 0017               DIMENSION ANFLQ(50),ANFHQ(50)                                    GAR40170
 0018               DIMENSION TFLQ(50),TFHQ(50)                                      GAR40180
 0019               DIMENSION WIDTHQ(5),ANPLQ(5)                                     GAR40190
 0020               DIMENSION ANPHQ(5),ALNQ(5)                                       GAR40200
 0021               DIMENSION HPLQ(5),HPHQ(5)                                        GAR40210
 0022               DIMENSION TEST1Q(5),BWL(5)                                       GAR40220
 0023               DIMENSION BWH(5),WTF(5)                                          GAR40230
 0024               DIMENSION AK(5),HEAD(20)                                         GAR40240
 0025               DIMENSION ELCORQ(5),DPCORQ(5)
 0026           600 READ (5,6)HEAD                                                   GAR70010
 0027               WRITE (6,7)HEAD                                                  GAR70020
             C READ CONTROL CARD FOR THE TABLES                                      GAR70030
 0028               READ (5,1)NVIS,NVISH,NFF,NFFH,NLEX,NLCON,NTEX,NTCON,NTURN        GAR70040
             CREAD THE NINE DIFFERENT TABLES                                         GAR70050
 0029               READ (5,2)(TEMP(I),VIS(I),I=1,NVIS)                              GAR70060
 0030               READ (5,2)(TEMPH(I),VISH(I),I=1,NVISH)                           GAR70070
 0031               READ (5,2)(RE(I),FF(I),I=1,NFF)                                  GAR70080
 0032               READ (5,2)(REH(I),FFH(I),I=1,NFFH)                               GAR70090
 0033               READ (5,2)(ARAT1(I),EXL(I),I=1,NLEX)                             GAR70100
 0034               READ (5,2)(ARAT2(I),CONL(I),I=1,NLCON)                           GAR70110
 0035               READ (5,2)(ARAT3(I),TEX(I),I=1,NTEX)                             GAR70120
 0036               READ (5,2)(ARAT4(I),TCON(I),I=1,NTCON)                           GAR70130
 0037               READ (5,2)(THETA(I),TURN(I),I=1,NTURN)                           GAR70140
             C READ CONTROL CARD FOR OTHER VARIABLES                                 GAR70150
 0038           601 READ (5,1)J1,J2,J3                                               GAR70160
             C READ OTHER VARIABLES                                                  GAR70170
 0039               DO 10 N1=1,J1                                                    GAR70180
 0040            10 READ (5,2) WIDTHQ(N1),ANPLQ(N1),ANPHQ(N1),ALNQ(N1),HPLQ(N1),HPHQ( GAR70190
                   1N1),TEST1Q(N1),BWL(N1),BWH(N1),WTF(N1),AK(N1),ELCORQ(N1),
                   1DPCORQ(N1)
 0041               DO 11 N2=1,J2                                                    GAR70210
 0042            11 READ (5,2) WLQ(N2),WHQ(N2),TINLQ(N2),TINHQ(N2),TOUTLQ(N2),TOUTHQ( GAR70220
                   1N2),PINLQ(N2),PINHQ(N2),POUTLQ(N2),POUTHQ(N2),ROELQ(N2),ROEHQ(N2) GAR70230
 0043               DO 12 N3=1,J3                                                    GAR70240
 0044            12 READ (5,2) HTQ(N3),RATIOQ(N3),ANFLQ(N3),ANFHQ(N3),TFLQ(N3),TFHQ(N3GAR70250
                   1)
 0045               K=1                                                              GAR70270
 0046               DO 1000 N3=1,J3                                                  GAR70280
```

```
      DO 1000 N2=1,J2                                  GAR70290
      DO 1000 N1=1,J1                                  GAR70300
      K3=0
      WIDTH=WIDTHQ(N1)                                 GAR70310
      ANPL=ANPLQ(N1)                                   GAR70320
      ANPH=ANPHQ(N1)                                   GAR70330
      ALN=ALNQ(N1)                                     GAR70340
      HPL=HPLQ(N1)                                     GAR70350
      HPH=HPHQ(N1)                                     GAR70360
      TEST1=TEST1Q(N1)                                 GAR70370
      ELCORE=ELCORQ(N1)
      DPCORE=DPCORQ(N1)
      WL=WLQ(N2)                                       GAR70380
      WH=WHQ(N2)                                       GAR70390
      TINL=TINLQ(N2)                                   GAR70400
      TINH=TINHQ(N2)                                   GAR70410
      TOUTL=TOUTLQ(N2)                                 GAR70420
      TOUTH=TOUTHQ(N2)                                 GAR70430
      PINL=PINLQ(N2)                                   GAR70440
      PINH=PINHQ(N2)                                   GAR70450
      POUTL=POUTLQ(N2)                                 GAR70460
      POUTH=POUTHQ(N2)                                 GAR70470
      ROEL=ROELQ(N2)                                   GAR70480
      ROEH=ROEHQ(N2)                                   GAR70490
      HT2=HTQ(N3)
      RATIO2=RATIOQ(N3)
      ANFL=ANFLQ(N3)                                   GAR70520
      ANFH=ANFHQ(N3)                                   GAR70530
      TFL=TFLQ(N3)                                     GAR70540
      TFH=TFHQ(N3)                                     GAR70550
      ALAML=1.0-TFL*ANFL                               GAR70560
      ACPL=(1.0-TFL/HPL)*ALAML                         GAR70570
      ATPL=2.0*ALAML+2.0*ANFL*(HPL-TFL)                GAR70580
      RHL=HPL*ACPL/(ATPL*12.0)                         GAR70590
      ALAMH=1.0-TFH*ANFH                               GAR70600
      ACPH=(1.0-TFH/HPH)*ALAMH                         GAR70610
      ATPH=2.0*ALAMH+2.0*ANFH*(HPH-TFH)                GAR70620
      RHH=HPH*ACPH/(ATPH*12.0)                         GAR70630
      HT=HT2
      RATIO=RATIO2
      K2=0
      K1=0
      ARGOLD=1.
      EPS=0.1
      EPS2=0.1*HT2
      KK1=0
      IF (TEST1-1.0)109,300,300                        GAR70640
  108 K1=0
  109 A=WIDTH*RATIO                                    GAR70650
      B=WIDTH-A                                        GAR70660
      X=(HT*HT+A*A)**0.5                               GAR70670
      Y=(HT*HT+B*B)**0.5                               GAR70680
      WIDL=HT*WIDTH/Y                                  GAR70690
      ALENX=HT*WIDTH/(X*2.0)                           GAR70700
      WIDH=ALENX*2.0                                   GAR70710
```

```
      ALENL=Y/2.0
      ALENH=X/2.0                                                       GAR70720
      THETL=HT/Y                                                        GAR70730
      THETH=HT/X                                                        GAR70740
      ACL=ACPL*WIDL*HPL*ANPL/144.0                                      GAR70750
      AFRL=X*ALN/144.0                                                  GAR70760
      ARATL=ACL/AFRL                                                    GAR70770
      COREL=ACPL*WIDL/(BWL(N1)*WIDTH)                                   GAR70780
      ACH=ACPH*WIDH*HPH*ANPH/144.0                                      GAR70790
      AFRH=Y*ALN/144.0                                                  GAR70800
      ARATH=ACH/AFRH                                                    GAR70810
      COREH=ACPH*WIDH/(BWH(N1)*WIDTH)                                   GAR70820
      ALPHA=(HT*WIDTH)/(X*Y)                                            GAR70830
      CALL LAGIN2(51,THETA,NTURN,3,ALPHA,CTM,TURN)                      GAR70840
      GOUTL=[illegible]/ACL
      CALL LAGIN2(7,THETA,NTURN,3,THETL,CTOL,TURN)
      CALL LAGIN2(8,TEMP,NVIS,3,TOUTL,VOL,VIS)                          GAR71010
      REOL=GOUTL*4.*RHL/VOL
      CALL LAGIN2(9,RE,NFF,3,REOL,FFOL,FF)                              GAR71030
      IF (2000.-REOL)222,222,219                                        GAR71040
  219 CALL LAGIN2(10,ARAT2,NLCON,3,COREL,COROL,CONL)                    GAR71050
      CALL LAGIN2(11,ARAT1,NLEX,3,ARATL,EXOL,EXL)                       GAR71060
      GO TO 224                                                         GAR71070
  222 CALL LAGIN2(12,ARAT4,NTCON,3,COREL,COROL,TCON)                    GAR71080
      CALL LAGIN2(13,ARAT3,NTEX,3,ARATL,EXOL,TEX)                       GAR71090
  224 DENOL=ROEL*POUTL/TOUTL                                            GAR71100
      QQOL=GOUTL*GOUTL/(64.4*DENOL)
      DPOL=QQOL*(FFOL*ALENL/(RHL*12.)+COROL+EXOL+CTOL)/144.
      DPPOL=DPOL*100./PINL
      XXOL=QQOL*(FFOL*ALENL/(RHL*12.0))/144.0
      XXXOL=XXOL*100.0/PINL
      GH=WH/ACH                                                         GAR71150
      CALL LAGIN2(14,TEMPH,NVISH,3,TINH,VIH,VISH)                       GAR71160
      REIH=GH*4.0*RHH/VIH                                               GAR71170
      CALL LAGIN2(15,REH,NFFH,3,REIH,FFIH,FFH)                          GAR71180
      IF (2000.-REIH)236,236,233                                        GAR71190
  233 CALL LAGIN2(16,ARAT2,NLCON,3,ARATH,CONIH,CONL)                    GAR71200
      CALL LAGIN2(17,ARAT1,NLEX,3,COREH,CORIH,EXL)                      GAR71210
      GO TO 238                                                         GAR71220
  236 CALL LAGIN2(18,ARAT4,NTCON,3,ARATH,CONIH,TCON)                    GAR71230
      CALL LAGIN2(19,ARAT3,NTEX,3,COREH,CORIH,TEX)                      GAR71240
  238 CALL LAGIN2(20,THETA,NTURN,3,THETH,CTIH,TURN)                     GAR71250
      DENIH=ROEH*PINH/TINH                                              GAR71260
      QQIH=GH*GH/(64.4*DENIH)                                           GAR71270
  241 DPIH=QQIH*(FFIH*ALENH/(RHH*12.0)+CONIH+CORIH+CTIH)/144.0
      DPPIH=DPIH*100.0/PINH                                             GAR71300
      XXIH=QQIH*(FFIH*ALENH/(RHH*12.0))/144.0
      XXXIH=XXIH*100.0/PINH
  510 A2=WIDTH*RATIO2
      B2=WIDTH-A2
      X2=(HT2*HT2+A2*A2)**0.5
      Y2=(HT2*HT2+B2*B2)**0.5
      WIDL2=HT2*WIDTH/Y2
      ALENX2=HT2*WIDTH/(X2*2.)
      WIDH2=ALENX2*2.
```

```
      ALENL2=Y2/2.
      ALENH2=X2/2.
      THETL2=HT2/Y2
      THETH2=HT2/X2
      ACL2=ACPL*WIDL2*HPL*ANPL/144.
      AFRL2=X2*ALN/144.
      ARATL2=ACL2/AFRL2
      COREL2=ACPL*WIDL2/(BWL(N1)*WIDTH)
      ACH2=ACPH*WIDH2*HPH*ANPH/144.
      AFRH2=Y2*ALN/144.
      ARATH2=ACH2/AFRH2
      COREH2=ACPH*WIDH2/(BWH(N1)*WIDTH)
      ALPHA2=(HT2*WIDTH)/(X2*Y2)
      CALL LAGIN2(61,THETA,NTURN,3,ALPHA2,CTM2,TURN)
      GINL=WL/ACL2
      CALL LAGIN2(1,TEMP,NVIS,3,TINL,VIL,VIS)
      REIL=GINL*4.*RHL/VIL
      CALL LAGIN2(2,RE,NFF,3,REIL,FFIL,FF)
      IF (2000.-REIL)208,208,205
  205 CALL LAGIN2(3,ARAT2,NLCON,3,ARATL2,CONIL,CONL)
      CALL LAGIN2(4,ARAT1,NLEX,3,COREL2,CORIL,EXL)
      GO TO 210
  208 CALL LAGIN2(5,ARAT4,NTCON,3,ARATL2,CONIL,TCON)
      CALL LAGIN2(6,ARAT3,NTEX,3,COREL2,CORIL,TEX)
  210 CALL LAGIN2(62,THETA,NTURN,3,THETL2,CTIL,TURN)
      DENIL=ROEL*PINL/TINL
      QQIL=GINL*GINL/(64.4*DENIL)
      DPIL=QQIL*(FFIL*ALENL2/(RHL*12.)+CONIL+CORIL+CTIL)/144.
      DPPIL=DPIL*100./PINL
      XXIL=QQIL*(FFIL*ALENL2/(RHL*12.))/144.
      XXXIL=XXIL*100./PINL
      GH2=WH/ACH2
      CALL LAGIN2(21,TEMPH,NVISH,3,TOUTH,VOH,VISH)
      REOH=GH2*4.*RHH/VOH
      CALL LAGIN2(22,REH,NFFH,3,REOH,FFOH,FFH)
      IF (2000.-REOH)250,250,247
  247 CALL LAGIN2(23,ARAT2,NLCON,3,COREH2,CONOH,CONL)
      CALL LAGIN2(24,ARAT1,NLEX,3,ARATH2,EXOH,EXL)
      GO TO 252
  250 CALL LAGIN2(25,ARAT4,NTCON,3,COREH2,CONOH,TCON)
      CALL LAGIN2(26,ARAT3,NTEX,3,ARATH2,EXOH,TEX)
  252 DENOH=ROEH*POUTH/TOUTH
      CALL LAGIN2(63,THETA,NTURN,3,THETH2,CTOH,TURN)
      QQOH=GH2*GH2/(64.4*DENOH)
      DPOH=QQOH*(FFOH*ALENH2/(RHH*12.)+CONOH+EXOH+CTOH)/144.
      DPPOH=DPOH*100./PINH
      XXOH=QQOH*(FFOH*ALENH2/(RHH*12.))/144.
      XXXOH=XXOH*100./PINH
      VOLM=(HT*WIDTH*ALN+HT2*WIDTH*ALN)/2.
      WEIGT=VOLM*WTF(N1)
      DPTOT=DPPOH+DPPIH+DPPOL+DPPIL
      IF(ABS((XXIL-XXOL)/XXIL) .LE. .05) GO TO 701
      HT=HT*(XXOL/XXIL)**.5
      IF(HT .GT. HT2) HT=HT2
      IF(HT .LT. .01) HT=.01
```

```
      K1=K1+1
      IF(K1 .GT. 10) K3=1
      IF(K1 .GT. 10) GO TO 500
      GO TO 109
  701 IF(ABS((XXIH-XXOH)/XXOH) .LE. .05) GO TO 500
      ARG=XXOH-XXIH
      IF(ARG/ARGOLD .LT. 0.0) EPS=.25*EPS
      DEL=SIGN(EPS,ARG)
      RATIO=RATIO+DEL
      ARGOLD=ARG
      IF(RATIO .GT. 1.) RATIO=1.
      IF(RATIO .LT. 0.0) RATIO=0.0
      K2=K2+1
      IF(K2 .GT. 10) K3=1
      IF(K2 .GT. 10) GO TO 500
      GO TO 108
  300 CONTINUE
      RATIO=0.0
      RATIO2=0.0
      DPIL=0.0
      DPOL=0.0
      DPPIL=0.0
      DPPOL=0.0
      XXIL=0.0
      XXOL=0.0
      XXXIL=0.0
      XXXOL=0.0
      REIL=0.0
      REOL=0.0
      ACH=ACPH*HT*HPH*ANPH/144.0                                        GAR71740
      ALENH=WIDTH/2.                                                    GAR71750
      X=WIDTH                                                           GAR71760
      Y=HT                                                              GAR71770
      ACH1=WIDTH*HPH*BWH(N1)*ANPH/144.
      GH=WH/ACH                                                         GAR71800
      GH1=WH/ACH1                                                       GAR71810
      ARATH=ACH*144.0/(HT*ALN)                                          GAR71820
      COREH=ACH/ACH1                                                    GAR71830
      CALL LAGIN2(35,TEMPH,NVISH,3,TINH,VIH,VISH)                       GAR71840
      REIH=GH*4.0*RHH/VIH                                               GAR71850
      CALL LAGIN2(36,REH,NFFH,3,REIH,FFIH,FFH)                          GAR71870
      IF (2000.0-REIH)419,419,416                                       GAR71890
  416 CALL LAGIN2(38,ARAT2,NLCON,3,ARATH,CONIH,CONL)                    GAR71900
      CALL LAGIN2(39,ARAT1,NLEX,3,COREH,CORIH,EXL)                      GAR71910
      GO TO 421                                                         GAR71930
  419 CALL LAGIN2(40,ARAT4,NTCON,3,ARATH,CONIH,TCON)                    GAR71940
      CALL LAGIN2(41,ARAT3,NTEX,3,COREH,CORIH,TEX)                      GAR71950
  421 DENIH=ROEH*PINH/TINH                                              GAR71970
      QQIH=GH*GH/(64.4*DENIH)                                           GAR71980
      DPIH=QQIH*(FFIH*ALENH/(RHH*12.)+CONIH+CORIH+AK(N1))/144.
      DPPIH=DPIH*100.0/PINH                                             GAR72030
      XXIH=QQIH*(FFIH*ALENH/(RHH*12.))/144.
      XXXIH=XXIH*100./PINH
      CALL LAGIN2(42,TEMPH,NVISH,3,TOUTH,VOH,VISH)                      GAR72040
      ACH2=ACPH*HT2*HPH*ANPH/144.
```

```
      Y2=HT2
      GH2=WH/ACH2
      ARATH2=ACH2*144./(HT2*ALN)
      COREH2=ACH2/ACH1
      REOH=GH2*4.*RHH/VOH
      CALL LAGIN2(43,REH,NFFH,3,REOH,FFOH,FFH)
      IF (2000-RFOH)433,433,430
  430 CALL LAGIN2(45,ARAT1,NLEX,3,ARATH2,EXOH,EXL)
      CALL LAGIN2(46,ARAT2,NLCON,3,COREH2,COROH,CONL)
      GO TO 435
  433 CALL LAGIN2(47,ARAT3,NTEX,3,ARATH2,EXOH,TEX)
      CALL LAGIN2(48,ARAT4,NTCON,3,COREH2,COROH,TCON)
  435 DENOH=ROLH*POUTH/TOUTH
      QQOH=GH2*GH2/(64.4*DENOH)
      DPOH=QQOH*(FFOH*ALENH/(RHH*12.)+EXOH+COROH+AK(N1))/144.
      DPPOH=DPOH*100./PINH
      XXOH=QQOH*(FFOH*ALENH/(RHH*12.))/144.
      XXXOH=XXOH*100./PINH
      VOLM=(HT+HT2)*WIDTH*ALN/2.
      WEIGT=VOLM*WTF(N1)
      DPTOT=DPPIH+DPPOH
      DELP1=XXIH+(HT/ELCORE)*(DPCORE/2.)
      DELP2=XXOH+(HT2/ELCORE)*(DPCORE/2.)
      IF(ABS((DELP1-DELP2)/DELP1) .LE. .05) GO TO 500
      ARG=DELP2-DELP1
      IF(ARG/ARGOLD .LT. 0.0) EPS2=.25*EPS2
      DEL=SIGN(EPS2,ARG)
      HT=HT-DEL
      ARGOLD=ARG
      IF(HT .LT. .01) HT=.01
      IF(HT .GT. HT2) HT=HT2
      KK1=KK1+1
      IF(KK1 .GT. 10)K3=1
      IF(KK1 .GT. 10)GO TO 500
      GO TO 300
  500 CONTINUE
      IF(K3 .EQ. 1) HT=0.0
      IF(K3 .EQ. 1) RATIO=0.0
      WRITE (6,3)WL,TINL,TOUTL,PINL,POUTL,WH,TINH,TOUTH,PINH,POUTH,HT2,
     1RATIO2,HT,RATIO,TEST1,AK(N1),ANFL,ANFH,TFL,TFH
      WRITE (6,4)WIDTH,ALN,HPL,HPH                                      GAR72280
      IF(K3 .EQ. 0) WRITE (6,5)DPIL,DPOL,DPPIL,DPPOL,DPIH,DPOH,DPPIH,
     1DPPOH,XXIL,XXOL,XXXIL,XXXOL,XXIH,XXOH,XXXIH,XXXOH,VOLM,WEIGT,X,Y,
     2RHL,RHH,REIL,REOL,REIH,REOH
      IF(K3 .EQ. 0) WRITE(6,14) DPTOT
      IF(K3 .EQ. 1) WRITE (6,13)
      WRITE (6,8)                                                       GAR72310
 1000 CONTINUE                                                          GAR72320
      READ (5,1)M                                                       GAR72330
      GO TO (600,601),M                                                 GAR72340
    1 FORMAT (9I5)                                                      GAR72350
    2 FORMAT (8F10.4)                                                   GAR72360
    3 FORMAT (1H0,18X,19HLOW  PRESSURE  SIDE,44X,20HHIGH  PRESSURE  SIDEGAR72370
     1,/,3X,4HFLOW,4X,10HINLET TEMP,2X,11HOUTLET TEMP,2X,8HPRESS IN,2X, GAR72380
     18HPRES OUT,12X,4HFLOW,4X,10HINLET TEMP,2X,11HOUTLET TEMP,2X,8HPRESGAR72390
```

```
                1S IN,2X,8HPRES OUT,/,2X,6HLB/SEC,7X,1HR,12X,1HR,9X,4HPSIA,6X,      GAR72400
                14HPSIA,13X,6HLB/SEC,8X,1HR,11X,1HR,9X,4HPSIA,6X,4HPSIA,/,F10.4,F10GAR72410
                1.3,F12.3,F12.3,F10.3,9X,F10.4,F10.3,F12.3,F12.3,F10.3//,3X,15HLOW
                1PRESSURE IN,5X,16HHIGH PRESSURE IN,/,2X,9HHEIGHT,IN,4X,5HRATIO,4X,
                19HHEIGHT,IN,4X,5HRATIO,4X,5HTEST1,2X,13HRECT.TURN CON,2X,10HNO.FIN
                1 LP ,2X,10HNO.FIN HP ,2X,15HFIN THICK LP,IN,2X,15HFIN THICK HP,IN,
                1/,F10.3,F10.3,F12.3,F10.3,F8.1,F12.3,F14.2,F12.2,F14.4,7X,F10.4)
0317          4 FORMAT (1H0,/2X,9HWIDTH,IN ,F7.4,5X,11HNO.FLOW,IN ,F7.3,5X,16HPASSGAR72460
                1AGE HT. LP  ,F4.3,5X,16HPASSAGE HT. HP  ,F4.3)                    GAR72470
0318          5 FORMAT (1H0,//,10X,32HLOW PRESSURE SIDE,PRESSURE DROPS,29X,33HHIGHGAR72480
                1 PRESSURE SIDE,PRESSURE DROPS,/,2X,10HINLET,PSIA,3X,11HOUTLET,PSIAGAR72490
                1,3X,13HINLET,PERCENT,3X,14HOUTLET,PERCENT,5X,10HINLET,PSIA,2X,11HOGAR72500
                1UTLET,PSIA,2X,13HINLET,PERCENT,2X,14HOUTLET,PERCENT,/,F12.4,F13.4,GAR72510
                1F14.4,F16.4,7X,F12.4,F13.4,F13.4,F16.4,/F12.4,F13.4,F14.4,F16.4,7X
                1,F12.4,2. 13.4,F16.4,2X,8HFRICT DP/,2X,12HVOLUME,CU.IN,2X,
                1                                                              9H
                1WEIGHT,LB,3X,13HDIMENSIONS,IN,3X,10HL.P. RH,FT,2X,10HH.P. RH,FT,2XGAR72530
                1,10HIN RE  LP ,2X,11HOUT RE  LP ,2X,10HIN RE  HP ,2X,             GAR72540
                111HOUT RE  HP ,/,F12.4,F13.4,F10.3,F8.3,F12.6,F12.6,F10.2,3(F13.2)GAR72550
                1,//)
0319          6 FORMAT (20A4)                                                     GAR72570
0320          7 FORMAT (1H1,20A4)                                                 GAR72580
0321          8 FORMAT (40X,40H* * * * * * * * * * * * * * * * * * * * )          GAR72590
0322         13 FORMAT(1H0,///,10X,'NO SOLUTION IN 10 ITERATIONS',////)
0323         14 FORMAT(1H+,2X,'TOTAL PRESSURE DROP=',F9.4,1X,'PERCENT',//)
0324            END                                                               GAR72600
```

DISTRIBUTION LIST

NASA-Lewis Research Center
21000 Brookpark Road
Cleveland, Ohio 44135
Attention: (See list below)
G. M. Ault (MS 3-13) - 1
R. E. English (MS 500-201) - 1
H. O. Slone (MS 500-201) - 1
J. A. Heller (MS 500-201) - 1
E. E. Kempke, Jr. (MS 500-201) - 1
J. P. Joyce (MS 500-201) - 1

D. C. Guentert (MS 500-201) - 1
D. R. Packe (MS 500-201) - 1
D. G. Beremand (MS 500-201) - 1
W. T. Wintucky (MS 500-201) - 1
R. R. Miller (MS 500-202) - 1
M. J. Saari (MS 500-202) - 1

P. A. Thollot (MS 500-201) - 1
W. L. Stewart (MS 77-2) - 1
P. T. Kerwin (MS 500-201) - 53
G. M. Thur (MS 500-202) - 1
S. J. Kaufman (MS 49-2) - 1
V. F. Hlavin (MS 3-14) - 1

J. E. Dilley (MS 500-309) - 1
Technology Utilization (MS 3-19) - 1
Report Control (MS 5-5) - 1
Reliability & Quality Assurance (MS 500-111) - 1
Library (MS 60-3) - 2
R. L. Johnsen (MS 500-201) - 1

NASA-Lewis Research Center
Plum Brook Station
Sandusky, Ohio 44870
Attention: D. B. Fenn (MS 1441-1) - 2

National Aeronautics & Space Administration
Washington, D.C. 20546
Attention: (See list below)
RNP/P. R. Miller - 1
RNP/H. D. Rochen - 1
RNT/J. Lazar - 1

NASA Scientific & Technical Information
P. O. Box 33
College Park, Maryland 20740
Attention: Acquisitions Branch (SQT-34054) - 1

NASA-Marshall Space Flight Center
Marshall Space Flight Center, Alabama 35812
Attention: (See list below)
Library - 1
C. Graff - 1
W. Brantley - 1

NASA-Flight Research Center
P. O. Box 273
Edwards, California 93523
Attention: Library - 1

NASA-Ames Research Center
Moffitt Field, California 94035
Attention: Library - 1

NASA-Goddard Space Flight Center
Greenbelt, Maryland 20771
Attention: Library - 1

NASA-Langley Research Center
Langley Station
Hampton, Virginia 23365
Attention: Library - 1

Jet Propulsion Laboratory
4800 Oak Grove Drive
Pasadena, California 91103
Attention: Library - 1

NASA-Manned Spacecraft Center
Houston, Texas 77058
Attention: (See list below)
Library - 1
A. Redding - 1
J. Grayson - 1

AEC Headquarters
Space Nuclear Systems Division
Germantown, Maryland 20545
Attention: C. Johnson - 2

Air Force Systems Command
Aeronautical Systems Division
Wright-Patterson Air Force Base, Ohio 45438
Attention: Library - 1

U.S. Army Engineer R&D Labs
Gas Turbine Test Facility
Fort Belvoir, Virginia 22060
Attention: W. Crim - 1

Bureau of Naval Weapons
Department of the Navy
Washington, D.C. 20025
Attention: Code RAPP - 1

Institute for Defense Analyses
400 Army-Navy Drive
Arlington, Virginia 22202
Attention: Library - 1

Office of Naval Research
Department of the Navy
Washington, D. C. 20025
Attention: Dr. Ralph Roberts - 1

Naval Facilities Engineering Command
P. O. Box 610
Falls Church, Virginia 22046
Attention: Graham Heggy, Code 042 - 1

Bureau of Ships
Department of the Navy
Washington, D. C. 20025
Attention: L. Graves - 1

University of Virginia
School of Engineering & Applied Science
Dept. of Mechanical Engineering
Charlottesville, Virginia 22903
Attention: Dr. E. J. Gunter, Jr. - 1

University of Maryland
College of Engineering
College Park, Maryland 20740
Attention: M. E. Talast - 1

Massachusetts Institute of Technology
Cambridge, Massachusetts 02139
Attention: Library - 1

Battelle Memorial Institute
505 King Avenue
Columbus, Ohio 43201
Attention: Library - 1

Power Information Center
University of Pennsylvania
3401 Market Street, Room 2107
Philadelphia, Pennsylvania 19104

Aerospace Corporation
2350 East El Segundo Blvd.
El Segundo, California 90045
Attention: H. T. Sampson - 1

AVCO-Bay State Abrasives Division
Westboro, Massachusetts 01581
Attention: George Herterick - 1

Aerojet-General Corporation
Von Karman Center
Azusa, California 91702
Attention: Library - 1

Bendix Research Labs. Division
Detroit, Michigan 48232
Attention: Library - 1

Borg-Warner Corporation
Pesco Products Division
24700 North Miles Road
Bedford, Ohio 44014
Attention: Library - 1

Continental Aviation & Engineering Corporation
12700 Kercheval Avenue
Detroit, Michigan 48215
Attention: Library - 1

The Boeing Company
Aero-Space Division
Box 3707
Seattle, Washington 98124
Attention: Library - 1

Curtiss-Wright Corporation
Wright Aero Division
Main and Passaic Streets
Woodridge, New Jersey 07075
Attention: Library - 1

Consolidated Controls Corp.
15 Durant Avenue
Bethel, Connecticut 06801
Attention: Library - 1

Garrett Corporation
AiResearch Manufacturing Company
402 South 36 Street
Phoenix, Arizona 85034
Attention: R. A. Rackley - 2

Garrett Corporation
AiResearch Manufacturing Company
9851 Sepulveda Blvd.
Los Angeles, California 90009
Attention: M. G. Coombs - 1

General Dynamics Corporation
16501 Brookpark Road
Cleveland, Ohio 44142
Attention: Library - 1

General Electric Company
Missile & Space Vehicle Dept.
3198 Chestnut Street
Philadelphia, Pennsylvania 19104
Attention: Library - 1

General Electric Company
Lynn, Massachusetts 01905
Attention: Library - 1

General Electric Company
Mechanical Technology Laboratory
R&D Center
Schnectady, New York 12301
Attention: Library - 1

General Electric Company
Flight Propulsion Laboratory Div.
Cincinnati, Ohio 45215
Attention: Library - 1

General Motors Corporation
Indianapolis, Indiana 46206
Attention: Library - 1

Franklin Institute Research
Laboratories
Benjamin Franklin Parkway at
20th Street
Philadelphia, Pennsylvania 19103
Attention: Library - 1

General Electric Company
Missile and Space Division
Cincinnati, Ohio 45215
Attention: D. Huebner - 2

Lear Siegler, Inc.
3171 S. Bundy Drive
Santa Monica, California 90406
Attention: Library - 1

Lockheed Missiles & Space Co.
P.O. Box 504
Sunnyvale, California 94088
Attention: Library - 1

McDonnell-Douglas Corporation
Space Station Office
Huntington Beach, California
Attention: R. Gervais - 2

McDonnell-Douglas Corporation
Lambert Field
St. Louis, Missouri 63166
Attention: Library - 1

North American Rockwell Corp.
Space Division
12214 Lakewood Blvd.
Downey, California
Attention: (See list below)

- A. Nusseberger - 1
- C. Gould - 1
- W. Schmill - 1

North American Rockwell
Atomics International Division
P. O. Box 309
8900 DeSota Avenue
Canoga Park, California 91304
Attention: (See list below)

- T. A. Moss - 1
- W. Botts - 1

Northern Research & Engineering Co.
219 Vassar Street
Cambridge, Massachusetts 02139
Attention: Library - 1

Mechanical Technology Inc.
968 Albany-Shaker Road
Latham, New York 12110
Attention: Library - 2

Solar Division of International
Harvester
2200 Pacific Highway
San Diego, California 92112
Attention: Library - 1

Sunstrand Denver
2480 West 70 Avenue
Denver, Colorado 80221
Attention: Library - 1

TRW Systems Division
One Space Park
Redondo Beach, California 90278
Attention: Library - 1

Union Carbide Corporation
Linde Division
P. O. Box 44
Tonawanda, New York 14152
Attention: Library - 1

United Aircraft Corporation
Pratt & Whitney Aircraft
West Palm Beach, Florida 33402
Attention: Dr. R. A. Schmidtke - 1

United Aircraft Research Lab.
East Hartford, Connecticut 0610
Attention: Library - 1

Westinghouse Electric Corporation
Aerospace Electrical Division
P. O. Box 989
Lima, Ohio 45802
Attention: A. King - 1

Westinghouse Electric Corporation
Astronuclear Laboratory
P. O. Box 10864
Pittsburth, Pennsylvania 15236
Attention: Library - 1

Williams Research
Walled Lake, Michigan 48088
Attention: Library - 1

Naval Ship Engineering Center
Hyattsville, Maryland 20782
Attention: Frank Welling - 2

TRW, Inc.
23555 Euclid Avenue
Euclid, Ohio 44117
Attention: Bill Davis - 1